Optics and Fluid Dynamics Department annual progress report for 2003

Bindslev, H.; Hanson, Steen Grüner; Lynov, Jens-Peter; Petersen, Paul Michael; Skaarup, Bitten

Publication date:
2004

Document Version
Publisher's PDF, also known as Version of record

Risø-R-1453(EN)

Optics and Fluid Dynamics Department Annual Progress Report for 2003

Edited by H. Bindslev, S.G. Hanson, J.P. Lynov, P.M. Petersen and B. Skaarup

Risø National Laboratory, Roskilde, Denmark
May 2004

Abstract The Optics and Fluid Dynamics Department performs basic and applied research within three scientific programmes: (1) laser systems and optical materials, (2) optical diagnostics and information processing and (3) plasma and fluid dynamics. The department has core competences in: optical sensors, optical materials, optical storage, biophotonics, numerical modelling and information processing, non-linear dynamics, fusion plasma physics and plasma technology. The research is supported by several EU programmes, including EURATOM, by Danish research councils and by industry. A summary of the activities in 2003 is presented.

ISBN 87-550-3301-6 (Internet)
ISSN 0106-2840
ISSN 0906-1797

Contents

1. Introduction 7

2. Laser systems and optical materials 9

2.1 Introduction 9

2.2 Laser systems 10

2.2.1 High-brightness laser source for the graphics industry based on very broad-area semiconductor laser diodes 10

2.2.2 Improvement of spatial and temporal coherence of a broad-area laser diode using an external-cavity design with double grating feedback 11

2.3 Active and passive polymer technology 14

2.3.1 Orientational dynamics in electro-optical polymers 14

2.3.2 Transport and polymer light sources 15

2.4 Laser ablation and pulsed laser deposition 16

2.4.1 Plume dynamics of UV laser ablation of silver in vacuum with fs pulses 16

2.4.2 Deposition of polyethylene glycol by matrix-assisted pulsed laser evaporation 17

2.4.3 Large-area pulsed laser deposition 18

2.5 Optical sensors 19

2.5.1 Absolute refractive index determination by micro-interferometric backscatter detection 19

2.5.2 Reverse-symmetry multimode waveguide 20

2.5.3 Holographic design of integrated surface-plasmon resonance sensor chip 21

2.5.4 Waveguide sensor for on-line monitoring of bacteria with increased probing depth 22

2.6 Holographic storage 23

2.6.1 Photoinduced anisotropy in a family of amorphous azobenzene polyesters for optical storage 23

2.6.2 Polarization holographic and surface relief gratings at 257 nm in an amorphous azobenzene polyester 24

2.6.3 Evanescent polarization holographic recording of sub 200 nm gratings in an azobenzene polyester 25

2.7 Collaboration with Danish and foreign universities 26

2.7.1 Center for Biomedical Optics and New Laser Systems – BIOP 26

2.7.2 VELI – Virtual European Laser Institute 27

3. Optical diagnostics and information processing 29

3.1 Introduction 29

3.2 Biooptics 30
3.2.1 Bio-photonics: new lasers for diagnostic and therapeutic applications – BIOLASE 30
3.2.2 BIOP Graduate School: "Biomedical Optics and New Laser Systems" 31
3.2.3 Optical coherence tomography in clinical examinations of skin cancer 33
3.2.4 Image processing tools for quantifying biofilm growth and structure 34
3.2.5 Aligning noisy signals for enhancing the signal-to-noise ratio of retinal OCT scanners 35
3.2.6 Determination of optical scattering properties of highly-scattering media in optical coherence tomography images 36
3.2.7 Quantitative distinction between bound and free NADH in biological systems 39

3.3 Optical tweezers 41
3.3.1 Controllable mode-launching in micro-structured fibres 41
3.3.2 User-interactive microscopy 43
3.3.3 Multiple-beam optical tweezers based on Shack-Hartmann setup 44

3.4 Speckle techniques 46
3.4.1 Miniaturisation of optical sensors 46
3.4.2 Variance of intensity for Gaussian statistics and partially developed speckle in complex *ABCD* optical systems 48
3.4.3 Applicability of the singular-optics concept for diagnostics of random and fractal rough surfaces 49

3.5 IR techniques 51
3.5.1 Measurements of glucose in aqueous solutions with dual-beam FTIR 51
3.5.2 MENELAS 52
3.5.3 Infrared temperature calibration and related projects 54
3.5.4 Optical thickness measurement at industrial demands 56
3.5.5 Optical inspection of "reliable" plastic weldings 56

3.6 Calibration 57
3.6.1 Calibration of temperature measuring equipment 57
3.6.2 Calibration of voltage, resistance current and pressure measuring equipment 58
3.6.3 Process measurement 58

4. Plasma and fluid dynamics 59

4.1 Introduction 59
4.1.1 Fusion plasma physics 60
4.1.2 Low temperature plasma technology 61

4.2 Turbulence and transport in fusion plasmas 61
4.2.1 Impurity and trace tritium transport in tokamak edge turbulence 63
4.2.2 Intermittent transport in scrape-off layer plasmas 64
4.2.3 Self-regulation, bursting and large-scale intermittency in convective turbulence 66
4.2.4 Study of intermittent small-scale turbulence in Wendelstein 7-AS plasmas during controlled confinement transitions 67
4.2.5 Statistical properties of transport in plasma turbulence 68
4.2.6 Evaluation of measured turbulent particle fluxes in toroidal devices 69
4.2.7 Shear flow generation in electromagnetic plasma edge turbulence 70
4.2.8 Numerical investigations of large-scale zonal flows in drift wave turbulence 71
4.2.9 Do sheared flows inhibit interchange instability? 72

4.3 Millimetre waves used for diagnosing fast ions in fusion plasmas 72
4.3.1 Construction of the collective Thomson scattering diagnostic upgrade for TEXTOR 74
4.3.2 Construction and installation of the collective Thomson scattering diagnostic at ASDEX Upgrade 75
4.3.3 Quasi-optical transmission line of the fast ion millimetre wave collective Thomson scattering diagnostics on TEXTOR and ASDEX Upgrade 76
4.3.4 Electronics for the CTS diagnostics at ASDEX Upgrade and TEXTOR 78
4.3.5 Data acquisition software and calibration for collective Thomson scattering 79
4.3.6 Diagnosing fast ions in ITER by collective Thomson scattering, feasibility study covering systems from millimetre waves to far infrared 80
4.3.7 Preliminary design studies of a 60 GHz CTS diagnostic for ITER 81
4.3.8 Microwave transmission system for audio signals 84

4.4 Low temperature plasmas with environmental and industrial applications 86
4.4.1 Remediation of nitrogen oxide (NO) in the flue gas of a gas power plant 86

4.5 Fluid dynamics 88
4.5.1 Toroidal bubbles with circulation in ideal hydrodynamics: a variational approach 88
4.5.2 The shape and stability of a falling liquid thread 89
4.5.3 Dynamics of vortex lines 89

4.6 Optics and acoustics 89
4.6.1 Interaction of nonlocal dark optical solitons 90
4.6.2 Quadratic solitons as nonlocal solitons 90
4.6.3 Beam stabilization in the 2D nonlinear Schrödinger equation by attractive potentials and radiation 91
4.6.4 Fractional generalization of the Ginzburg-Landau equation: implications for high-temperature superconductivity 91
4.6.5 Inspection of steel bars with laser-generated ultrasound at high scanning velocities 92

5. Publications and educational activities 93

5.1 Laser systems and optical materials 93

5.2 Optical diagnostics and information processing 96

5.3 Plasma and fluid dynamics 102

6. Personnel 93

1. Introduction

J.P. Lynov
jens-peter.lynov@risoe.dk

The Optics and Fluid Dynamics Department performs basic and applied research in laser systems, optical sensors and optical materials as well as in plasma physics and plasma technology. The research is conducted as a combination of science and technology with the following core competences:

- Diode laser systems
  - Biomedical applications
  - Industrial applications
- Optical sensors
  - Light propagation in complex systems
  - Laser-based sensors
  - Diffractive optical components
  - Phase contrast methods
- Optical materials
  - Passive and active polymers
  - Laser ablation and pulsed laser deposition
- Optical storage
  - Holographic techniques
  - Optical encryption
- Biooptics
  - Light/tissue interaction
  - Biosensors
  - Time-resolved fluorescence spectroscopy
  - Optical tweezers
  - IR spectroscopy
- Numerical modelling and information processing
  - Plasma and fluid dynamics, optics
  - Image processing
  - Knowledge-based processing
- Non-linear dynamics
  - Turbulence
  - Vortex dynamics
  - Light propagation in non-linear media
- Fusion plasma physics
  - Theoretical plasma physics
  - Laser and millimetre wave diagnostics
- Plasma technology
  - Pollution reduction
  - Surface treatment
  - Sterilization

The output from the research activities is new knowledge and technology. The users are within industry, research communities and government, and the department is responsible for the Danish participation in EURATOM's fusion energy programme.

For the solution of many of the scientific and technological problems the department employs the following key technologies:

- Microtechnology for optical systems
  - Analogue and digital laser recording of holograms
  - Injection moulding of diffractive optical elements
- Optical characterisation
  - Determination of material surfaces
  - Phase contrast measurements
- Temperature calibration and IR measurement techniques
  - Accredited temperature calibration including IR techniques
  - Fourier transform infrared (FTIR) measurements

The department is organised in three scientific programs

- Laser systems and optical materials
- Optical diagnostics and information processing
- Plasma and fluid dynamics

In the following sections, the scientific and technical achievements during 2003 for each of these programmes are described in more detail.

2. Laser systems and optical materials

2.1 Introduction

P. M. Petersen
paul.michael.petersen@risoe.dk

The research programme on Laser Systems and Optical Materials (LSO) has its main competence within the areas of laser systems, active and passive polymer technology, laser ablation, pulsed laser deposition, biomedical optics, optical sensors, nonlinear properties of materials, holographic storage and nanotechnology. We have close collaboration with Danish and foreign universities, research institutes and industry. Nationally, we participate in the Danish Polymer Centre and the Centre for Biomedical Optics and New Laser Systems. Moreover, the research programme plays a key role in the Danish Graduate School on Biomedical Optics and New Laser Systems. The research programme undertakes significant teaching activities at both the University of Copenhagen and the Technical University of Denmark. Internationally, the programme participates in the Virtual European Laser Institute (VELI) with financial support from the European Commission; the purpose of VELI is to enhance and promote the available laser expertise in Europe.

Development of new laser systems is an important activity in LSO. We carry out fundamental studies as well as applied research where new industrial lasers are constructed. We are currently developing new and improved laser systems for medical applications, materials processing, printing, rapid prototyping, biotechnology and optical sensing. An important research area is the development of new high-power, tunable semiconductors with high spatial and temporal coherence.

The polymer optics activities in LSO are currently involved in the fabrication and replication of diffractive optics, dynamic holographic recording materials, liquid crystalline polymers as well as laser-assisted deposition of transparent coatings (indium tin oxide, ITO) on polymers. Moreover, active polymers research is undertaken with the purpose of developing new light sources.

Laser ablation is also performed in LSO with facilities that comprise a vacuum chamber for studying fundamental laser plume properties, a vacuum chamber for thin film production by pulsed laser deposition and a test chamber for production of polymer films. The facilities are based on UV light from an Nd:YAG laser with pulse energies up to 200 mJ at 355 nm.

Nonlinear optics has been a research subject of intense investigations for many years. The field covering the dynamics of optical materials is concentrated on both inorganic and organic materials. Among the inorganic materials the efforts have been within photorefractives and semiconductors in which nonlinear effects such as parametric oscillation and amplification, optical phase conjugation and four-wave mixing have been studied. The organic studies are focused on surface as well as on bulk effects. More specifically, storage effects, surface relief gratings, molecular reorientation dynamics, electrooptic properties and rotational effects are being investigated.

Finally, holographic data storage and nanotechnology in polymers are important activities that have recently led to collaboration with industry. The activities within optical storage and nanotechnology comprise development and application of polyesters and peptides.

2.2 Laser systems

2.2.1 High-brightness laser source for the graphics industry based on very broad-area semiconductor laser diodes

M. Chi, B. Thestrup and P.M. Petersen
birgitte.thestrup@risoe.dk

High-power, broad-area semiconductor laser diodes are attractive laser sources for a number of applications within industry and medicine due to their small physical size, low costs, high efficiency and long lifetimes. In addition, broad-area single emitters can deliver up to several watts of output power. However, these diodes suffer from poor spatial coherence due to multimode lasing along the emitter stripe. A way of improving the spatial coherence properties and, thereby, the brightness of such lasers is to introduce feedback to the diodes by off-axis self-injection locking.[1]

In the present project, we are developing a high-brightness laser source for the graphics industry, based on very broad-area single emitters, using the off-axis self-injection locking principle. The high-brightness source will be implemented in an image-setter machine developed by the Danish company Esko-Graphics. By increasing the laser power density on illuminating the offset plates in the machine, the exposure time can be decreased substantially. This is important for, e.g., the newspaper industry.

Figure 1 shows a photo of the basic laser system, developed at Risø. The final system will consist of two similar systems coupled together by polarization coupling.[2]

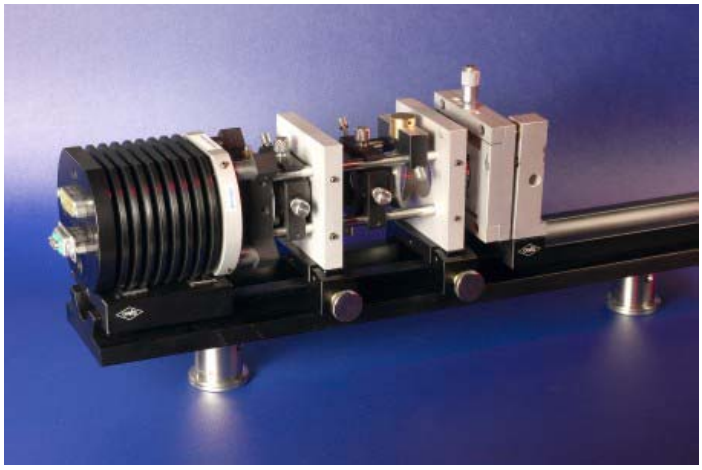

Figure 1. Photo of a single diode laser system based on a broad-area diode laser.

Figure 2 shows what happens to the far-field intensity profile along the emitter stripe of a very broad-area diode laser when external feedback is applied to the diode. The beam width (FWHM), measured in the far-field plane, is narrowed ten times when compared with the freely running laser system. The diode is an 830 nm, 10 W laser with an emitter width of 1000 μm.

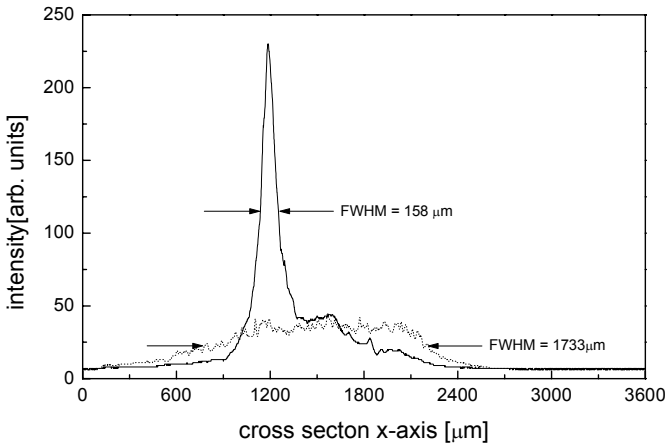

Figure 2. Far-field intensity profiles measured along the emitter for a diode laser with (solid curve) and without (dotted curve) external feedback measured at an operating current of 7.0 A.

The current project is partly financed by Esko-Graphics.

1. M. Løbel, P.M. Petersen and P.M. Johansen, "Single-mode operation of a laser-diode array with frequency-selective phase-conjugate feedback", Opt. Lett. **23**, 825-827 (1998).
2. B. Thestrup, M. Chi, B. Sass and P.M. Petersen, "High brightness laser source based on polarization coupling of two diode lasers with asymmetric feedback", Appl. Phys. Lett. **82**, 680-682 (2003).

2.2.2 Improvement of spatial and temporal coherence of a broad-area laser diode using an external-cavity design with double grating feedback

E. Samsøe (also at the Department of Physics, Lund Institute of Technology, Lund, Sweden), P.E. Andersen, S. Andersson-Engels (Department of Physics, Lund Institute of Technology, Lund, Sweden) and P. Michael Petersen
eva.samsoe@risoe.dk, peter.andersen@risoe.dk, stefan.andersson-engels@fysik.lth.se, paul.michael.petersen@risoe.dk

Due to their compactness, low costs and high efficiency, laser diodes are used in a wide range of applications from medical diagnostics and therapies to printing technologies. Since the invention of semiconductor lasers in 1962,[1] their performance has improved steadily, primarily in terms of lifetime and power level. The output power, however, is limited due to catastrophic optical damage of the laser output facet. This limitation may be overcome by increasing the width of the injection stripe, thus manufacturing broad-area lasers (BALs) or by fabricating monolithic laser diode arrays with several injection stripes separated by, e.g., proton implantations. However, these techniques result in uncontrolled emission of several lateral modes with a double-lobe far field pattern[2] and, thus, lasers with poor spatial and temporal coherence. The coherence properties are crucial in many applications, such as efficient coupling to optical fibres or nonlinear generation of new frequencies. For example, crystals for second harmonic generation or optical parametric oscillators require pump lasers with high spatial and temporal coherence. A remaining problem using diode lasers as pump sources for such applications is maintaining high power while improving their coherence.

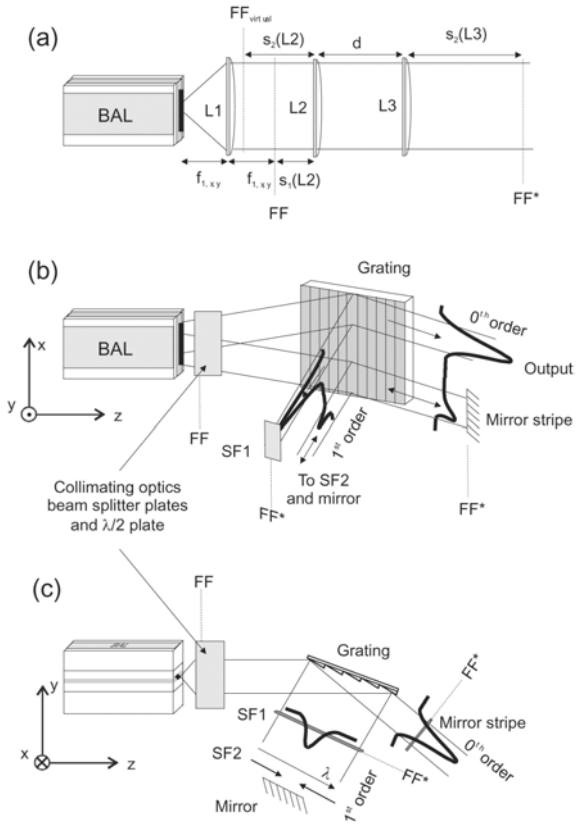

Figure 3. Collimation and generation of image planes (a), side view (b), and top view (c) of experimental set-up. BAL: broad area laser; Li: collimating lenses; f1,x: focal length of L1, s1(Li): distance from object plane to Li; s2(Li): distance from Li to image plane; FF: lateral far field plane; FFvirtual: virtual image plane of FF; FF*: image plane of FF; SF1: spatial filter in the lateral direction; SF2: spatial filter in the transverse direction; x, y, z: lateral, transverse and longitudinal directions, respectively. The shapes of the intensity profiles have been outlined in black.

In this work,[3] we demonstrate a novel technique for narrow bandwidth and highly improved lateral mode operation of a high-power broad-area laser diode. The system, see Figure 3 and Figure 4, uses simultaneous asymmetric feedback from the first diffracted order and the zeroth reflected order of a diffraction grating. The grating is arranged in a configuration similar to a Littman configuration, but with additional feedback from the zeroth order. By means of spatial filters the two feedback paths are arranged to operate in a constructive manner leading to simultaneously improvement of the spectral and spatial properties of the laser diode, respectively. The output from the system is extracted from the zeroth order. The laser system operates in the well-known asymmetric double-lobed far field pattern with the larger lobe being extracted as the output. The bandwidth of the enhanced output beam has been measured to 0.07 nm, which corresponds to an improvement of a factor of 17 compared with the bandwidth of the freely running laser, see Figure 5. The output from the system contains 54% of the energy reaching the grating, or 75% of the power reflected into the zeroth order. The overall efficiency from the freely running laser to the output of the system is 43%. This figure can be improved remarkably by using microoptics and better coatings.

The improvements in both the spatial and the temporal coherence open the possibility of using this laser system in applications such as frequency doubling and pumping of optical parametric oscillators.

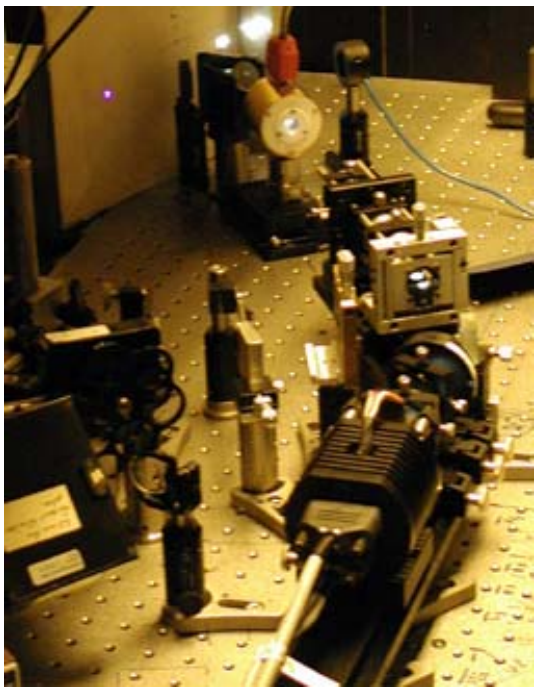

Figure 4. The laser running with single-pass frequency doubling in PP-KTP (405 nm out is viewed as the blue dot on the screen).

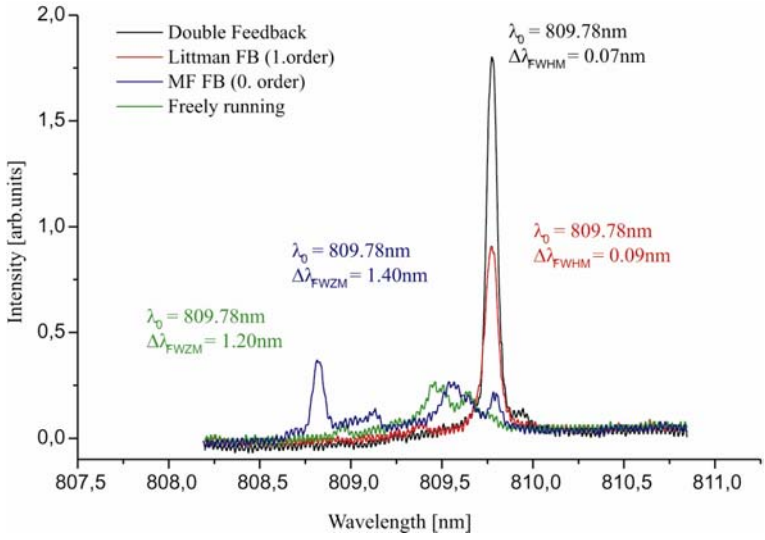

Figure 5. Spectrum of the double and single feedback laser. Black spectrum: double feedback applied; red spectrum: feedback from first order applied; blue spectrum: feedback from zeroth order applied; green spectrum: freely running laser.

1. R. N. Hall, G. E. Fenner, J. D. Kingsley, T. J. Soltys and R. O. Carlson, Phys. Rev. Lett. **9**, 366-368 (1962).
2. J.-M. Verdiell, H. Rajbenbach and J. P. Huignard, J. Appl. Phys. **66**, 1466-1468 (1989).
3. E. Samsøe, P. E. Andersen, S. Andersson-Engels and P. M. Petersen, "Improvement of spatial and temporal coherence of a broad area laser diode using an external-cavity design with double grating feedback", Optics Express **12**, 609-616 (2004).

2.3 Active and passive polymer technology

2.3.1 Orientational dynamics in electro-optical polymers

D. Apitz, K. G. Jespersen (now at Chemical Physics Dept., Lund University, Lund, Sweden), T. G. Pedersen (Institute of Physics, University of Aalborg, Denmark) and P. M. Johansen
per.michael.johansen@risoe.dk

Efficient electro-optic applications are possible in materials based on polymers doped with a substantial amount of nonlinear chromophores. The interest is, e.g., for applications in high-speed photonics such as broadband modulation of light using electro-optic polymers. However, before we can apply polymers effectively in the field of electro-optics, the intricate interaction between dipolar dye molecules embedded in a viscoelastic polymer host material must be established. To further this understanding, we have established a novel model for electro-optic response of chromophores in a viscoelastic polymer matrix to a combined dc and ac applied poling field. The chromophore-matrix interaction is modelled by inferring a local molecular field of a constant magnitude, but with random orientation in space. The model results in explicit dependence on frequency and local molecular field, and can be extended to cover explicit temperature dependence by introducing a temperature-dependent molecular field. Moreover, the model constitutes the basis for inclusion of the effect of chromophore-chromophore interaction.[1] In Figure 6 the in-phase spectrum of the electro-optic response of PMMA containing DR1 has been displayed at frequencies ω and 2ω, respectively. The dots represent experimental data and the full lines are obtained by fitting the data using the present model.

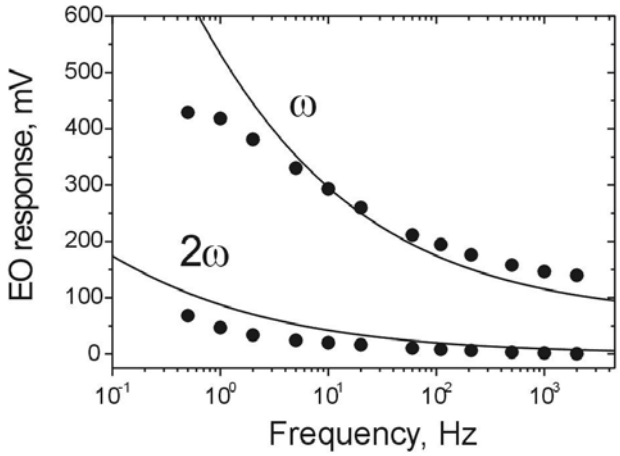

Figure 6. In-phase spectrum of the electro-optic response of PMMA containing DR1.

In addition, the time-dependent birefringence of a polymer-based electro-optic material has been investigated experimentally using ellipsometry.[2] It was shown experimentally that choosing poling times for different poling voltages makes it possible to reach the same level of birefringence in a chromophore-doped polymer. The investigations of turn-on and turn-off behaviour from a common level revealed that at least two processes occur simultaneously when chromophores align or the alignment relaxes. The fast process depends only little on the poling voltage in turn-on experiments and not at all in a turn-off process. This process is, furthermore, insensitive to temperature changes. The slow process, on the other hand, depends highly on both the poling time and temperature. The fast process is explained by a

local deformation of the matrix polymer by the chromophores, whereas the slow process represents a long-range deformation.

1. K. G. Jespersen, T. G. Pedersen and P. M. Johansen, J. Opt. Soc. Am B Vol. 20, 2179 (2003).
2. D. Apitz, C. Svanberg, K. G. Jespersen, T. G. Pedersen and P. M. Johansen, J. Appl. Phys. Vol. 94, 1 (2003).

2.3.2 Transport and polymer light sources

P. Kjær Kristensen (also at University of Aalborg, Denmark) T. G. Pedersen (Institute of Physics, University of Aalborg, Denmark) and P. M. Johansen
per.michael.johansen@risoe.dk

Intense research in organic polymers for applications in the fields of optoelectronics, solar cells and light emitting diodes is carried out these years in practically all the western industrialized countries. Just imagine being able to produce an electro-optic modulator at the telecommunication wavelength in plastics or being able to fabricate large-area colour displays of high contrast in an organic material. Conducting polymers belong to the group of spatially disordered materials. Conjugated polymers like PPV have a backbone that consists of alternating single and double carbon-carbon bonds. The overlap of the π orbitals forms a continuous system of electron density along the backbone. The extent of this overlap together with the bond alternation determines the HOMO-LUMO band gap (HOMO: Highest Occupied Molecular Orbital; LUMO: Lowest Unoccupied Molecular Orbital). PPV and derivates thereof are of great interest since they are capable of emitting in the range from the near infrared to the ultraviolet. The wavelength of emission depends on the extent of conjugation and can be controlled by modification of the chemical structure by adding various functional groups such as, e.g., adding of the MeH-group to improve material solvability. Currently, we are in the process of establishing a platform for fabrication, testing and modelling PLED devices. On the long-term basis we plan on incorporating complexes for infrared emission into the polymers. In Figure 7 we have displayed our own first results observed with PPV and PF diodes fabricated in our labs.

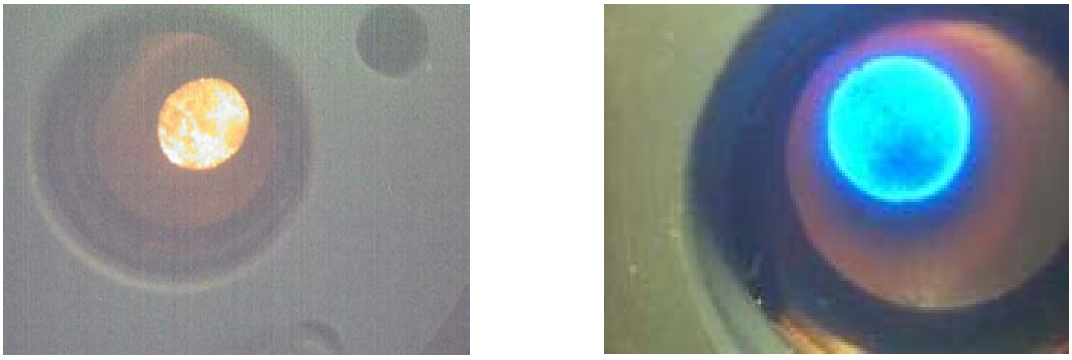

Figure 7. Digital camera pictures of diodes fabricated from PPV and PF shown in the left and right picture, respectively.

1. P. K. Kristensen, T. G. Pedersen and P. M. Johansen, DOPS-NYT Vol. 2, 9 (2003).

2.4 Laser ablation and pulsed laser deposition

2.4.1 Plume dynamics of UV laser ablation of silver in vacuum with fs pulses

B. Toftmann (also at Southern University of Denmark, Odense, Denmark), J. Schou, C. Budtz-Jørgensen and J. Lunney* (*Physics Department, Trinity College, Dublin, Ireland)*
j.schou@risoe.dk

The dynamics of the ablation plume expansion in *fs* laser ablation of solids is important for micromachining, microanalysis and thin film production by laser. Moreover, knowledge of the velocity and the angular distribution of the ablation plume particles yields useful information for developing a physical understanding of *fs* laser ablation. We have studied the angular shape and the ion time-of-flight (TOF) distribution of the plasma plume ions as well as the total ablation yield for *fs* UV ablation of a pure silver target in vacuum. This study is similar to previous experiments on *ns* laser ablation of silver.

The experiments were carried out at the *fs* UV facility at IESL-FORTH on Crete, Greece, using a 500 fs laser pulse at 248 nm. A semicircular array of 13 planar (2×2 mm^2) Langmuir probes in horizontal plane at a distance of 80 mm from the target was used to measure the angular variation of the TOF spectra of the ablated ions. The angular variation of the deposition was found by measuring the optical transmission of a thin film deposited on a transparent flexible substrate.

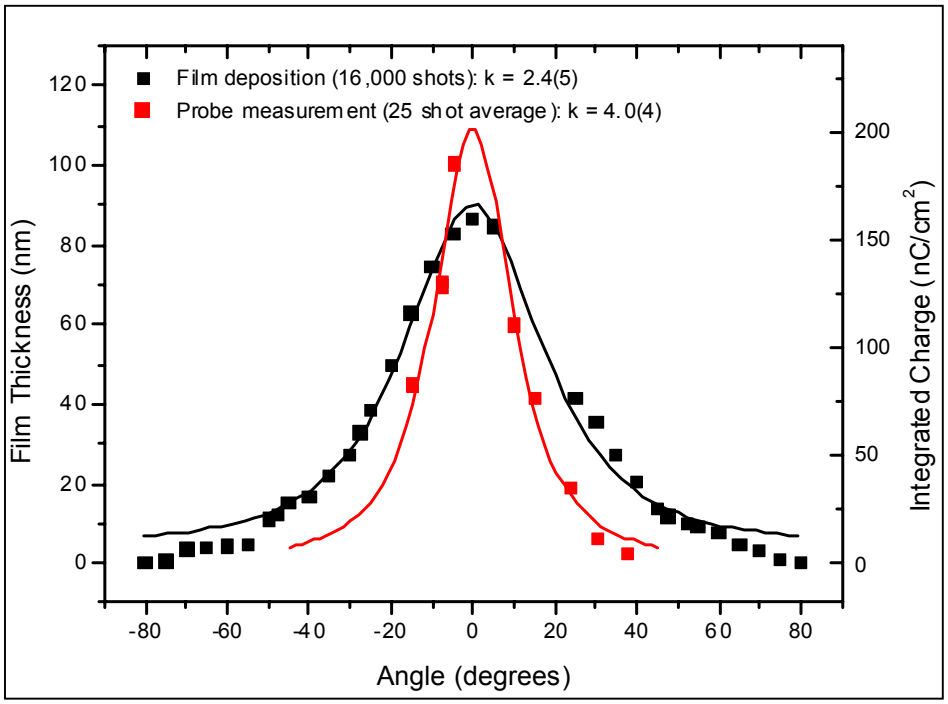

Figure 8. The angular distribution of ions (narrow peak) and of the total flow (e.g. ions and neutrals) (broad peak) for laser ablation at 248 nm with 500 fs pulses.

The angular distribution of the ions (red curve) and the total distribution of ions and neutrals (black) are shown in Figure 8. The distribution of ions is clearly more peaked in forward direction. The beam spot on target was 0.35 mm × 0.6 mm, and the laser fluence was varied in the range 0.1 to 2.0 J/cm^2.

2.4.2 Deposition of polyethylene glycol by matrix-assisted pulsed laser evaporation

K. Janik, B. Toftmann (also at Southern University of Denmark, Odense, Denmark), J. Schou and R. Pedrys* (*Physics Department, Jagiellonian University, Krakow, Poland)*
bo.toftmann.christensen@risoe.dk

For many years it has been possible to make high-quality thin films of hard materials by pulsed laser deposition (PLD). In this process UV light energy is coupled into a target material at such a high rate that a thin volume of the irradiated material will evaporate or explode away. Then the ablated atoms are collected for film growth on a suitable substrate. Soft materials generally need to be treated much more gently, since they otherwise decompose and create films without the desired functionality. To overcome this problem, we have deposited material by matrix-assisted pulsed laser evaporation (MAPLE). By this method the organic material is dissolved in an appropriate solvent and subsequently frozen into a matrix. Usually, this matrix is irradiated at a comparatively low fluence whereby the solvent evaporates and the organic material is collected on a suitable substrate.

We have made deposition of the biotechnically important polyethylene glycol (PEG), in this case with an average molecular weight of 1500 a.m.u., and have studied how the deposition rate depends on deposition parameters like target temperature, laser spot size and solvent. Also the deposition yield as a function of PEG concentration in water has been measured using a quartz crystal microbalance as detector. The results of these measurements are shown in Figure 9 where the yield is expressed as the number of equivalent deposited molecules. However, the chain length of the deposited material has not yet been measured.

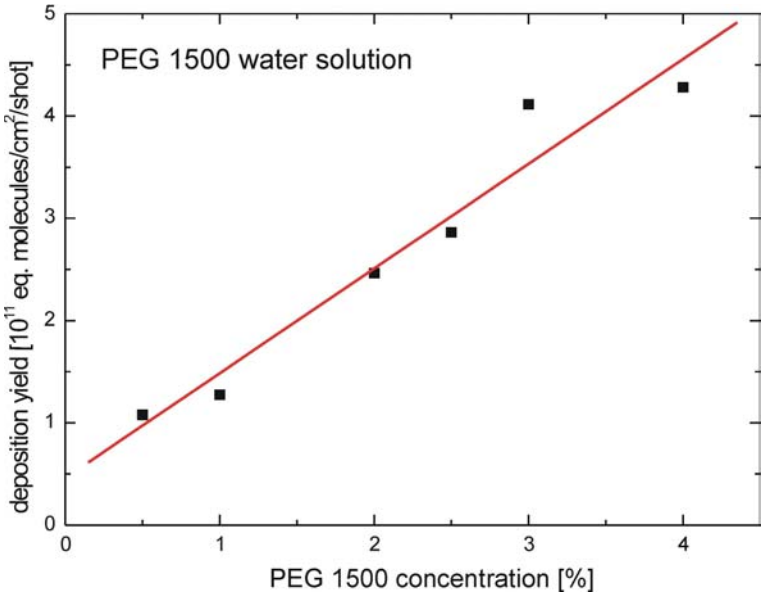

Figure 9. The deposition yield of PEG plotted as a function of the PEG concentration in water ice. Laser wavelength: 355 nm (6 ns); spot size: 0.8 mm^2; target temperature -50^0 C; laser fluence: 6 J/cm^2.

2.4.3 Large-area pulsed laser deposition

J. Schou, B. Toftmann (also at University of Southern Denmark, Odense, Denmark), N. Pryds and Søren Linderoth* (*Materials Research Department, Risø National Laboratory, Denmark)*
j.schou@risoe.dk

Pulsed laser deposition (PLD) is a newly established method for producing thin films of a thickness ranging from a fraction of a nanometer up to more than a few μm. One advantage of PLD is that even films of complicated stoichiometry, e.g. oxides or nitrides, can relatively easily be produced. Typically, the films are manufactured from laser irradiation of one or more pressed targets, so that mono- or multilayers can be deposited with well-known or completely new composition. Another advantage is the high kinetic energy with which the ablated atoms arrive at the growing film surface, which leads to films of a high crystalline quality even for substrates at room temperature.

Figure 10. Photograph of the new set-up.

A new large-area PLD facility will be established at Risø. The Danish Technical Research Council has supported this facility with a major grant. The new PLD system offers the possibility of increasing the size of the film from 1 cm^2 to more than 100 cm^2, which means that large-area films, for example for solid oxide fuel cells, can be manufactured. The system will be computer-controlled and is in many respects superior to the existing set-up: The substrate can be heated to 900 K, several targets are available in the same deposition sequence (gives the possibility of making new multilayer structures), and there is a load-lock so that interchange of target and substrates is fast. The film production is performed with an excimer laser with a power of 80 W (40 times more than the present Nd:YAG laser). The pulse repetition frequency is 200 Hz compared with 10 Hz for the existing laser at Risø. In addition, the new laser operates at 248 nm which is generally more efficient for producing ablation than the present one (at 355 nm).

The system is expected to be delivered from the manufacturer in the beginning of May 2004 and will be fully operating in the summer 2004.

2.5 Optical sensors

2.5.1 Absolute refractive index determination by micro-interferometric backscatter detection

H. S. Sørensen (also at Dept. of Manufacturing Engineering and Management, Technical University of Denmark, Denmark), H. Pranov (Dept. of Manufacturing Engineering and Management, Technical University of Denmark, Denmark), N. B. Larsen (Danish Polymer Centre, Risø National Laboratory, Denmark), D. J. Bornhop (Department of Chemistry, Vanderbilt University, Nashville, TN, USA) and P. E. Andersen
henrik.schioett.soerensen@risoe.dk, henrik.pranov@risoe.dk, niels.b.larsen@risoe.dk, darryl.bornhop@vanderbilt.edu, peter.andersen@risoe.dk

It is of great interest to be able to measure small changes in the refractive index in small volumes of fluid. This may be achieved by using the micro-interferometric backscatter detection (MIBD) scheme,[1] which is based on a simple optical system. MIBD is universal since the refractive index varies with a wide range of parameters. Changes in temperature, concentration and pressure may be detected inside a small volume of the liquid by this method. MIBD has previously been shown capable of measuring changes in the refractive index of liquids in the order of 10^{-7}.[2] The MIBD technique is based on interference of laser light after it has been reflected from different regions in a capillary. These reflections generate an interference pattern that moves upon changing refractive index of the liquid in the capillary. The small angle interference pattern traditionally considered has a repetition frequency in the refractive index space that limits the ability to measure refractive-index-to-refractive index changes causing one repetition. Such refractive index changes are typically in the order of three decades. Recent modelling and experiments with the MIBD technique has shown that other intensity variations in the pattern are present for larger backscattered angles.[3,4]

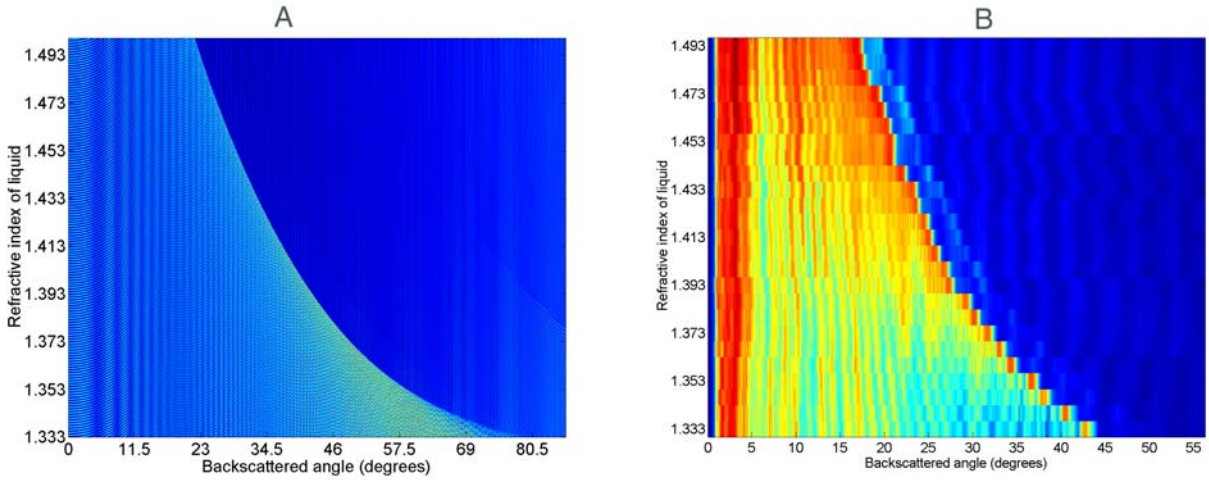

Figure 11. Simulated (A) and experimental (B) interference pattern.

By considering these variations we have shown two methods by which it is possible to extend the dynamic measurement range to make an absolute refractive index measurement. One method utilizes variations in the Fresnel coefficients while the second approach is based on the refractive index dependent onset of total internal reflection angles.[3] The model predicts an abrupt change in intensity that moves towards lower backscatter angles as the refractive

index of the liquid approaches the one of the glass tubing, see Figure 11A. This feature of the interference pattern has also been observed experimentally, see Figure 11B, and it agrees with the predicted feature in position refractive index space within experimental error. From our experiments, the precision of the absolute determination of the refractive index is found to be 2.5 10^{-4} with the refractive index in the range of 1.33 to 1.5. With our current technique and set-up, we are able to perform an absolute refractive index measurement with accuracy on this level on a 180 nL volume. The main limitations for accuracy such as temperature control and detector resolution are the same as for conventional MIBD. The theoretical limit using this approach is therefore similar to the limit achievable by conventional MIBD and it is possible to perform a conventional MIBD measurement simultaneously to our newly proposed method. In principle, if the dimensions and the refractive index of the capillary tube are known, then there is a one to one relationship between the backscatter angle and the refractive index of the liquid enabling determination of the absolute refractive index.

1. D. J. Bornhop, Appl. Opt. **34**, 3234-3239 (1995).
2. K. Swinney, D. Markov and D. J. Bornhop, Rev. of Scien. Instruments **71**, 2684-2692 (2000).
3. H. S. Sørensen, H. Pranov, N. B. Larsen, D. J. Bornhop and P. E. Andersen, Anal. Chem. **75**, 1946-1953 (2003).
4. H. S. Sørensen, H. Pranov, P. E. Andersen and D. J. Bornhop, Patent application (US), PCT/US03/25849.

2.5.2 Reverse-symmetry multimode waveguide

N. Skivesen (also at University of Copenhagen, Copenhagen, Denmark),
R. Horváth and H. C. Pedersen
nina.skivesen@risoe.dk, robert.horvath@risoe.dk, henrik.pedersen@risoe.dk

Planar optical waveguides can be used as optical sensors to detect changes in the media that surround the waveguide as the eletromagnetic field propagating in the waveguide will extend into the surrounding media as an evanescent eletromagnetic field. The refractive index of the surrounding media will thereby contribute to the effective refractive index detected by the waveguide. Planar optical waveguides can for example be used for biological applications detecting the change in refractive index due to the adhesion of bacterial substances to the sensor surface. A waveguide consists of a substrate (S), a waveguiding film (F) and a cover medium (C), where the cover medium is the substance to be characterized by determining the refractive index. It has been shown that the reverse-symmetry ($n_S<n_C$) waveguide is more sensitive than the normal-symmetry waveguide as the penetration depth of the evanescent wave in the cover medium is increased by the reverse symmetry [1].

We have developed a multimode planar optical waveguide with reverse symmetry for the use as a refractometer. To achieve reverse symmetry, air is used as substrate; hence, a free-standing waveguiding film. Because of this, the waveguiding film has to be mechanically stable which is difficult to achieve with a monomode waveguide that is a few 100 nm thick. However, by using a multimode waveguide with a film that is about 100 times thicker, the mechanical stability is significantly increased and at the same time an easier fabrication of the waveguide is achieved.

The waveguiding film used is a simple glass plate that is 50 µm thick. The glass plate is coated with a 40 nm thick polymer grating layer and air is used as substrate material, thus a freestanding waveguide. Experiments for determining changes in the refractive index of the cover medium have been carried out by using different concentrations of NaSCN-solutions.

In Figure 12 the intensity measurements for three different aqueous solutions are shown. The peaks in the spectra correspond to the guided modes in the waveguide. As the refractive index of the solution changes, the number of guided modes changes. By detecting the coupling angle of the highest order mode, the refractive index of the solution can be determined, see Figure 13. The developed sensor has a measuring range between the refractive index of the substrate and of the film, which gives a detection range from 1-1.52 and a resolution that varies from 0.007 to $5x10^{-5}$ depending of the refractive index of the cover solution [2].

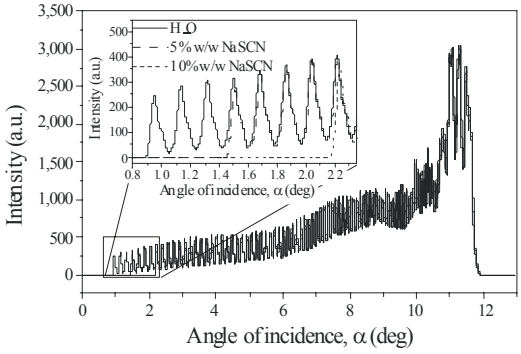

Figure 12. Measured intensity spectra for water, 5% w/w and 10% w/w NaSCN.

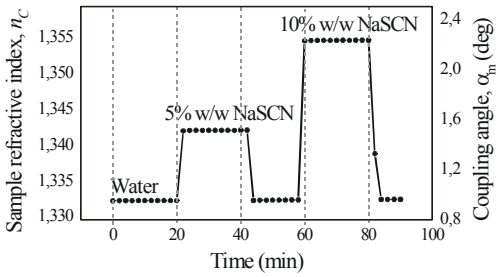

Figure 13. Measured coupling angle and corresponding n_C.

1. R. Horváth, L. R. Lindvold and N. B. Larsen, Appl. Phys B **74**, 383 (2002).
2. N. Skivesen, R. Horváth and H.C. Pedersen, Opt. Lett. 28 (24), 2473 (2003).

2.5.3 Holographic design of integrated surface-plasmon resonance sensor chip

H. C. Pedersen and C. Thirstrup (Vir Biosensor, Vir A/S, Denmark)
henrik.pedersen@risoe.dk

A new integrated design of a surface-plasmon resonance (SPR) sensor has been developed. As opposed to the conventional Kretschmann configuration in which a laser beam is focused via a lens and a prism at a metal-coated glass slide and recollimated via a second lens to reach a CCD camera, the present design comprises a simple planar injection moulded polymer chip with focusing gratings and metal coating integrated in the surface of the chip. With the integrated design, all light coupling and focusing is achieved without lenses or prisms, and because of the very inexpensive manufacturing process the sensor chip can be made disposable.

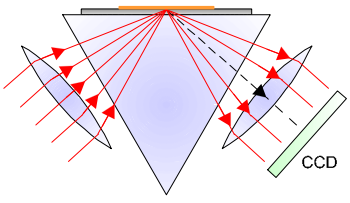

Figure 14. Conventional Kretschmann SPR sensor configuration.

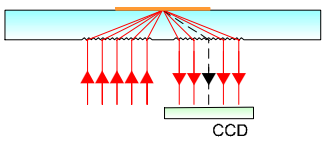

Figure 15. New integrated SPR sensor chip design.

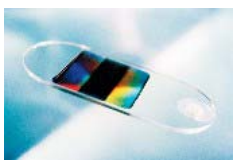

Figure 16. Injection moulded SPR sensor chip.

The two focusing coupling gratings are mastered holographically by recording the interference between two HeCd laser beams in photoresist. However, since the diffraction angles have to span the expected SPR angular range, which assumes values of up to 77 deg, the resulting holographic gratings appear to be far from paraxial. This implies that the classical holographic design techniques reported by Latta[1,2] in the early 1970's are pushed far beyond the paraxial limit and therefore break down. It has therefore been necessary to develop an alternative design algorithm to achieve a sufficiently accurate chip in the grating profiles. The new algorithm is based on matching the local grating spacing of the recording interference pattern to the desired grating spacing in the injection moulded sensor chip. This is opposed to the classical method that is based on aberration balancing. The new design algorithm was demonstrated to have superior performance for the design of non-paraxial holograms.[3]

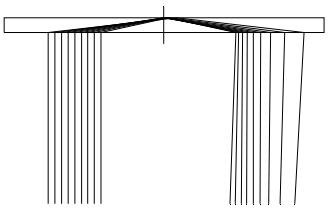

Figure 17. Ray trace of sensor chip with aberration balanced holograms.

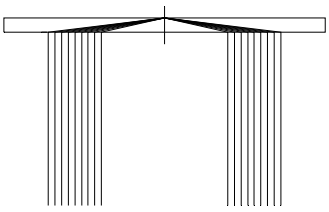

Figure 18. Ray trace of sensor chip with grating-matched holograms.

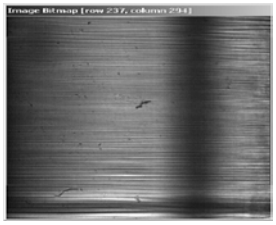

Figure 19. CCD image of SPR dip.

1. J. N. Latta, "Computer-based analysis imagery and aberrations. I. Hologram types and their nonchromatic aberrations," Appl. Opt. **10,** 599-608 (1971).
2. J. N. Latta, "Computer-based analysis imagery and aberrations. II. Aberrations induced by a wavelength shift," Appl. Opt. **10,** 609-618 (1971).
3. H. C. Pedersen and C. Thirstrup, "Design of near-field holographic optical elements by grating matching", to appear in Appl. Opt.

2.5.4 Waveguide sensor for on-line monitoring of bacteria with increased probing depth

R. Horváth, H. C. Pedersen, N. Skivesen (also at University of Copenhagen, Copenhagen, Denmark), D. Selmeczi and N.B. Larsen* (*Danish Polymer Centre, Risø National Laboratory, Denmark)*
robert.horvath@risoe.dk and henrik.pedersen@risoe.dk

In recent years, sensor systems for the detection of pathogenic bacteria have received renewed interest, especially within the fields of food safety, medical diagnostics and biological warfare. This interest is due to the increasing number of illnesses caused by bacteria which account for up to 40% of the 50 million annual deaths worldwide. The main goal of the new sensor systems has been to encompass a rapid alternative to the very time-consuming culturing methods that usually require several days to give a result.

Grating coupled planar optical waveguides have been used for many biosensing applications.[1] In these sensors, the electromagnetic field of the modes interacts with the analyte layer (for example: protein layer) deposited on the surface of the sensor. Because the optical evanescent field decays exponentially from the sensor surface into the sample volume, only changes within the penetration depth of the evanescent field are probed. Under normal conditions, this penetration depth has an upper limit of 100 – 200 nm. Thus, for a bacterial

cell of typically 1-3 μm in size, only a small fraction is actually probed by the evanescent field which results in severe reduction in sensitivity.

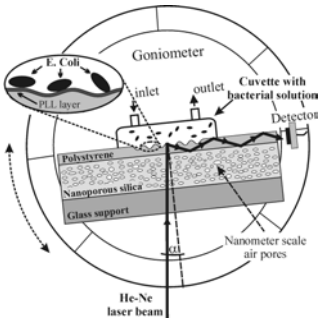

Figure 20. Reverse symmetry waveguide sensor.

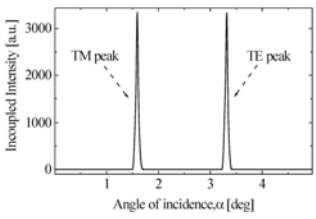

Figure 21. Incoupled light intensity versus angle of incidence.

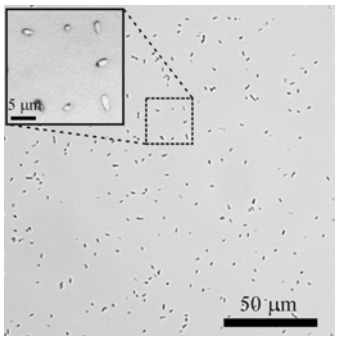

Figure 22. Microscope image of the waveguide surface after *E. Coli* attachment.

In our novel waveguide sensor design, the use of a nanoporous silica substrate layer which supports the waveguiding film and which has a refractive index smaller than that of water implies that the penetration depth of the evanescent field has no upper limit.[2-3] This design makes it possible to increase the penetration depth of the evanescent field to cover micron-scale biological objects and also places a higher amount of relative electromagnetic mode power into the sample volume, resulting in increased sensitivity. By using *E. coli K12* cells to test the sensor detection limit of 60 cells/mm^2 has been demonstrated.[4]

1. J. Voros, J. J. Ramsden, G. Csucs, I. Szendro, S. M. de Paul, M. Textor and N. D. Spencer, "Optical grating coupler biosensors," Biomaterials, **23,** 3699 – 3710 (2002).
2. R. Horvath, L. R. Lindvold and N. B. Larsen, "Reverse-symmetry waveguides: theory and fabrication," Applied Physics B **74**, 383 – 393 (2002).
3. R. Horvath, H. C. Pedersen and N. B. Larsen, "Demonstration of reverse symmetry waveguide sensing in aqueous solutions," Appl. Phys. Lett. **81**, 2166 - 2168 (2002).
4. R. Horvath, H. C. Pedersen, N. Skivesen, D. Selmeczi and N. B. Larsen, "Optical waveguide sensor for on-line monitoring of bacteria," Opt. Lett. 28, 1233 - 1235 (2003).

2.6 Holographic storage

2.6.1 Photoinduced anisotropy in a family of amorphous azobenzene polyesters for optical storage

L. Nedelchev (Central Laboratory of Optical Storage and Processing of Information, Sofia, Bulgaria), A. Matharu (Division of Chemistry, Nottingham Trent University, Nottingham, England), S. Hvilsted (Department of Chemical Engineering, Technical University of Denmark, Lyngby, Denmark) and P. S. Ramanujam
p.s.ramanujam@risoe.dk

We investigate parameters associated with optical data storage in a variety of amorphous side-chain azobenzene-containing polyesters, denoted E1aX. The polyesters possess a common cyano-substituted azobenzene chromophore as side chain, but differ in their main-chain polyester composition. Seventeen different polymers from the E1aX family divided into four classes, depending on the type of the main-chain substituent (one-, two-, three-ring aromatic or alicyclic), have been thoroughly investigated.[1] Various parameters characterizing the

photoinduced birefringence in these materials such as response time, thermal and light stability and long-term stability under ambient light at room temperature have been measured. Each of these parameters is quantitatively represented and it is therefore possible to make a clear comparison between the properties of the polymers. The results indicate that the long-term stability at ambient temperature is closely related to the thermal stability of the photoinduced birefringence. A strong correlation has also been found between the response time and the stability of the induced anisotropy towards illumination with unpolarized white light. One of the classes of E1aX polymers characterized by a two-ring aromatic substituent in the main chain is a good candidate for optical data storage media, see Figure 23. Recording energy of approximately 2 J/cm^2 is sufficient to induce high refractive index modulations of Δn = 0.13 in these materials, which is retained even at elevated temperatures (> 130 °C). Long-term stability, i.e. more than one year, for the induced anisotropy has also been achieved.

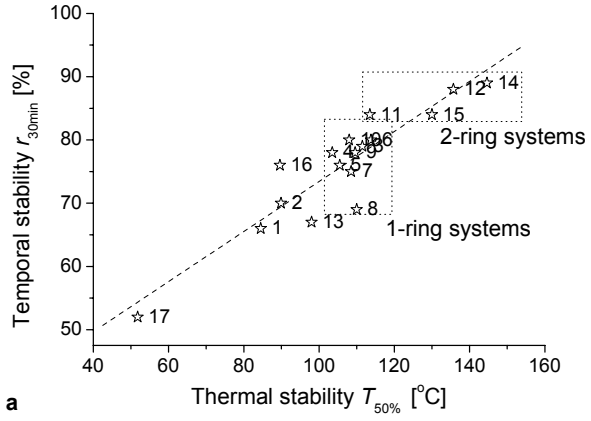

Figure 23. Dependence between the different parameters describing the behaviour of the photoinduced anisotropy in the E1aX polymers: (a) temporal vs. thermal stability.

1. L. Nedelchev, A. Matharu, S. Hvilsted and P. S. Ramanujam, *Appl. Opt.* **42**, 5918-5927 (2003).

2.6.2 Polarization holographic and surface relief gratings at 257 nm in an amorphous azobenzene polyester

L. Nedelchev (Central Laboratory of Optical Storage and Processing of Information, Sofia, Bulgaria), A. Matharu (Division of Organic Chemistry, Nottingham Trent University, Nottingham, England) and P. S. Ramanujam
p.s.ramanujam@risoe.dk

Polarization holographic and surface relief gratings have been recorded in an amorphous azobenzene polyester using a frequency doubled argon ion laser beam at 257 nm.[1] Higher excited states of azobenzene in the *trans* and *cis* configurations contribute to the formation of diffraction gratings in this experiment. A combination of right and left circularly polarized writing beams has been found to give the highest diffraction efficiency. The contributions to the total phase difference arising from anisotropy and surface relief have been separated experimentally (see Figure 24), and it has been shown that the surface relief grating contributes a larger phase difference than that due to anisotropy.

1. P. S. Ramanujam, L. Nedelchev and P. S. Ramanujam, *Opt. Lett.* **28**, 1072-1074 (2003).

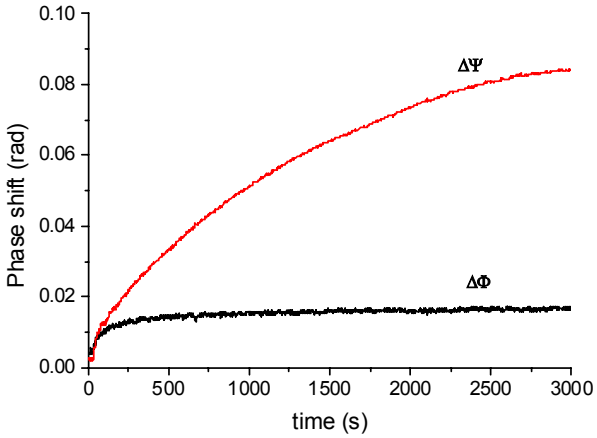

Figure 24. Phase difference induced in E1aP due to anisotropy ($\Delta\phi$) and surface relief ($\Delta\psi$).

2.6.3 Evanescent polarization holographic recording of sub 200 nm gratings in an azobenzene polyester

P. S. Ramanujam
p.s.ramanujam@risoe.dk

High-resolution polarization holographic recording with evanescent waves in a thin film of an azobenzene polyester deposited directly on the hypotenuse of a high refractive prism has been demonstrated.[1] A spatial frequency of more than 7000 lines/mm and a diffraction efficiency larger than 1% have been achieved, see Figure 25. It has been found that the diffraction efficiency increases in the dark after the writing beams have been switched off. The biphotonic effect found in other azobenzene polymers, which converts *cis* states of the azobenzene to *trans* states followed by an ordering process due to aggregation, is proposed as the reason for this increase in diffraction efficiency.

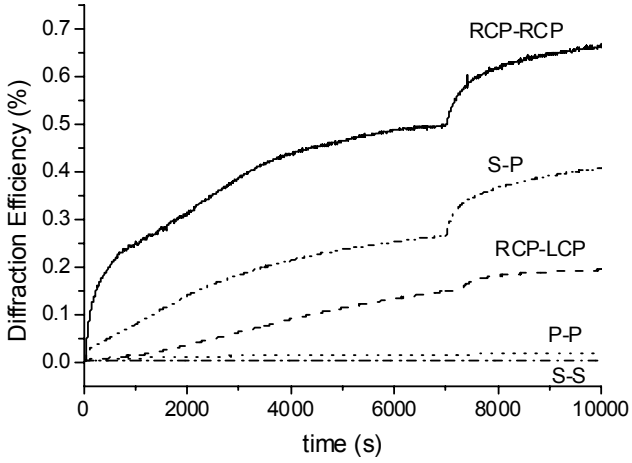

Figure 25. Diffraction efficiency at 633 nm at various polarization combinations of the write beams at 488 nm. The write laser is switched off after 7000 s. The diffraction efficiency is measured at 633 nm.

1. P. S. Ramanujam, *Opt. Lett.* **28**, 2375-2377 (2003).

2.7 Collaboration with Danish and foreign universities

2.7.1 Center for Biomedical Optics and New Laser Systems – BIOP

P. Michael Petersen, P. E. Andersen and T. M. Jørgensen
paul.michael.petersen@risoe.dk, peter.andersen@risoe.dk, thomas.martini@risoe.dk,
www.biop.dk

The Center for Biomedical Optics and New Laser Systems (BIOP), established in 2000, is a Danish initiative where engineers, physicists, chemists and physicians collaborate on the development of new biomedical applications based on the most recent progress in lasers and optical measurement techniques. The aim of the centre is to conduct research and develop advanced laser systems and optical measurement technologies, and to apply these systems within dermatology, ophthalmology and biosensing.

The main purposes of the BIOP research programme are (i) to demonstrate and develop state-of-the-art diagnostic procedures and (ii) to improve therapeutic facilities at Danish hospitals. The collaboration has resulted in the development of novel biomedical applications of modern laser technology, including three-dimensional imaging in human tissue, blood flow visualization, non-invasive spectroscopy and fluorescence measurements for diagnostics and biosensors for measurements of concentrations of, e.g., glucose and protein. As an example, new frequency lasers for diagnostics have been developed (see Figure 26 and 2.2.2).

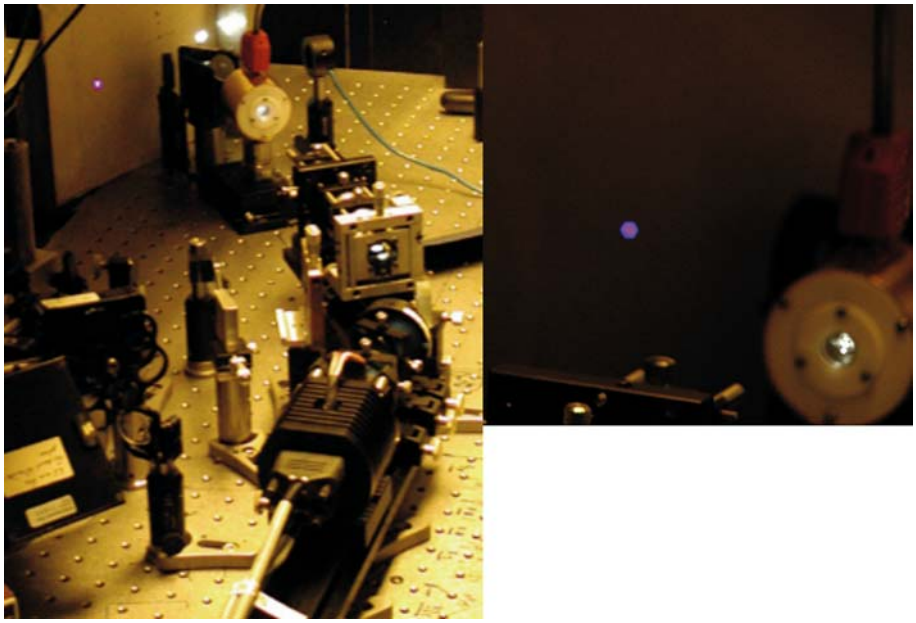

Figure 26. The laser running with single-pass frequency doubling in PP-KTP (405 nm out is viewed as the blue dot on the screen).

In the BIOP centre the following five focus areas have been selected:

- Biomedical imaging systems
- New laser systems for diagnostic and therapeutic applications
- Optical tweezers systems
- Bio-sensing
- Biomedical image and data processing

Education in BIOP

Young scientists are offered coordinated training and education at MSc and PhD levels within the areas of laser technology, imaging, medicine and biotechnology through undergraduate courses and graduate schools, see also BIOP Graduate School. One of the objectives of this approach is that the education of PhD students takes place in close cooperation with the Danish business sector. The PhD projects carried out in BIOP are all structured as interinstitutional collaborative efforts. Moreover, permanently employed members of staff are given the possibilities of using facilities at other institutions and of participating in the education programme - an initiative that contributes to further strengthening of mobility.

Participants

Partners who hold strong positions in their own fields participate in BIOP. The following partners participate in BIOP:

- Department of Dermatology, Aarhus Amtssygehus, University of Aarhus
- Department of Mathematical Modelling, Technical University of Denmark
- Department of Ophthalmology, Herlev Hospital, University of Copenhagen
- Department of Physics, Technical University of Denmark
- Optics and Fluid Dynamics Department, Risø National Laboratory
- Research Center COM, Technical University of Denmark

Located in the vicinity of Copenhagen, BIOP has strong collaboration with Lund Institute of Technology and Lund Medical Laser Centre, Lund (Sweden)

Another important aspect of BIOP is to establish collaboration with industrial partners through joint projects in which the developed technology is transferred to the industrial partner. Such collaborative projects may involve PhD students who participate in the research projects at the premises of the industrial partners as well as at the involved research institution.

2.7.2 VELI – Virtual European Laser Institute

P. E. Andersen and P. M. Petersen
peter.andersen@veli.net, paul.michael.petersen@veli.net, www.veli.net, www.eli-online.org

In 2001, a multidisciplinary Virtual European Laser Institute (VELI) was formed with support from the European Commission in order to enhance and promote the available laser expertise in Europe. The BIOP Center (www.biop.dk) was invited to join VELI in order strongly to promote use of lasers and optical methods in the field of biophotonics.

The motivation for establishing VELI is to create one main portal through which access to experts in the fields of laser physics, technology and applications is enabled. Industry in general, but in particular small and medium sized enterprises may experience significant difficulties in reaching the enormous body of knowledge that exists at the various laser institutes across Europe. Moreover, from the point of view of industry, it is difficult to gain insight into the existing and available expertise in lasers and optical measurement technologies at the various dispersed laser centres. Therefore, a multidisciplinary Virtual European Laser Institute (VELI) was formed. The purposes of VELI are:

- to increase the transparency and knowledge of available laser expertise in Europe,
- to remove the current inefficiency (or lack) of exploitation of new laser knowledge and techniques,
- to create common agreements and procedures for knowledge transfer.

This European effort will achieve the critical mass in human and technological terms bringing together the expertise and resources needed and will thus enhance the competitiveness of European industry.

In the VELI network, the BIOP Center collaborates with 15 leading research institutions that have specialized in laser physics and applications of lasers. The wide variety of competencies of the participating scientists representing different disciplines support the creation of an outstanding state-of-the-art knowledge base on a European level, including advanced applications of lasers in biophotonics.

The major output of the VELI project is:

- A fully operational core network consisting of 15 leading professional laser institutes in Europe possessing core competencies in the fields of laser technology.
- A database containing state-of-the-art expertise, experience and knowledge formerly dispersed at various laser institutes. Moreover, the database also contains the gathered knowledge that has been generated from the extensive list of industrial needs at small and medium sized enterprises.
- A virtual surrounding, i.e. a site where the requests coming from the small and medium sized enterprises (industrial needs/demand) meet the available expertise and the wide array of possible applications of laser and laser technology (laser institute supply) speeding up the realisation of potentially new and highly competitive applications.

In accordance with the aims (see the first bullet in the list above), an important milestone was achieved during 2003 when the European Laser Institute (ELI) was founded. This new association is now operational and open to new members. The organization is responsible for the online laser portal and its contents are available at www.eli-online.org.

3. Optical diagnostics and information processing

3.1 Introduction

S.G. Hanson
steen.hanson@risoe.dk

During the last couple of years the impact of the research performed in the research programme has expanded from basic research into related areas and, in particular, into the area of applications. In this way innovation has become a key word that has been successfully pursued by the research programme. Two new companies launched in 2002 based on ideas and intellectual rights from Risø have in 2003 made great efforts to establish and maintain their positions. The outcome of their efforts will be revealed in the near future. An investigation has been conducted into the possibilities of further dissemination of latent ideas for industrial implementation. Some of these ideas may prosper in the years to come. A further indicator of our commitment to serve national interests and promote the visibility of our scientific achievements is our contribution to the Danish higher educational system. The research programme has addressed this aspect partly by being responsible for lectures at the Danish Technical University within the field of bio-optics (Graduate School on Biomedical Optics and New Laser Systems), partly by offering a lecture series on statistical optics at the University of Southern Denmark.

In addition to coping with the change in focus, the research programme has managed to increase the contribution to the scientific community by steadily augmenting the number of peer reviewed scientific articles, while at the same time being able to protect commercially attractive scientific ideas – two issues that are likely to provoke a conflict when they are to be addressed simultaneously. But as it has turned out that a mere delay in making the ideas public has been the result; basically, the protection of ideas does not give rise to a reduction in the number of articles.

A series of dissertation projects, primarily in the field of electronic processing, have been successfully conducted during the period. It is our feeling that not only have the students obtained a good supplement to their study, but we in the research programme have benefited strongly by their efforts. Another advantage of conducting lectures at the universities is the direct access to and frequent discussions with the students. This initiates interest in our work and mitigates the start of MSc projects.

An escalating increase in the use of infrared techniques in combustion and biological research has resulted in new and interesting projects, especially within the national PSO (Public Service Obligations) programme frame. Our capability within this field has resulted in Risø being appointed as the national reference site for non-contact temperature measurements, i.e. IR-calibration. In 2003 the laboratory for temperature calibration has been heavily involved in a project where the ability to perform low-temperature calibration has been crucial.

In the following, we will present some of the focal points of our optically related research that have taken place in 2003.

3.2 Biooptics

3.2.1 Bio-photonics: new lasers for diagnostic and therapeutic applications – BIOLASE

P. E. Andersen
peter.andersen@risoe.dk, www.bio-lase.dk

The frame programme "Bio-photonics: new lasers for diagnostic and therapeutic applications – BIOLASE" is a collaborative project between the Optics and Fluid Dynamics Department at Risø National Laboratory, COM at the Technical University of Denmark, the company Crystal Fibre A/S and the Department of Dermatology at Roskilde Regional Hospital. BIOLASE is funded for a five-year period from the Danish Technical Research Council under grant no. 26-02-0020 and was initiated in 2003.

One major reason for the high current and rapidly increasing research activities in the field of bio-photonics is that optics inherently has the potential of providing non-invasive diagnostic and therapeutic procedures, which may lead to novel and improved methods. The aim of BIOLASE is to combine fundamental research in nonlinear optics and lasers to create novel laser systems and light sources for use in biomedical applications. The primary target is to develop laser systems for diagnostic purposes in collaboration with medical doctors, thus incorporating their needs and requirements at the earliest stage in the developmental process. The primary target for the clinical applications in BIOLASE is within the field of dermatology.

In the short term, BIOLASE will provide novel biomedical applications, such as ultrahigh-resolution imaging of skin tissue, fluorescence-based diagnosis of cancerous lesions and skin diseases, new laser-based treatment procedures of skin cancer and fibre-optic delivery of high-power treatment light. The essential component to ensure such development is the light source. BIOLASE therefore enhances research in advanced laser systems and light sources, and simultaneously points out new areas for applications of lasers. Furthermore, the programme also provides education of scientists highly specialized in optics, engineering and medical science.

In the long term, new diagnostic and therapeutic procedures will emerge from the joint efforts of the collaborators. Hence, the interdisciplinary collaboration provides a firm basis for transferring results from basic research to applications, which is emphasized by the participation of the company Crystal Fibre A/S.

In 2003, two PhD-projects funded directly by BIOLASE were initiated: one project anchored at the Optics and Plasma Research Department focused on developing a high-power, frequency doubled diode laser system for fluorescence diagnostics of cancer, and one project anchored at COM on developing a broad-bandwidth white-light source based on photonic crystal fibres (PCFs) for optical coherence tomography (OCT). Furthermore, BIOLASE had a femtosecond laser installed. This source, which has an ultra-high bandwidth itself, is to be used for two main projects within BIOLASE: firstly, to be used as a pumping source for white-light sources based on PCFs and, secondly, to be used in an ultra-high resolution OCT system centred at 800 nm. An example of white-light generation using the femtosecond laser for pumping a PCF is shown in Figure 27.

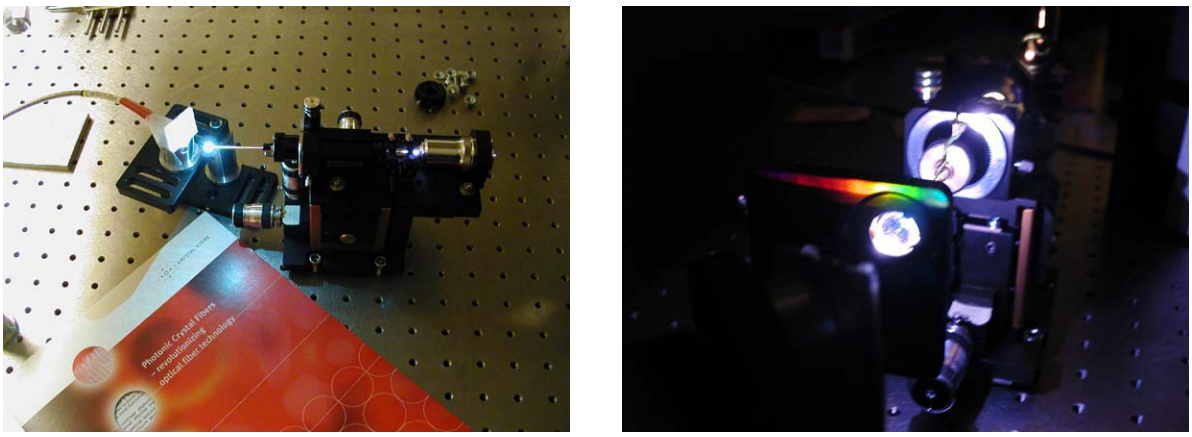

Figure 27. White-light generation by using a femtosecond laser to pump a photonic crystal fibre.

3.2.2 BIOP Graduate School: "Biomedical Optics and New Laser Systems"

P. E. Andersen and T. M. Jørgensen
peter.andersen@risoe.dk, thomas.martini@risoe.dk, www.biop.dk/graduateschool/

The BIOP Graduate School: "Biomedical Optics and New Laser Systems" has been formed under the BIOP centre, which is part of collaboration between the Technical University of Denmark and Risø National Laboratory. The graduate school received funding from the Danish Research Agency under grant no. 643-01-0092 for a three-year educational programme, which started August 2002.

The BIOP Graduate School is administered by the BIOP centre. The school is supervised by a board that coincides with the board of the BIOP centre. Professor Preben Buchhave, Dept. Physics, Technical University of Denmark, heads the graduate school and he is also a member of the board of the BIOP centre. The school board has appointed Peter E. Andersen from Risø National Laboratory school director along with a management team.

The purpose of the BIOP graduate school is to strengthen the educational efforts within the area of biomedical optics in Denmark emphasizing use of lasers and optical methods for diagnostics, manipulation and therapy. In this new interdisciplinary research area, the focus of the school will be on strengthening research activities and educational efforts and on enhancing collaboration between the fundamental physical and technical sciences and the medical, clinical and biological sciences.

Therefore, the graduate school supports PhD projects, conferences, graduate summer schools, visiting scientists and exchange students within the areas of the school.

Areas of the graduate school

The following list, although not exhausted, shows the main research and educational areas for the graduate school:

- Laser physics, laser technology and non-linear optics for biological and medical applications
- Inference based on mathematical processing of spatial and temporal structures
- Advanced data and image processing
- Optical sensors based on optical fibres and photonic crystal fibres for biological and medical applications
- Tissue optics and light propagation in tissue

- Optical excitation of biochemical processes
- Optical tweezers systems
- Lasers and optical methods for applications in ophthalmology
- Lasers and optical methods for applications in dermatology
- Lasers and optical methods for applications in cardiology

Graduate summer school: Bio-Photonics '03

One major event organized by the graduate school was the Graduate Summer School Bio-Photonics '03. The school was organized in collaboration with Lund Institute of Technology in Sweden and the school itself was located on the island of Hven. During one intense week, 50 graduate students and postdoctoral fellows in the field of biophotonics from 20 different countries attended lectures with ten internationally renowned lecturers from Europe and the US. The initiative caught the eye of several international associations, see e.g. the list of co-sponsors, and SPIE profiled the event in their monthly magazine.[1] The success of this first graduate school in this field has spurred interest in organizing a series of graduate schools. Therefore, the second school in the series has been announced to take place in June 2005.

More information on the recent Bio-Photonics '03 and the forthcoming Bio-Photonics '05 can be found at:

- Bio-Photonics '03: www.biop.dk/biophot03/
- Bio-Photonics '05: www.biop.dk/biophotonics05

Figure 28. Steven Jacques, Oregon Medical Laser Center, answers questions from students between lectures at the school.

1. OE Magazine, published by the International Society for Optical Engineering, Oct. issue 2003, p. 30. http://oemagazine.com/fromTheMagazine/oct03/edu.html.

3.2.3 Optical coherence tomography in clinical examinations of skin cancer

L. K. Jensen (also at COM Center, Technical University of Denmark, Denmark), L. Thrane, P. E. Andersen, A. Tycho, F. Pedersen, S. Andersson-Engels (Department of Physics, Lund Institute of Technology, Lund, Sweden), N. Bendsøe (Department of Dermatology, Lund University Hospital, Lund, Sweden), S. Svanberg (Department of Physics, Lund Institute of Technology, Lund, Sweden) and K. Svanberg (Department of Oncology, Lund University Hospital, Lund, Sweden)
peter.andersen@risoe.dk

During recent years the incidence of skin malignancies has increased. For the non-pigmented lesions there are a number of treatment modalities. Since topical application of δ-aminolevulinic acid (ALA) was introduced, photodynamic therapy (PDT) has been considered one way of treating these tumours. However, there are some limitations when PDT is applied with distant surface illumination and topical sensitisation both from the ALA diffusion point of view as well as from light penetration. Therefore, it is of importance to determine the tumour thickness in the planning of the treatment. For example, for nodular basal cell carcinomas (nBCCs) it is often needed to apply PDT more than once. Another possibility is to perform cryosurgery, curettage or some other tumour thickness reducing modality before PDT. The clinical way to determine the thickness of a non-pigmented skin malignancy is to visualise and palpate the tumour area provided a punch biopsy has not been performed.

In this study,[1] a non-invasive way to visualise the tumour thickness by means of OCT[2] has been investigated. This study has been focused on basal cell carcinomas (BCC) as it is the most common type of non-pigmented skin cancer and, therefore, gives the possibility of obtaining thorough understanding of what the OCT images represent.[3]

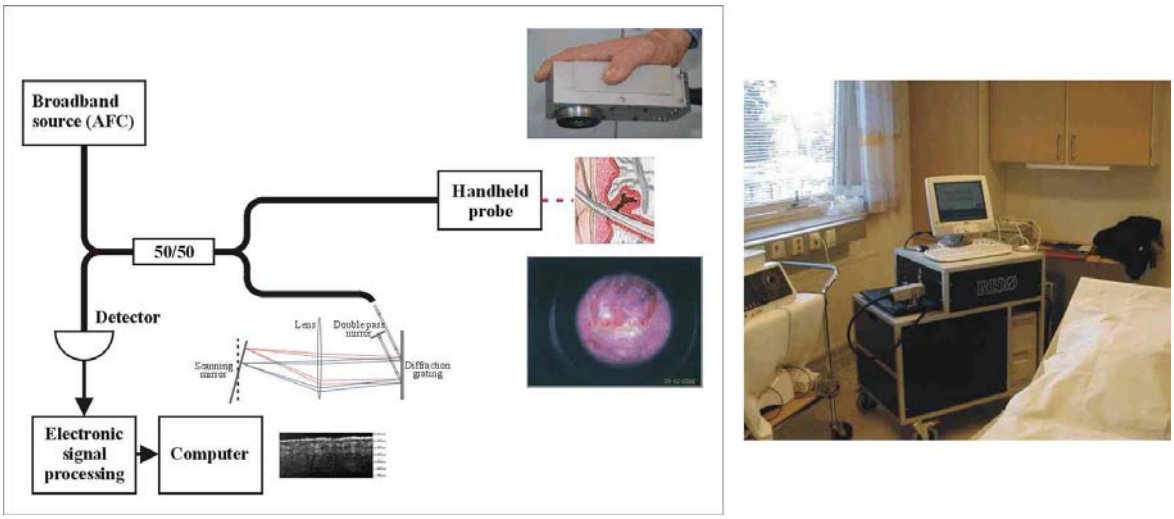

Figure 29 Left: Sketch of the mobile OCT system and compact handheld probe with integrated video camera. The pictures in the sketch demonstrate the size of the probe and show an example of a skin surface image from the video camera. Right: Picture of the mobile OCT system is shown in the clinic at the Department of Oncology at Lund University Hospital.

Images have been acquired using a mobile OCT system in the clinic, see Figure 29. A handheld probe with an integrated video camera was used to locate the lesion and acquire the OCT scan. Each cross-sectional OCT image is correlated with a video image of the skin surface, which helps to document the OCT images for later purposes. An example of a BCC lesion is shown in Figure 30A and for comparison healthy tissue (close to the lesion) is shown

in Figure 30B. As a BCC develops, it breaks down the layered structure of the healthy skin, which is clearly seen comparing Figure 30A and B, where Figure 30A shows a cancerous area with homogenous structure and Figure 30B shows an obvious layered structure indicating healthy skin tissue. In this preliminary study, we have shown that it is possible to distinguish a BCC lesion from healthy tissue in OCT images. Furthermore, as described in Ref. 1 other lesions may be identified non-invasively by OCT. These results hold promise for developing future versatile, clinical apparatus with high diagnostic impact.

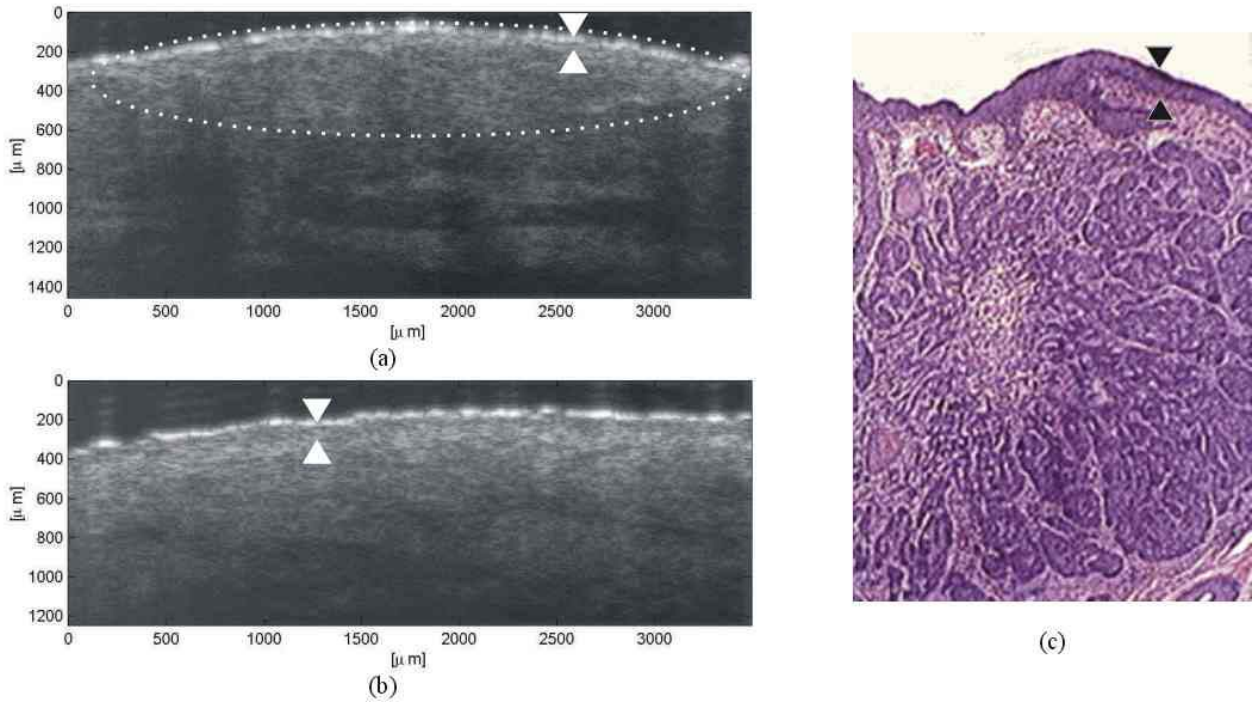

Figure 30. OCT images showing stratified BCC (a) marked with dotted ellipse, and healthy skin in the vicinity of the lesion (b). The triangles mark the thickness of the epidermis, and it is seen that though it is thinner in (a) than in (b) it is still intact. In (c) a histopathology of a similar stratified lesion is seen,[4] where the intact epidermis has also been marked (not correlated to (a) and (b)).

1. L. K. Jensen, L. Thrane, P. E. Andersen, A. Tycho, F. Pedersen, S. Andersson-Engels, N. Bendsøe, S. Svanberg and K. Svanberg, "Optical coherence tomography in clinical examinations of nonpigmented skin malignancies", Proc. SPIE **5140**, 160-167 (2003).
2. D. Huang, E.A. Swanson, C.P. Lin, J.S. Schuman, W.G. Stinson, W. Chang, M.R. Hee, T. Flotte, K. Gregory, C.A. Pulaifito and J.G. Fujimoto, Science, **254**, 1178 (1991).
3. J. Welzel, Skin Research and Technology, **7**, 1 (2001).
4. T.V. Rajan, M.D. UCHC, http://radiology.uchc.edu/code/1736.HTM.

3.2.4 Image processing tools for quantifying biofilm growth and structure

T. M. Jørgensen, A. Martiny, J. Haagensen* and S. Molin* (*Centre for Microbial Interactions, Biocentrum, Technical University of Denmark, Denmark)*
thomas.martini@risoe.dk

At the Molecular Microbial Ecology Group at Biocentrum DTU, physiological and structural interactions in multi-species biofilm communities are being investigated to bring important information about microbial interactions in heterogeneous environments. Another goal is to

gain a general understanding of biofilm development. During the last few years the fundamental knowledge built up within the group has been a platform for a currently increasing interest in microbial pathogenicity. The research is in particular focused on organisms that seem to be capable of shifting from a harmless environmental lifestyle to one associated with life-threatening infections.

The use of confocal laser scanning microscopy in combination with fluorescent probes is one important tool for studying the growth and development of biofilm structures. In order to quantify the development of the biofilm from the recorded time series of 3D images, adequate image processing and visualization algorithms are needed. The present project has focused on implementing software tools for this purpose by developing segmentation algorithms and quantification measures based on mathematical morphology (see Figure 31). The work includes the development of automatic thresholding techniques (biofilm versus background) as well as measures of following the sizes and numbers of microcolonies over time. The algorithms were specifically used in a project that examined the long-term development of the overall structural morphology and community composition of a biofilm formed in a model drinking water distribution system with biofilms from one day to three years old.[1]

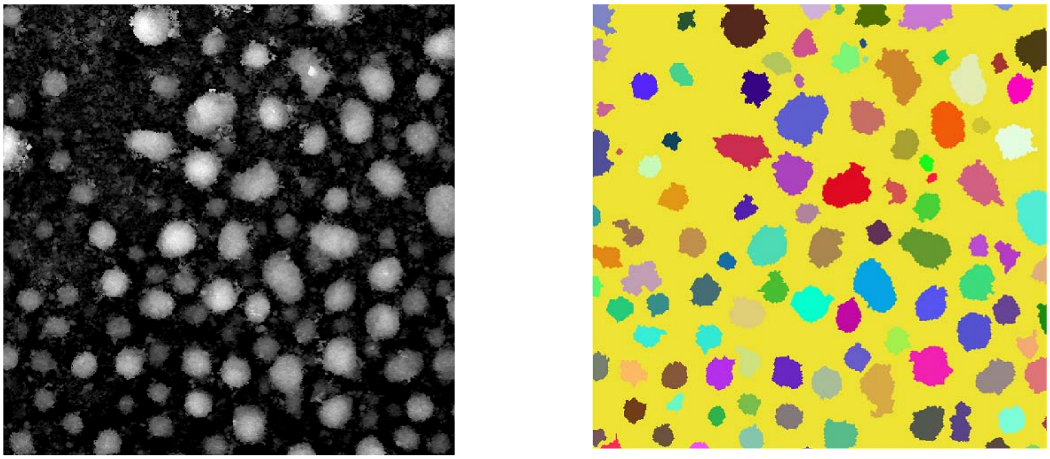

Figure 31. Left: A spatial thickness distribution of a biofilm (dark is "thin", light is "thick"). Right: By using a watershed transformation the dominating microcolonies are segmented from the background. From the segmented islands their sizes can be estimated and followed over a period of time.

1. A.C. Martiny, T.M. Jørgensen, H. Albrechtsen, E. Arvin and S.Molin, "Long-term succession of structure and diversity of a biofilm formed in a model drinking water distribution system," Appl. Environ. Microbiol. 69, 6899-6907 (2003).

3.2.5 Aligning noisy signals for enhancing the signal-to-noise ratio of retinal OCT scanners

T. M. Jørgensen, B. Sander, M. Larsen* (*Department of Ophthalmology, Herlev Hospital, University of Copenhagen, Denmark) and P.E. Andersen*
thomas.martini@risoe.dk

The application of optical coherence tomography (OCT) within ophthalmology is today relative widespread, the reason being that it is a major help in revealing details of structural damage and retinal patho-physiology that may otherwise be difficult to detect. Yet, there is still space for improvement, and due to the research efforts the OCT systems continuously improve both their speed and resolution. In addition, the possibility of improving the measuring system itself there is, however, also a possibility of "bootstrapping" the present

generation of commercial devices by adequate post-processing of the acquired signals. We have presented evidence that with existing commercial systems it is possible to improve the signal-to-noise ratio of the recorded images by fusing multiple scans of the same retinal region.[1,2] In order to achieve this improvement, it is necessary to align a number of noisy signals. We have explored a number of different techniques for achieving this goal. The developed algorithm has been tested on images recorded at Herlev Hospital, Denmark, using two commercial OCT retinal scanners, the older OCT1 and the recent OCT3 system from Humphrey-Zeiss. Between five and ten repetitive recordings were typically used for producing each picture. The improvement of the signal-to-noise-ratio is sufficient to reveal details that are impossible or difficult to observe from the individual OCT recordings (see Figure 32).

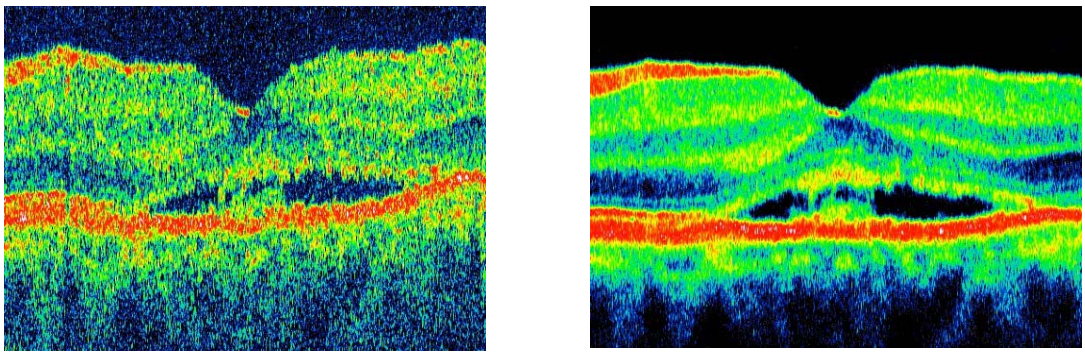

Figure 32. Left: A false-colour image of a single retinal OCT scan. Right: Result of aligning and averaging eight OCT scans of the same region as depicted in the single left image.

1. T.M. Jørgensen, J.L. Hougaard, B. Sander, L. Thrane and M. Larsen, "Image processing scheme for enhancing retinal OCT scans" (oral presentation). In: Book of abstracts. 3. International Workshop on Computer Assisted Fundus Image Analysis (CAFIA 2003), Turin (IT), 28-30 Mar 2003.
2. M. Larsen, L. Thrane, J.L. Hougaard, B. Sander and T.M. Jørgensen, "Enhanced-resolution optical coherence tomographic imaging of ischemic and edematous retinal damage" (oral presentation). In: Book of abstracts. 3. International Workshop on Computer Assisted Fundus Image Analysis (CAFIA 2003), Turin (IT), 28-30 Mar 2003.

3.2.6 Determination of optical scattering properties of highly-scattering media in optical coherence tomography images

D. Levitz, L. Thrane, M. H. Frosz (COM, Technical University of Denmark), P. E. Andersen, C. B. Andersen (Department of Pathology, Rigshospitalet, Copenhagen, Denmark), J. Valanciunaite, J. Swartling*, S. Andersson-Engels* (*Department of Physics, Lund Institute of Technology, Lund, Sweden) and P. R. Hansen (Department of Cardiology, Amtssygehuset i Gentofte, Hellerup, Denmark)*
peter.andersen@risoe.dk

Over the last few decades there has been a continuing search for a high-resolution imaging modality that can quickly and accurately measure the optical properties of layered tissue *in vivo*. Here, the optical properties of interest are those that primarily guide light transport inside the tissue, namely the scattering coefficient μ_s and the anisotropy factor g. A valid method with which these measurements can be done has many important biomedical

implications, such as identifying vulnerable atheromatous lesions during percutaneous coronary interventions.[1]

Optical coherence tomography (OCT) is an imaging technology measuring the backscattering properties of tissues.[2] OCT signals are mainly influenced by the scattering properties of the examined sample, i.e. μ_s and g. These are macroscopic physical properties unique to the tissue, which play a vital role in the modelling of OCT signals. By properly modelling an OCT signal as a function of depth so that multiple scattering events are included, and fitting the depth profile of coherent backscattered light in an OCT image to such model, it is possible to extract both μ_s and g. Additionally, OCT has the important advantage that images can be obtained *in vivo* from which optical properties may be extracted, thereby enabling in situ assessment of the tissue and/or lesion.

In this study,[3] we have developed a new algorithm, see Figure 33, that fits OCT signals as a function of depth to a general theoretical OCT model which takes into account multiple scattering effects.[4] Our objectives in this study were twofold: firstly, to demonstrate that the curve fitting algorithm we employed compared well with controlled experimental measurements and theoretical calculations. This evaluation was conducted on a set of tissue phantoms using integrating sphere measurements to determine optical scattering properties. Secondly, we applied the OCT extraction method on normal and atherosclerotic human aortic samples, see Figure 34, in a preliminary *ex vivo* study in order to demonstrate that the technique may provide a basis for distinguishing between different tissues by their optical properties.

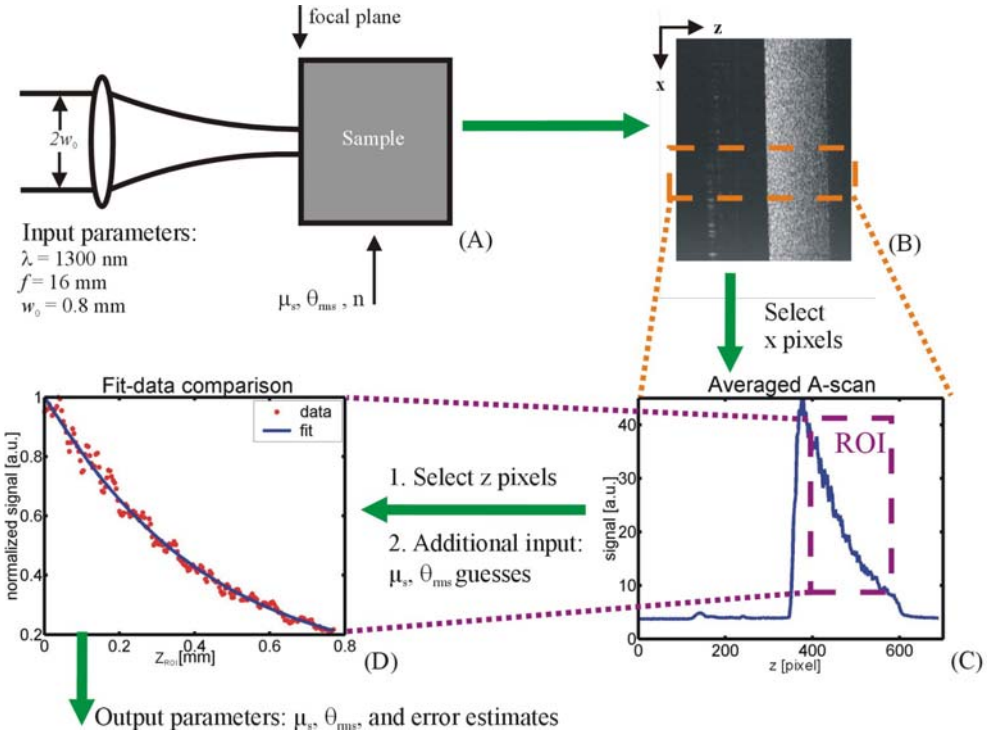

Figure 33. A schematic representation of the principles of the extraction algorithm. The sample arm geometry and the input parameter values from our OCT set-up are shown in (A). These parameters were used to generate an image (B) and were also employed during curve fitting (C-D). A transverse region of interest was selected in (B, inset), averaged, smoothed, and plotted in (C). The axial pixels of the ROI were chosen in (C, inset), and shown as points in (D). z_{ROI} represents the probing depth within the region of interest in (D). The fit was performed on the resulting data points using μ_s and θ_{rms} initial value guesses as additional input. The algorithm returned μ_s, θ_{rms}, the fit's error estimates, and a plot comparing the fit with the data points (D).

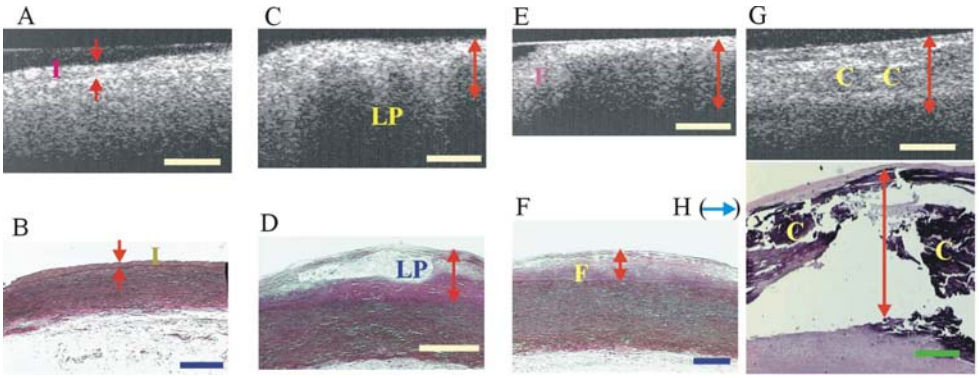

Figure 34. Correlation of raw OCT images (A, C, E and G) and histopathology (B, D, F and H). Normal intima labelled 'I' in (A-B). Lipid-rich lesion (C-D), with a lipid pool marked 'LP'. Fibrous plaque (E-F), with fibrous area marked 'F'. Fibrocalcific lesion (G-H), with the calcifications denoted 'C'. Rupture artifacts caused by the decalcifying process are clearly seen in (H). The arrows represent the intima in (A-F) and the fitting region in (G-H), respectively. Bars = 500 µm.

(A)

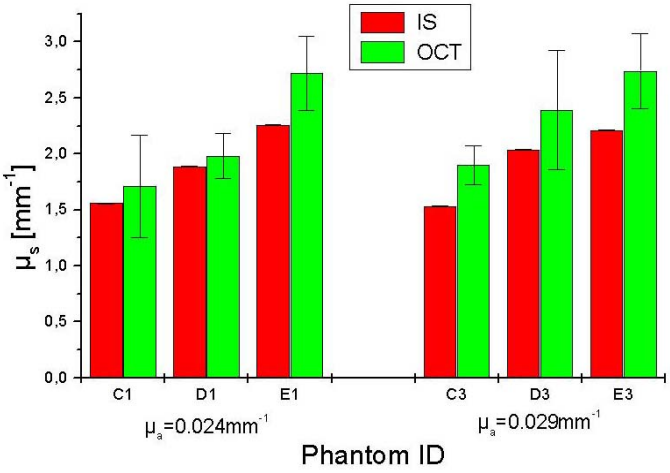

(B)

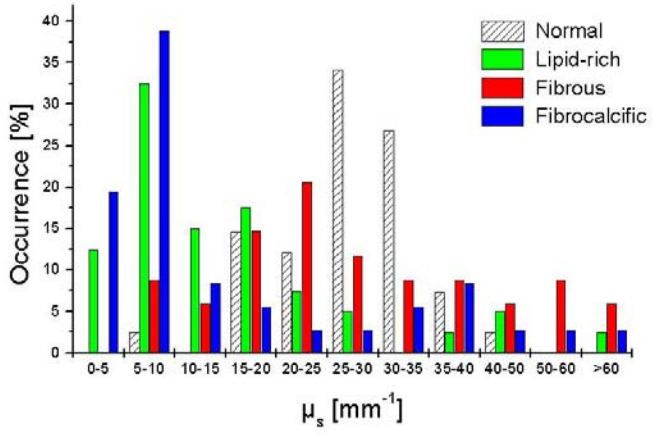

Figure 35 (A) Comparison of μ_s values (means ± standard deviation) obtained from measurements on tissue phantoms with OCT extractions (green) and the integrating sphere (IS, in red). Note a stepwise increase on two separate sets of three phantoms purposely prepared to exhibit such an increase. (B) Distribution of μ_s for normal arteries and lipid-rich, fibrous and fibrocalcific atherosclerotic plaques, respectively. In (B), μ_s for normal samples (striped) were centred between 15 and 40 mm^{-1}, but were centered at lower values for lipid-rich (green) and fibrocalcific (blue) plaques, and were randomly distributed for fibrous plaques (red). Details can be found in Ref. 3.

The study[3] demonstrated that with use of the outlined algorithm the optical scattering properties of tissue may be obtained from OCT images. The evaluation study on phantoms showed that OCT is capable of accurately determining the optical scattering properties of highly scattering media whereby we obtain results in agreement with a well-established experimental method (see Figure 35A). Using this technique, we were able for the first time to conduct a preliminary investigation that quantitatively compared the optical scattering properties of the human arterial intima *ex vivo*, see Figure 35B. Furthermore, our preliminary *ex vivo* tissue data indicated that differences in scattering properties data may exist between normal and atherosclerotic arterial segments and that optical scattering data provided by OCT can potentially contribute to plaque characterization. The OCT technique presented here opens many new avenues of research combining high-resolution tissue visualization and scattering properties measurements. This feature, if successfully implemented, holds considerable promise for future clinical utility.

1. Z. Fayad and V. Fuster, "Clinical imaging of the high-risk or vulnerable atherosclerotic plaque," Circ. Res. **89**, 305-316 (2001).
2. D. Huang, E. A. Swanson, C. P. Lin, J. S. Schuman, W. G. Stinson, W. Chang, M. R. Hee, T. Flotte, K. Gregory, C. A. Puliafito and J. G. Fujimoto, "Optical coherence tomography," Science **254**, 1178-1181 (1991).
3. D. Levitz, L. Thrane, M. H. Frosz, P. E. Andersen, C. B. Andersen, J. Valanciunaite, J. Swartling, S. Andersson-Engels and P. R. Hansen, "Determination of optical scattering properties of highly-scattering media in optical coherence tomography images", *acc. for publication in* Optics Express, Jan. 2004.
4. L. Thrane, H. T. Yura and P. E. Andersen, "Analysis of optical coherence tomography systems based on the extended Huygens-Fresnel principle," J. Opt. Soc. Am. A **17**, 484-490 (2000).

3.2.7 Quantitative distinction between bound and free NADH in biological systems

M. R. Kasimova, K. Krab (Dept. of Molecular Cell Physiology, Earth and Life Sciences, Vrije Universiteit, Amsterdam, the Netherlands), P. E. Andersen, P. Hagedorn, H. Flyvbjerg* and I. Max Møller* (*Plant Research Department, Risø National Laboratory, Denmark)*
marina.kasimova@risoe.dk, peter.andersen@risoe.dk, max.moeller@risoe.dk

Without exceptions, in all living cells NADH is a key metabolite linking a large number of metabolic pathways. Flux rates through such pathways are an essential component in the understanding of the functioning of living cells. Knowledge about the way these fluxes depend on the concentrations of the metabolites involved (including NADH and its oxidized counterpart NAD^+) allows calculation of these fluxes. Therefore, a method to determine the concentration of free NADH is necessary. A distinction between the free and the protein-bound NADH can be made on the basis of its fluorescence emission spectrum and fluorescence lifetimes. A method for such measurements using a microscopic set-up for time-gated fluorescence spectroscopy has been introduced by Schneckenburger and co-workers.[1] We further improve this method by taking advantage of preliminary characterization of NADH binding to proteins in simple model systems. The binding is studied both by fluorescence and calorimetry, which allows a precise calculation of bound and free NADH and their respective spectra. An analysis of experimental data is advanced by applying singular value decomposition routine and subsequent fitting. Taken together these improvements allow a more accurate characterization of the NADH turnover in diverse biological systems and in the system of our interest – potato mitochondria.

NAD (oxidised NAD+, reduced NADH) and NADP (NADP+ and NADPH), collectively NAD(P), are two of the most used coenzymes in cellular metabolism. According to "Enzyme Nomenclature" more than 500 known enzymes use NAD(P) to catalyze reduction-oxidation reactions reversibly. Some of these enzymes are amongst the most abundant and well-studied enzymes participating in energy metabolism – glycolysis, the Krebs cycle, the Calvin cycle – biosynthesis, degradation, defense against oxidative damage, etc. NAD(P) is found in mitochondria, chloroplasts, peroxisome, the cytosol and other cellular compartments typically at a total concentration in the low mM range.

The reduced and oxidized forms of the two coenzymes have distinct spectroscopic characteristics, a fact that makes them easy to monitor and quantify. In particular, we rely on the differences in fluorescence spectra and fluorescence lifetimes between the bound and the free NADH.[3] Due to the necessity of measuring the oxygen concentration within the sample our set-up includes an oxygraph, see Figure 36. This arrangement allows simultaneous collection of fluorescence and the oxygen content data, see Figure 36.

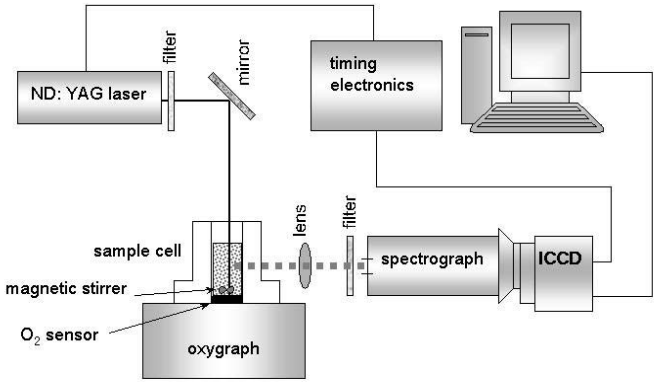

Figure 36. Sketch of the experimental set-up for measuring the time-gated fluorescence spectra.

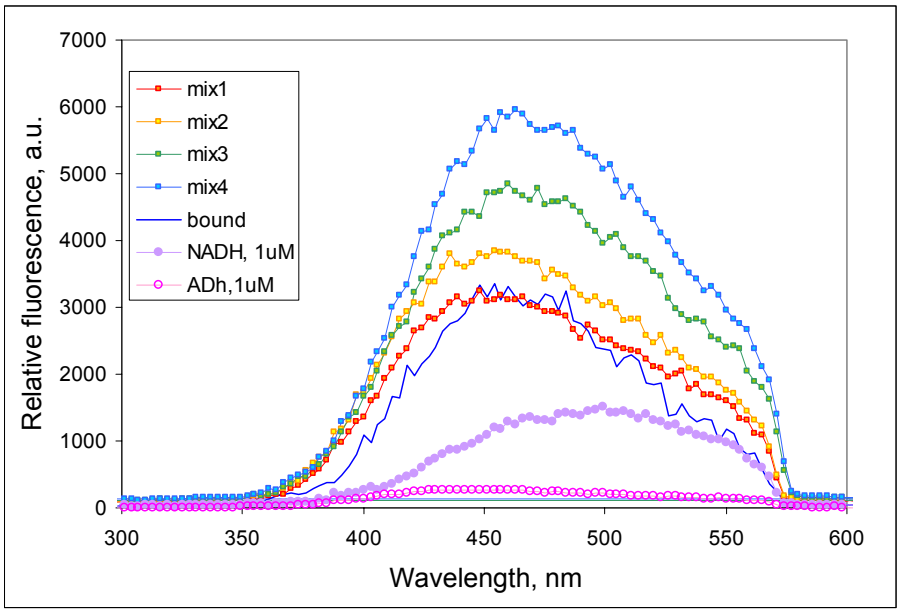

Figure 37. The relative fluorescence as a function of wavelength of NADH, alcohol dehydrogenase and their mixtures (mix1 through 4).

After the set-up was assembled, its performance was tested by examination of spectra of commonly known fluorophores. The fluorescent properties of free and bound NADH were also tested on several standard systems, consisting of NADH and NADH binding proteins, such as Alcohol Dehydrogenase (Adh), see example in Figure 37, and Bovine Serum Albumin (BSA). The binding properties of NADH to standard proteins were independently investigated by Isothermal Titration Calorimetry (ITC). Comparison of the results obtained by the two techniques suggests good performance of our instrument.[4]

1. R. J. Paul, H. Schneckenburger, Naturwissenschaften **83**, 32-35 (1996).
2. http://www.chem.qmul.ac.uk/iubmb/enzyme/
3. A. Gafni and L. Brand, Biochemistry **15**, 3165-3171 (1976).
4. M. R. Kasimova, K. Krabb, P. E. Andersen, P. Hagedorn, H. Flyvbjerg and I. M. Møller, "Quantitative distinction between bound and free NADH in biological systems", to appear in SPIE Proc. vol. **5322**, (2004).

3.3 Optical tweezers

3.3.1 Controllable mode-launching in micro-structured fibres

V. R. Daria, P. J. Rodrigo and J. Glückstad
jesper.glückstad@risoe.dk

The diverse possibilities for the design of micro-structured fibres[1] correspond to a broad range of guided modes that can be applied to a number of applications. Here we describe a coupling technique for controllable launching of high-order guided modes of such fibres[2]. The technique is based on a programmable input field distribution using a computer-controlled spatial light modulator (SLM). For this particular demonstration, we consider a phase-only binary grating to produce two distinct and phase-shifted first-diffraction orders to match the two lobes of the second-order guided mode of the fibre spatially. A binary grating modulated with 0 and π phase is appropriate for generating two distinct spots at the Fourier plane. The desired phase difference of the two first-order peaks is achieved at a prescribed position of the grating with respect to the optical axis. Controllable launching of the second-order guided mode is verified experimentally using a commercially available index-guided microstructured fibre with a triangular lattice air-hole structure.

Figure 38 shows the set-up to verify launching of the high-order guided modes of a micro-structured fibre. The beam from a He-Ne laser is expanded, collimated and incident on a phase-only SLM supplied by Hamamatsu Photonics. The SLM is based on a nematic liquid crystal, which is optically addressed by a 768x768-pixel extended video graphics array element. A simple graphical program has been developed to display binary gratings on the SLM so that the spatial frequency of the grating and the relative transverse and angular orientation can be tuned on the preference of the user. Figure 38b shows a typical binary grating and the corresponding diffraction orders (Figure 38c) at the Fourier plane of the coupling lens. For this demonstration, the coupling lens is a microscope objective lens (x20, 0.4NA and focal length 9 mm). The phase-encoded light is focused by the objective lens for coupling to the input facet of the fibre. The inset in Figure 38a is a micrograph showing the cross-section of the index-guided microstructured fibre (Crystal Fibre A/S, Denmark) with an index-guided core diameter of ~14 □m. The pitch or the periodicity of the air-hole structure in the cladding is 10.9 □m and the average hole size to pitch ratio is around 0.7. The

experimental set-up was designed in order to have negligible bending losses for a 20-cm-long fibre.

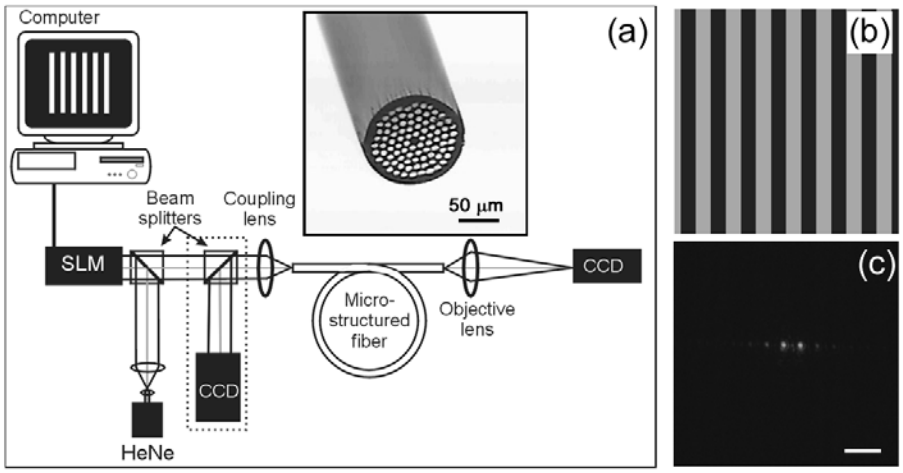

Figure 38. (a) Experimental set-up used to verify launching of high-order guided modes of a micro-structured fibre. Inset: Micrograph of the index-guided micro-structured fibre used in the experiments. (b) A binary phase grating encoded on the spatial light modulator and (c) corresponding optical Fourier transform measured after the coupling lens.

The second-order guided mode is characterized by a π-phase difference between the two amplitude-matched lobes. Transforming a single coherent TEM_{00} light source to match the two lobes of the second-order fibre mode spatially therefore requires that both amplitude and phase of the resulting input field follow these patterns. The frequency of the phase-only grating is chosen to position the two first-order peaks within the core of the fibre. To set a π-phase difference between the two lobes of the first-diffraction orders at the Fourier plane, the binary phase grating is positioned asymmetrically with respect to the optical axis. With a dynamically programmable SLM, the parameters of the grating can easily be changed. Changing the angle of the encoded binary grating can launch various orientations of second-order guided modes in a non-mechanical way. Figure 39a shows the intensity distribution at the output of the fibre when the binary grating is oriented to launch the second-order guided mode between two opposing holes of the six air holes surrounding the core. Changing the orientation angle of the grating by 60 and 120 degrees launches the two positions of the second-order mode as shown in Figure 39.b and Figure 39c, respectively.

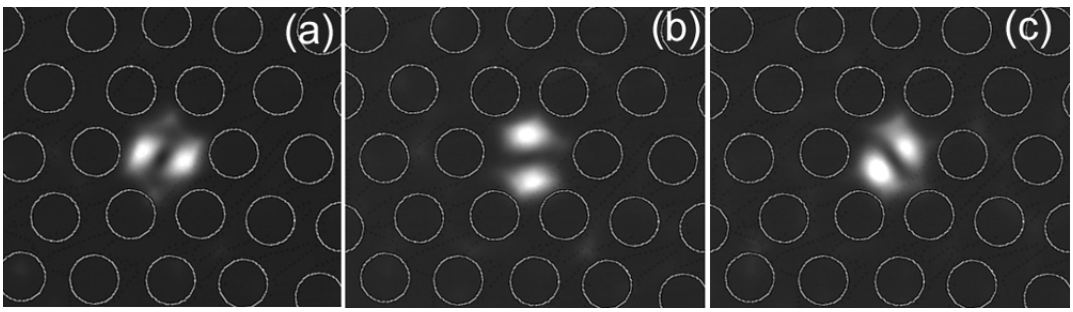

Figure 39. Non-mechanical rotation of the second-order guided mode. The output intensity distribution when the binary grating is encoded in (a) 0^o, (b) 60^o and (c) 120^o angular orientation.

We have demonstrated a technique for controllable launching of a high-order guided mode of an index-guided micro-structured fibre. The Fourier transform of a □-modulated binary grating encoded on a computer-programmable SLM generates the appropriate field distribution for controllable launching of the second-order guided mode of the fibre. The experimentally demonstrated programmable coupling to the second-order mode can be extended to other higher-order modes by encoding the SLM with an appropriate diffractive pattern.

1. J. C. Knight, T. A. Birks, P. S. J. Russel and D. M. Atkin, "All-silica single-mode optical fiber with photonic crystal cladding," *Opt Lett.* **21**, 1547-1549 (1996).
2. V. R. Daria, P. J. Rodrigo and J. Glückstad, "Programmable complex field coupling to high-order guided modes of micro-structured fibres," *Opt Comm.* **232**, 239-247 (2004).

3.3.2 User-interactive microscopy

P. J. Rodrigo, V. R. Daria and J. Glückstad
jesper.glückstad@risoe.dk

In 1970, Arthur Ashkin made pioneering experiments showing that light-induced forces are strong enough to trap and manipulate microscopic particles. Since then, optical micromanipulation has incessantly caught the attention of researchers in both physical and biological fields. In microscopy, it has supplemented the functionality of optical microscopes, bolstering the simple imaging instrument to one that allows pico-Newton forces to be applied to and measured from a microscopic specimen. Thus, increasing the number of light handles built into a microscope will open doors for many interesting studies on biological systems as well as applications in materials engineering – a transformation of the 'passive' to the 'active' type of microscope.

Using a virtually lossless phase-to-intensity converter based on the Generalized Phase Contrast method, user-configured arrays of dynamic optical traps have recently been demonstrated.[1,2] In a recent cover publication of Optics Express[1] the versatility of this system was demonstrated for simultaneous trapping and active control of a plurality of microstructures with different geometrical profiles. In this approach, the generation of arbitrarily shaped trapping beams is a result of a direct conversion of phase patterns into corresponding intensity distributions at the sample plane of the microscope. Two-dimensional phase patterns encoded on a programmable spatial light modulator (SLM) serve as input to the phase-to-intensity converter. The converter is composed of a 4-f lens imaging system and a spatial phase filter centred on the optical axis at the optical Fourier plane. The resulting output intensity distributions are obtained as direct mappings of the phase patterns encoded at the SLM. The interactive programmability of the SLM enables direct and simultaneous position control on an arbitrary number of trapping beams and permits individual specification of trap geometry and intensity. Compared with light pattern synthesis that uses an SLM for encoding computer-generated holograms, this phase-to-intensity conversion approach offers significant reduction in computational power requirements and does not suffer from the limited space bandwidth product and relatively poor modulation transfer function of currently available phase-encoding devices.[3]

The experimental results in Figure 40 illustrate versatile optical manipulation schemes of various clusters of microstructures using multiple traps[1,4]. Figure 40(a)-(c) show commercially dyed polystyrene spheres (diameter = 3 μm) trapped in unison and sorted according to colour. Figure 40(d)-(f) show simultaneous trapping and rearrangement of microspheres with different sizes. Figure 40(g)-(i) demonstrate the angular rotation or orientation of irregularly shaped particles using optical traps with rectangular symmetry.

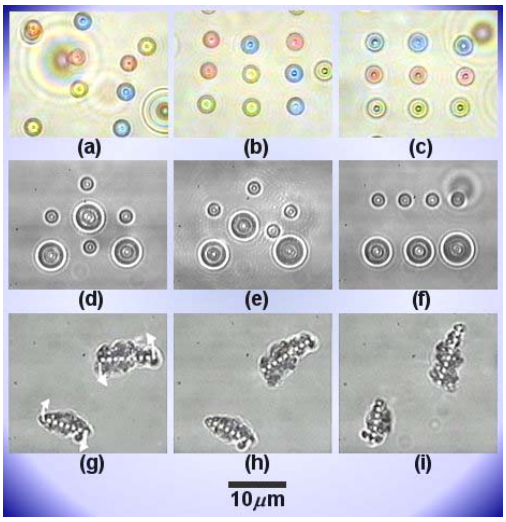

Figure 40. Optical manipulation of various assemblies of microscopic particles. Multiple optical traps with arbitrary spatial profiles are created for simultaneous trapping and dynamic manipulation of inhomogeneous colloidal mixtures.

The compact 200 mW laser diode source used for creating the multiple traps operates at 830 nm wavelength suitable for non-invasive manipulation of biological microstructures. Moreover, the profile of each trapping beam can be configured to incorporate an intensity void at its centre. For cells, this optical trap geometry avoids illumination of cell nuclei potentially reducing the damage or mutation to the specimen. With the functionalities of the multiple, dynamic optical traps described here, studies on cell biomechanics involving adhesion, growth, interactions, signalling and more can now be performed with superior flexibility and control.[5]

1. P. J. Rodrigo, R. L. Eriksen, V. R. Daria and J. Glückstad, "Interactive light-driven and parallel manipulation of inhomogeneous particles," *Opt. Express* **10**, 1550-1556 (2002).
2. R. L. Eriksen, V. R. Daria and J. Glückstad, "Fully dynamic multiple-beam optical tweezers," *Opt. Express* **10**, 597-601 (2002).
3. V. R. Daria, R. L. Eriksen and J. Glückstad, "Dynamic optical manipulation of colloidal structures using a spatial light modulator. *J. Mod Optic* **50**, 1601-1614 (2003).
4. R. L. Eriksen, V. R. Daria, P. J. Rodrigo and J. Glückstad, "Computer-controlled orientation of multiple optically-trapped microscopic particles," *Microelect. Eng*. **67-8**, 872-878 (2003).
5. J. Glückstad, "Sorting particles with light". *Nature Materials* **3**, 9-10 (2004).

3.3.3 Multiple-beam optical tweezers based on Shack-Hartmann setup

P. John Rodrigo, V. R. Daria and J. Glückstad
jesper.glückstad@risoe.dk

In optical micromanipulation, the demand for simultaneous control of a collection of particles has motivated the development of various multiple-beam trapping systems. Multiple optical traps have been produced by means of computer-generated holograms, generalised phase-contrast method, and vertical-cavity surface emitting laser (VCSEL) arrays as light sources. Here, we integrate the concept of light-induced confinement of microscopic particles with the theory of wavefront sensing by demonstrating a new multiple-beam optical tweezer system

with an architecture that is fundamentally based on the Shack-Hartmann wavefront sensor (SHWS) configuration.[1,2]

In the proposed optical tweezers configuration shown in Figure 41, the incident wavefront from a TEM_{00} source beam is spatially sampled by a microlens (lenslet) array creating multiple adjacent point sources distributed along a plane perpendicular to the optical axis. These beam spots are then imaged into the observation plane of an inverted microscope where particle trapping and manipulation by light-induced forces take place. A wavefront-engineering scheme is employed wherein slopes of the input field phase component are deliberately altered by a parallel-aligned nematic liquid crystal spatial light modulator (SLM) before the beam traverses the microlens array system. By encoding the appropriate phase patterns on the SLM, beam deflections in the transverse directions are controlled and as a consequence fine position tuning of trapped particles is achieved.

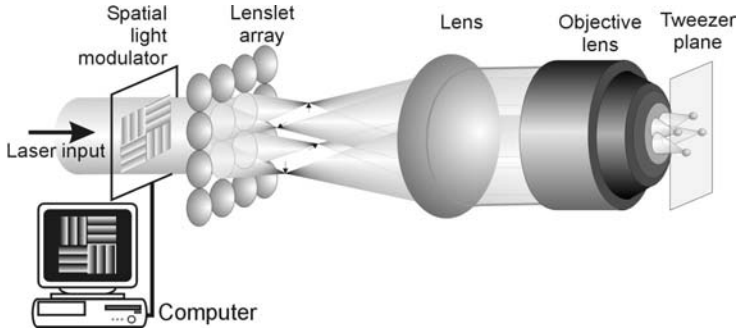

Figure 41. Shack-Hartmann multiple-beam optical tweezers setup. Optical Fourier-transforms of programmable blazed phase gratings are imaged onto the tweezer plane for parallel particle trapping with fine positioning modality. The computer addresses the SLM in four quadrants that allows for encoding of arbitrary grating orientations and frequencies at each quadrant. Deflection magnitude of each optical trap is proportional to the grating frequency.

Experimental results shown in Figure 42 verify the functionality of the SLM-encoded phase gratings to independently introduce small positional deflections to the trapped particles during simultaneous confinement in their respective optical traps. In the supplementary information linked to reference[1], a video clip shows the sequence of synchronized deflection of the four microspheres in a diamond-like path followed by the sequence where distinct deflections in the horizontal and vertical directions are obtained. In these experiments, particle deflections are achieved in discrete steps. But it must be stressed that continuous displacement of trapped particles can be attained with a sequence of phase gratings encoded with sufficiently smooth transition in periodicity and orientation.

A new methodology for generating multiple-beam optical tweezers has been proposed and demonstrated. The backbone of the optical setup is derived from that of the Shack-Hartmann wavefront sensing principle. A two-dimensional matrix of optical tweezers, produced from the passage of a single beam through a microlens array, is used to trap multiple microscopic particles in unison. All traps are highly stable in both the axial and the transverse directions. Phase perturbations of the input beam in the form of blazed grating functions are introduced by a computer-controlled SLM. The resulting array of diffracted spots defines the magnitude and direction of transverse deflections of the corresponding optical traps. Thus, independent positional fine-tuning of trapped particles has been achieved without any mechanical displacement in the setup.

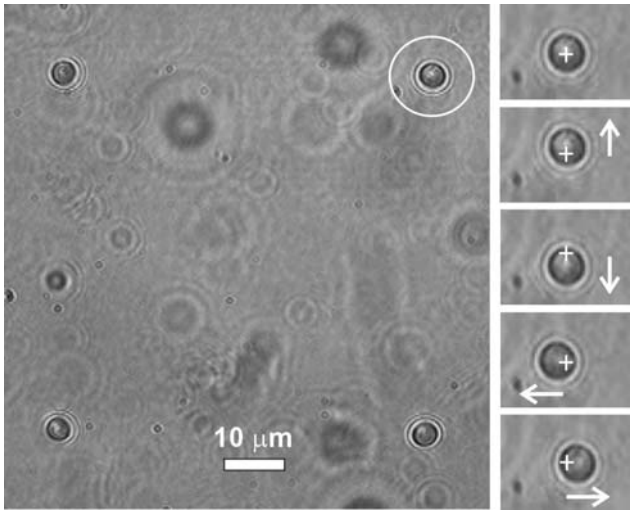

Figure 42. Parallel trapping of polystyrene microspheres with independent deflection control. Shown at the right is a sequence of magnified images of one trapped particle (encircled in the left frame) illustrating different directions of deflection (magnitude ~ 1.5 μm).

1. P. J. Rodrigo, R. L. Eriksen, V. R. Daria and J. Glückstad, "Shack-Hartmann multiple-beam optical tweezers," *Opt. Express* **11**, 208-214 (2003).
2. R.L. Eriksen, P. J. Rodrigo, V. R. Daria and J. Glückstad, "Spatial light modulator-controlled alignment and spinning of birefringent particles optically trapped in an array". *Appl. Opt.* **42** , 5107-5111 (2003).

3.4 Speckle techniques

3.4.1 Miniaturisation of optical sensors

M. L. Jakobsen, H. E. Larsen, F. Pedersen and S. G. Hanson
michael.linde.jakobsen@risoe.dk

Technologies providing low cost, miniaturisation and high reliability are essential for optical sensors in order to find commercial interests within industrial applications and products. Within the Centre for Miniaturizing of Optical Sensors (MINOS) (http://www.sensortec.dk/stc.htm), concepts of such micro-optical sensor systems have been studied over the last three years, including miniature light sources, detectors, diffractive gratings and refractive miniature structures. Replications in polymers as well as technologies for packing the micro-optical components have also been studied. After finishing MINOS early this year, related and new concepts and designs have been developed within new commercial contracts to the point of having alpha-prototypes ready for performance tests.

The main achievements in 2003 have been the development and testing of two optical sensor designs, both using speckle translation, to measure rotation or in-plane translation of solid objects with a non-specular surface. One sensor design required a high-precision displacement sensor, while the priorities of the other sensor design were applicability to many types of target surfaces, low-power consumption and eye safety.

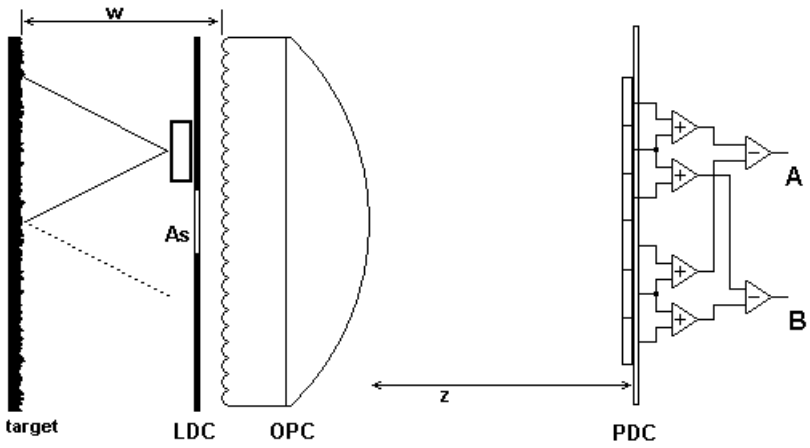

Figure 43. The schematic presentation illustrates the spatial filtering velocimetry sensor for surfaces.

The sensors illuminate the target surface with coherent light from a vertical cavity surface emitting laser (VCSEL). The light scattered from the surface propagates either in free space (Figure 43) or through an optical arrangement. The latter isolates speckle translation from a single mechanical measurand, such as either in-plane translation or out-of-plane rotation. The speckle translation is formed at a lenticular array (f_1), which together with a large spherical lens (f_2) forms a narrow spatial band-pass filter. The filter provides a spatial quasi-sinusoidal intensity distribution at the detector plane, which moves with the movement of the speckle patterns. A photodetector array provides temporal information about the spatial intensity distribution at various spatial phase steps. The difference in photocurrents from photodetectors spaced over a 180 degrees phase step offers suppression of common mode intensity variations and higher harmonics, while photodetectors spaced over a 90 degrees phase step offer information about the direction of the speckle translation. The differential signal from two photodetectors spaced over a 180 degrees phase step is ideal for real-time zero-crossing detection. However, tests showed that more extensive signal conditioning in the procession algorithm is necessary. Without restrictions on the velocity range, a dynamical band-pass filter inserted in front of the zero-crossing detector is essential, and to improve the sensor's tolerance towards vibrations, evaluation of, e.g., signal phase quadrature is necessary.

The sensor illustrated in Figure 43 relies on free space propagation of speckles. In order to match the speckle size with the spatial filter at a reasonable working distance, the filter in this sensor is based on a microlenticular array with a lens spacing of 15 μm. In this case, diffraction effects and numerical aperture must be considered carefully. Furthermore, low-cost replication processes of such micro-structures in polymers becomes a challenging issue. The preliminary attempt to produce a miniaturised set-up with replicated optics is illustrated in Figure 44. One of the prototypes uses even smaller components. The opto-electronics, the interfacing electronics and the processor have been integrated on an application specific integrated circuit.

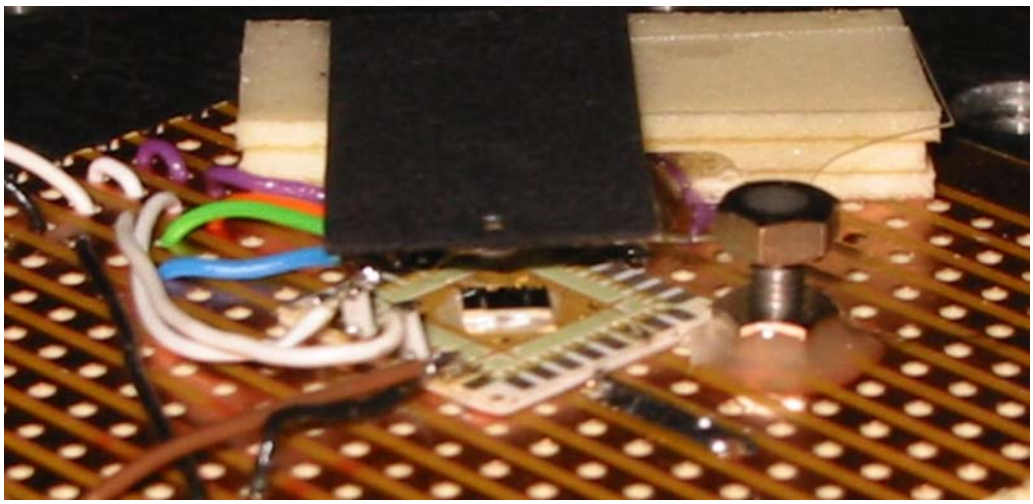

Figure 44. Preliminary optical design with a VCSEL and photodetector dices and replicated microlenticular arrays.

1. M. L. Jakobsen, H. E. Larsen and S.G. Hanson, ”Compact optical system for measuring linear and angular displacement of solid structures”, presented at the Sixth. Int. Conf. on Correlation Optics 2003, Ukraine.

3.4.2 Variance of intensity for Gaussian statistics and partially developed speckle in complex *ABCD* optical systems

H. T. Yura (The Aerospace Corporation, Los Angeles, USA) and S. G. Hanson
steen.hanson@risoe.dk

The fourth-order field correlation function for light scattered off a surface – or penetrating a diffusing medium - with a given surface roughness and a given lateral height correlation scale has been investigated. Results have previously been obtained in cases where the rms surface roughness is larger than the wavelength, and where the largest lateral height correlation scale is smaller than the illuminating spot. When these two restrictions are not fulfilled, the scattered field does not obey circularly symmetric Gaussian statistics, and the fourth-order field correlation function, i.e. the spatial intensity correlation function, becomes problematical to derive. Knowledge of the spatial height correlation function exceeding second order becomes important.

Attempts to apply a simplified model to analyze the problem and use the derivation for establishing a simple light scattering set-up for deriving the rms surface roughness and the lateral scale have been made.[1] A discussion of the applicability of this method has been offered.[2,3]

In order to present analytical expressions for the intensity variance, we have considered physical situations where both the real and the imaginary parts of the optical field obey Gaussian statistics. Within the limitations of the generalized ray-matrix method, an expression for the variance of intensity is obtained for arbitrary cylindrically symmetric optical systems in the presence of partially developed speckle, where the rms surface roughness is comparable with the optical wavelength. We assume beam illumination of reflective targets with arbitrary values of surface roughness whose surface-height fluctuations are taken as a zero-mean stationary Gaussian random process. In contrast to previous work, the present analysis is valid for an arbitrary complex optical system that can be characterized by an *ABCD* matrix (e.g., simple and complex imaging systems, free-space propagation in both the near- and the far-

field, and Fourier transform systems), including those systems that exhibit correlation between the real and imaginary parts of the optical field. As a direct application, we consider an optical system for probing angular deflections that are sensitive to the speckle dynamics, and derive the relationship between the surface roughness and the corresponding lateral scale length that yields the maximum AC signal strength.

The derived results are important for depicting the signal strength in light scattering systems based on speckles. Of special interest is the appearance of the effect of optical mixing of diffusely and specularly scattered light, giving rise to a strong intensity modulation for specific combinations of surface roughness and lateral scale.

1. C. F. Cheng, C. X. Liu, N. Y. Zhang, T. Q. Jia, R. X. Li and Z. Z. Xu, "Absolute measurement of roughness and lateral-correlation length of random surfaces by use of the simplified model of image-speckle contrast," *Applied Optics* **41**, 4148-4156 (2002).
2. C. F. Cheng, C. X. Liu, N. Y. Zhang, T. Q. Jia, R. X. Li and Z. Z. Xu, "Reply to comment: Absolute measurement of roughness and lateral-correlation length of random surfaces by use of the simplified model of image-speckle contrast," *Applied Optics* **42**, 2523-2525 (2003).
3. H. T. Yura and S. G. Hanson, "Variance of intensity for Gaussian statistics and partially developed speckle in complex ABCD optical systems," *Optics Communications* **228**, 263-270 (2003).

3.4.3 Applicability of the singular-optics concept for diagnostics of random and fractal rough surfaces

O. V. Angelsky, D. N. Burkovets*, A. V. Kovalchuk*, P. P. Maksimyak*, V. V. Ryukhtin* (*Department of Correlation Optics, Chernivtsi University, Ukraine) and S. G. Hanson*
steen.hanson@risoe.dk

New feasibilities have been considered for optical correlation diagnostics of rough surfaces with different distributions of irregularities. The influence of deviations of the height surface roughness distribution from a Gaussian probability distribution on the accuracy of optical analysis has been discussed. Possibilities for the optical diagnostics of fractal surface structures have been shown, and a set of statistical and dimensional parameters of the scattered fields for surface roughness diagnostics have been revealed. Finally, a multifunctional measuring device for estimating these parameters has been proposed.[3]

Later the multifractal description of rough surfaces has been discussed and the mechanisms for generation of fractal and multifractal height distributions of inhomogeneities for rough surfaces have been simulated. The original technique for estimating the spectrum of singularities was proposed for the study of these distributions.[1]

It has now been shown[2] that the spatial distribution of amplitude zeros of the field scattered by a rough surface, from the caustic zone to the far zone, reflects the irregularities of the surface of interest. The half-widths of histograms of local density of amplitude zeros estimated at various distances from a surface differ considerably from those of random and fractal surfaces. An example of an intensity distribution, the zerogram and the associated density of amplitude zeroes are shown in Figure 45 for a random rough surface and two fractal surfaces with varying degrees of spatial smoothing.

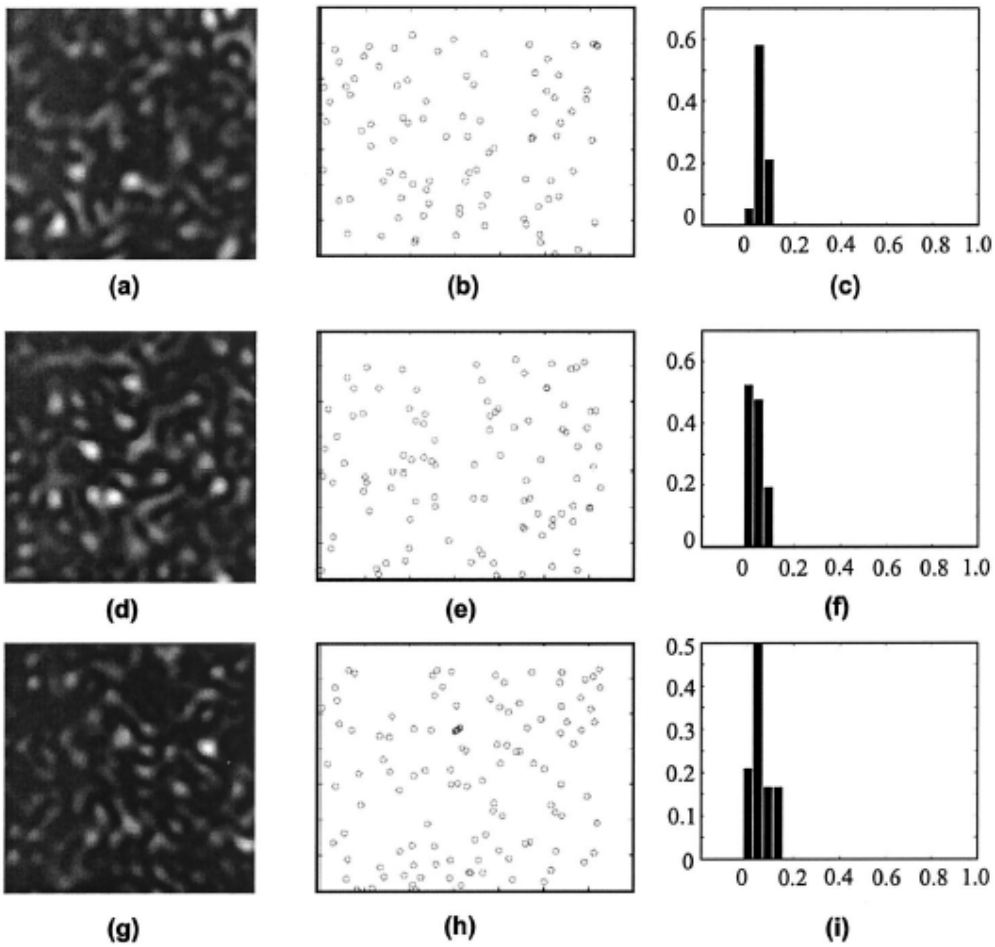

Figure 45. (a), (d), (g) Intensity distributions; (b), (e), (h) zerograms; (c), (f), (i) histograms of distributions of local density of amplitude zeros, Kp_K0, versus p [μm^{-2}] at a distance of 500 μm from the rough surfaces: (a)–(c) random and (d)–(f) fractal surfaces smoothed following a normal law over three pixels; (g)–(i) fractal surface smoothed following a normal law over five pixels.

For fractal rough surfaces, amplitude zeros are consequently clustered in specific zones, and one can easily understand this fact by taking into account the statistical self-similarity of such structures. This conclusion agrees with the prediction that the net of amplitude zeros of a scattered field unambiguously determines the phase distribution of a speckle field and, as a result, facilitates the prediction of some important peculiarities of the rough surface that produces this field. Moreover, the spatial instability of amplitude zeros with higher-order topological charge finds its experimental confirmation as a complex interference forklet decays owing to changes of geometry of the formation of the field. We believe that the next step in classification and diagnostics of the structures considered above could consist in looking for quantitative criteria for interconnections between the structural peculiarities of the intensity distribution and the zerogram of the scattered field as a function of the structural parameters of the object.

1. O. V. Angelsky, D. N. Burkovets, A. V. Kovalchuk and S. G. Hanson, "Fractal description of rough surfaces," *Applied Optics* **41**, 4620-4629 (2002).
2. O. V. Angelsky, D. N. Burkovets, P. P. Maksimyak and S. G. Hanson, "Applicability of the singular-optics concept for diagnostics of random and fractal rough surfaces," *Applied Optics* **42**, 4529-4540 (2003).

3. O. V. Angelsky, P. P. Maksimyak, V. V. Ryukhtin and S. G. Hanson, "New feasibilities for characterizing rough surfaces by optical-correlation techniques," *Applied Optics* **40**, 5693-5707 (2001).

3.5 IR techniques

3.5.1 Measurements of glucose in aqueous solutions with dual-beam FTIR

J. Bak
jimmy.bak@risoe.dk

In the search for more sensitive spectroscopic techniques for future applications within the biomedical field for non-invasive and on-line measurements of key-important biological compounds, an experimental set-up based on a dual-beam Fourier transform infrared spectrometer has been presented.[1,2] The experimental set-up has been used for measurements in the near-infrared spectral region. Details about optimisation and stability of the experimental set-up, data analytical procedures and chemometric modelling have been presented. The experimental set-up is exemplified by the measurements of glucose in water, see Figure 46. The improvements in detection limits obtained by using the dual-beam set-up has been demonstrated with respect to future biomedical applications.

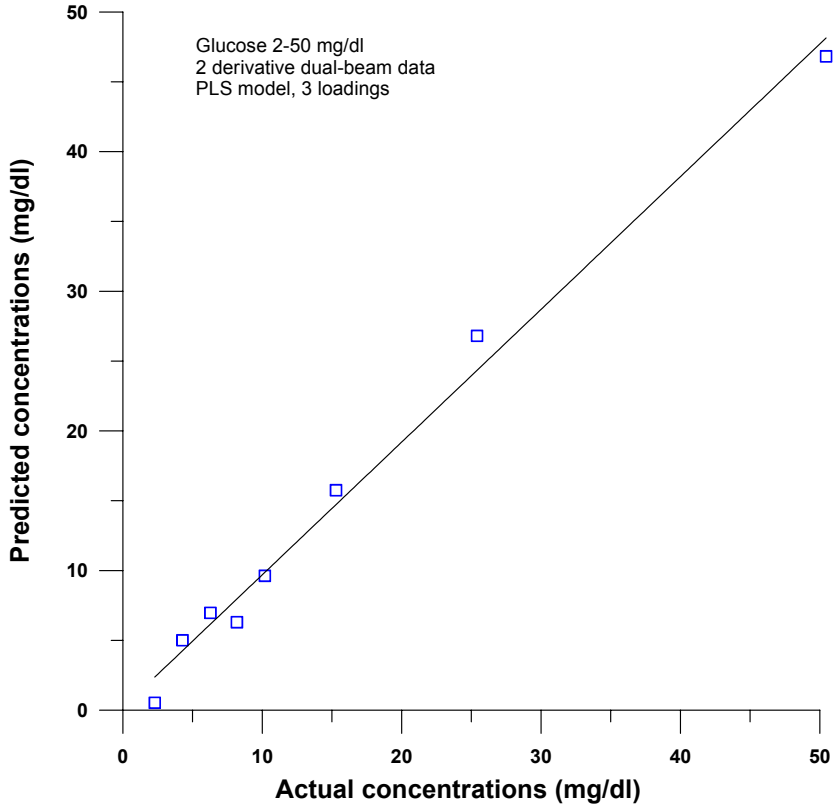

Figure 46. Predicted versus actual glucose concentrations measured with dual-beam FT-IR.

1. J. Bak, Peter S. Jensen & Tanja Begovic, Poster presented at the Pittcon Conf. 2003, Orlando (Fl).
2. P. S. Jensen, J. Bak & Andersson-Engels S, APPL SPEC. 57 (1): 28-36 Jan 2003.

3.5.2 MENELAS

S. Clausen
sonnik.clausen@risoe.dk

The goal of MENELAS is to develop innovative measurements and related apparatus that are capable of reducing time and costs for aeroplane engine development. These apparatus, with new technologies in accordance to present ICAO regulations, will bring to the aeronautics community original developments in infrared coherent sources specially designed for effluent trace detection in engine research and atmospheric impact studies.

The performances of the laser instruments developed in the project will be characterized through laboratory tests and cross-calibration experiments prior to campaign measurements. The Risø hot gas cell facility used in the EU-project AEROPROFILE for verification of methods based on FTIR spectroscopy has been upgraded in 2003 to cover the requirements in the MENELAS project.

The stainless steel surfaces of the inner hot cell parts have been covered with a ceramic coating to cope with reactive gases like CO and NO at high temperatures in the MENELAS project in order to avoid problems with gas reaction due to catalytic effects. Similarly, the gas cell windows have been replaced with wedged CaF_2 windows to reduce etalon effects. All temperature sensors have been calibrated. The gas cell cannot be operated at pressures far from ambient due to the use of graphite seals; however, a ceramic replacement inner cell with wedged sapphire windows will be available in the beginning of 2004 for experiments at low pressure.

Different water generators available on the commercial marked have been considered, e.g. NEOs Hovacal water generator and dew-point generators from Michell, but the water generators would be difficult to apply in the needed concentration range and with calibration gases. Therefore, a system for addition of water vapour has been designed, built and adapted, see Figure 47.

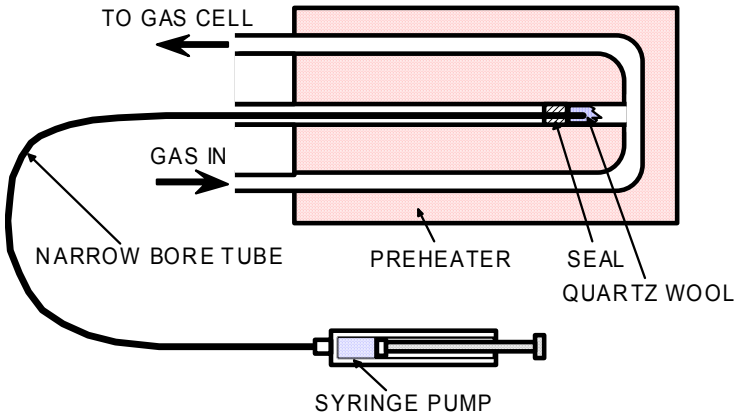

Figure 47. Water generator used in the MENELAS project. Gas from the Environics 4000 gas mixture system or from the bottle is preheated and water vapour is added to the gas flow before it enters the gas cell via a heated gas line. The syringe pump controls the water flow rate. The evaporation of the water leaving the narrow bore tube is smooth and effective through the large surface area of the quartz wool.

The upgraded hot gas cell facility at Risø was finally tested in August 2003 prior to experiments with the laser systems using an FTIR spectrometer with fibre optics sensitive in the spectral range 1800 – 6500 cm^{-1}. The test was performed with 1% CO, 1% CO_2 and 1% CH_4 in nitrogen at 800˚C in order to provoke gas reactions. We have concluded that gas reactions are very small with the ceramic coating and when the gas cell is operated with at a

flow rate of 2 l/min. Similarly, test measurements with the water generator were carried out at different water vapour levels. Experiments with approx. 1% CO_2, 1% CH_4 and nitrogen with and without high levels of water have been carried out at 1073 K, and it was shown that water could be removed by subtraction of the measured water spectrum in nitrogen.

It is concluded that the water vapour concentration is very stable, short term as long term, and it can be varied over a wide range.

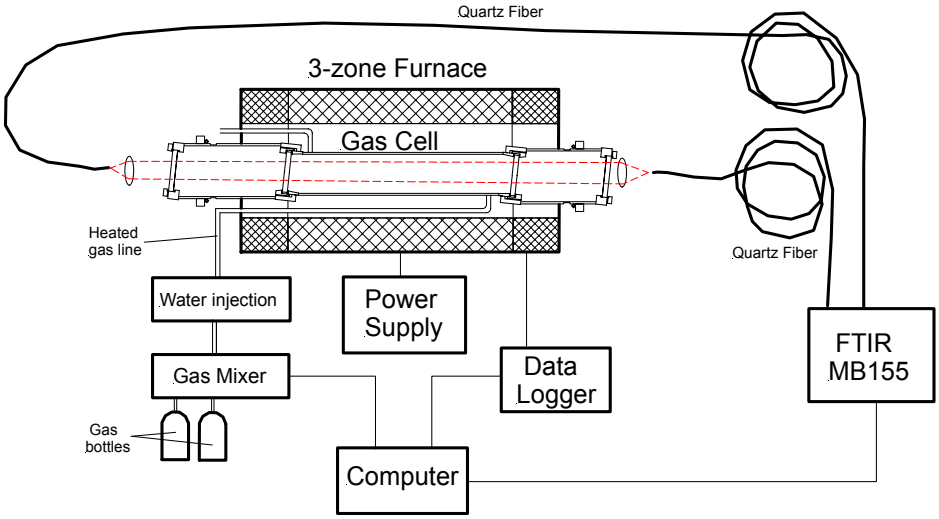

Figure 48. Experimental set-up in tests of upgraded hot gas cell. MIR (C2 chalcogenide) fibres were used in measurements with extended spectral range to cover fundamental bands of CO, CH_4 and CO_2. The temperature range is from ambient to 1073 K with gas cell windows of CaF_2.

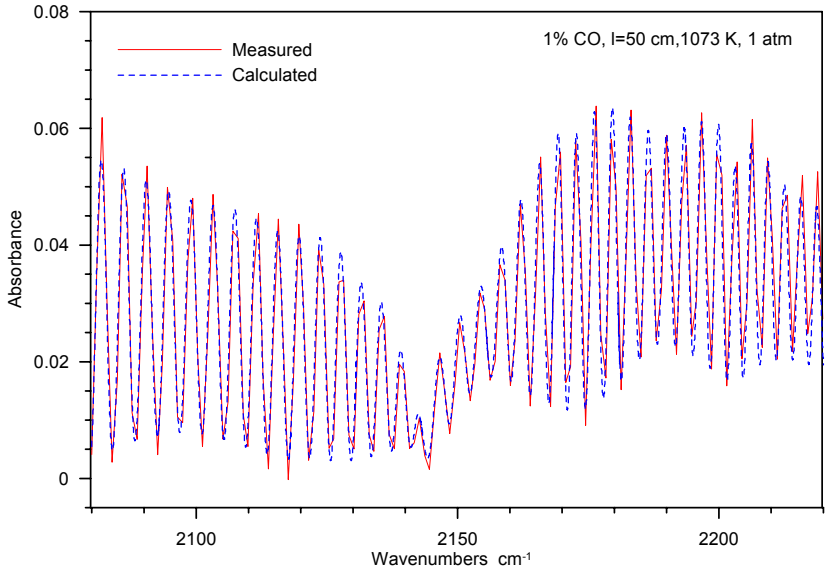

Figure 49. Measured CO spectrum compared with calculated spectrum from HITRAN96 for 1% CO at 1 atm, 1073 K and 50 cm path length. The spectral resolution in the calculated spectrum is 2.3 cm^{-1}. The deviation in area between the two curves is 1.3%. The gas flow rate through the gas cell was 2 l/min.

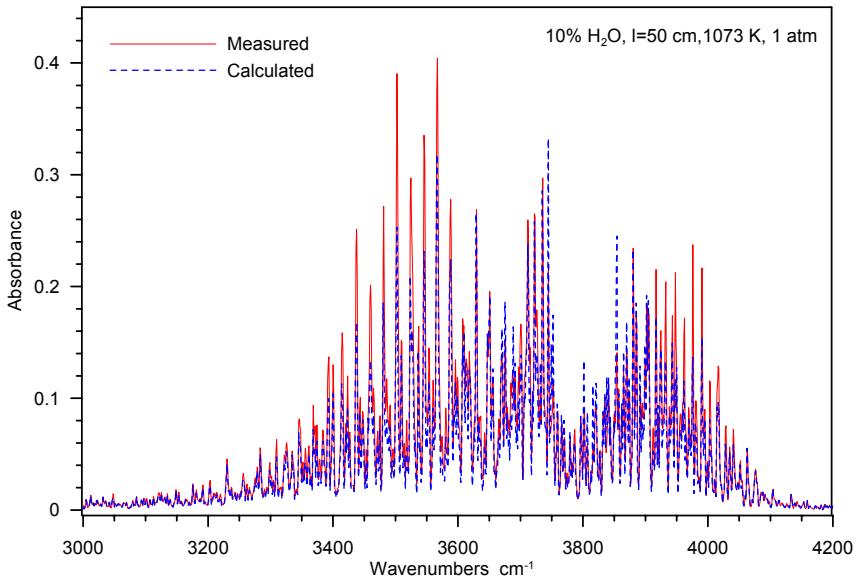

Figure 50. Measured H_2O spectrum compared with calculated spectrum using HITEMP for 10% H_2O at 1 atm, 1073 K and 50 cm path length. The spectral resolution has been set to 2 cm^{-1}. As expected, large deviations are seen between measured and calculated spectrum of water. The lifetime of the CaF_2 windows is reduced at high temperature as the surface seems to be attacked by water vapour (milky surface).

Technical University Clausthal in Germany visited Risø four days in week 50 for performing tests and line-broadening measurements at Risø's hot gas cell. Measurements were carried out for CH_4 in air, nitrogen and with addition of water vapour at temperatures from ambient and upwards in steps of 50 K.

3.5.3 Infrared temperature calibration and related projects

S. Clausen
sonnik.clausen@risoe.dk

A reference laboratory for calibration of infrared instruments was established at Risø in 1996. Traceable calibration of infrared thermometers and blackbodies is offered in the temperature range -50 °C to 1600 °C. In 2001 the laboratory was approved by the Danish Accreditation Scheme, DANAK, to issue certificates for calibration of non-contact temperature measuring equipment.

The work affects the following main topics to reduce uncertainties of non-contact temperature measurements:

- calibration service of infrared thermometers for customers;
- temperature measurements for customers;
- development of new and improved methods for infrared temperature measurements;
- measurement of spectral emissivity of samples and coatings;
- consultative service and information;
- international comparison of standards and procedures;
- design and construction of special blackbody sources for customers.

A large-area blackbody, ambient to 550 ºC, has been developed for FLS-Automation for calibration of infrared scanners. Risø has moreover been involved in the development of a new infrared calibrator from AMETEK Denmark. In addition, spectral emissivity measurements have been measured for customers.

With the combination of high-accuracy traceable blackbody sources and spectral measurements of infrared radiation with FTIR spectrometer Risø has state-of-art calibration capabilities in the spectral range from 1 – 25 μm. A powerful method has been developed for the measurement of spectral emissivity of samples, objects and blackbodies by an FTIR spectrometer.

In 2002 Risø was evaluated and given status as national reference laboratory for non-contact temperature measurements. The nomination was given by the Agency for Enterprise and Housing based on an evaluation led by Danish Fundamental Metrology, a private, non-profit institute that functions as the Danish national metrological institute. As a national reference laboratory Risø shall:

- disseminate traceable non-contact temperature measurements with the lowest degree of uncertainty in Denmark under the accreditation of DANAK;
- participate actively in national and international collaboration, carry out research and report in literature and at conferences;
- maintain broad knowledge of the field and communicate it to relevant institutions and users;
- contribute significantly to the evolution of temperature metrology in Denmark.

In the short term the nomination will strengthen Risø's contact to international project partners in the field, and over time improve measurement capabilities. The nomination is an important highlight and points out the importance and quality of the work carried out by the temperature laboratory at Risø.

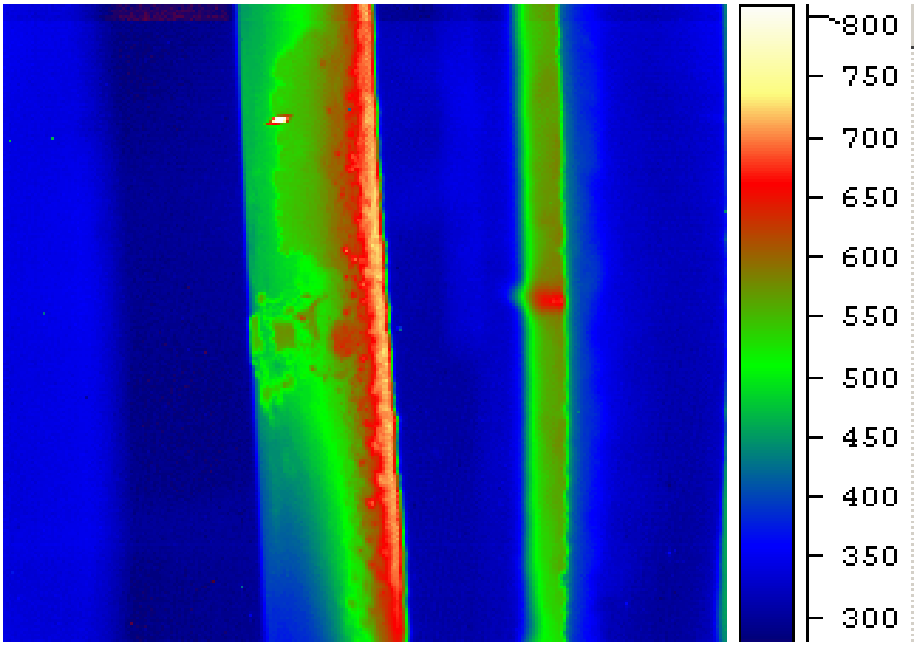

Figure 51. Infrared picture of surface temperatures of deposit layer on sampling probe and flying burning wood particle (white area). Result from experiment with Risø's IR-camera at the Technical University of Denmark.

Risø is involved in the EU project "EVITHEM" started in 2003 with participation of laboratories from most of Europe. The overall objective of the project is to form a European virtual institute in thermal metrology.

A new one-day course on infrared temperature measurement was held at the Danish Technological Institute (DTI) as the result of cooperation with DTI on technical courses for industry.

1. Clausen, S., Non-intrusive gas analysis at high temperature (invited talk). Meeting on non-intrusive gas analysis at high temperature, Risø (DK), 29 Sep 2003.
2. Sønnik Clausen, Guilin Hu, Peter Arendt Jensen, Lasse Holst Sørensen, ”Overfladetemperatur af belægningsprobe” (in Danish), Forskningscenter Risø, Roskilde, November 2003.

3.5.4 Optical thickness measurement at industrial demands

S. Arnfred Nielsen (FORCE Technology, Brøndby, Denmark) and P. E. Andersen
peter.andersen@risoe.dk

A co-operative project between FORCE Technology, Risø National Laboratory and Coloplast has resulted in the development of an optical thickness meter for the production of polymeric adhesives at Coloplast. Polymeric adhesives are a relatively expensive material in the production of colostomy bags, plasters, etc.

The thickness meter is a fibreoptic precision measuring instrument developed as part of the Centre for On-Line, Non-Contact Sensing, Monitoring and Control of Industrial Processes and Systems (BIPS) project and is based on low coherence interferometry. This technology is also applied in optical coherence tomography (OCT), which is a well-established diagnostic instrument for diagnostics of, e.g., skin diseases.

In addition to the high accuracy of this measuring method, OCT is also attractive, as it only requires access from one side of the material. Furthermore, OCT is a non-contact technique and very flexible. Additionally, in connection with the project we succeeded in developing algorithms for robust reproduction of 22 thickness measurements in nearly real time. The OCT22 instrument is now implemented on a production line moving at a speed of 40 m/s. The project was part of BIPS.

3.5.5 Optical inspection of ”reliable” plastic weldings

S. Arnfred Nielsen (FORCE Technology, Brøndby, Denmark) and S. Clausen
sonnik.clausen@risoe.dk

A co-operative project between FORCE Technology, Risø National Laboratory and Coloplast has resulted in the development of an optical method for detection of ”reliable” plastic weldings. The method was developed especially for the production of urine bags at Coloplast. A leaking urine bag would be very inconvenient for the incontinence patient and the plastic weldings therefore have to be most reliable.

This method is based on active pulsed thermography developed as part of the Centre for On-Line, Non-Contact Sensing, Monitoring and Control of Industrial Processes and Systems (BIPS). The infrared technique shows pictures in which the type of welding defects are revealed enabling the welder to adjust the welding parameters exactly. The pictures also reveal weak weldings that cause the bag to leak when burdened by the urine.

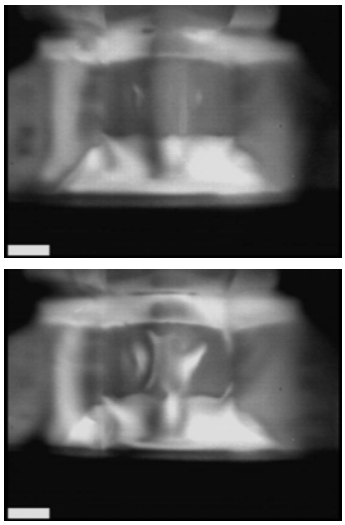

Figure 52. Example of welding defect in a reliable (upper photo) and leaking (lower photo) urine bag. Plastic foil with good adherence to the base appears as dark zones, while foil with no or poor adherence to the base appears as light zones.

3.6 Calibration

3.6.1 Calibration of temperature measuring equipment

M. Kirkegaard, F. Andersen and F. Eliasen
mogens.kirkegaard@risoe.dk

For more than 40 years the Thermometry Laboratory has calibrated temperature-measuring equipment. The Thermometry Laboratory was accredited in 1978 and has been approved by the Danish Accreditation Scheme, DANAK, to issue certificates for calibration of temperature-measuring equipment.

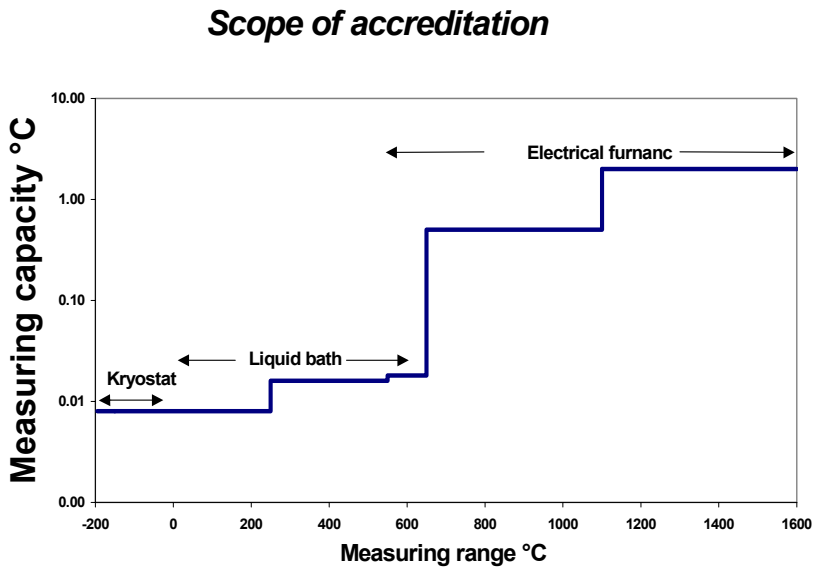

The instruments in the laboratory are traceable to international standards. The reference thermometers are regularly calibrated at National Physical Laboratory in London (NPL) to secure accordance with the international temperature scale, ITS-90.

The range has recently been raised and is now the largest for any Danish accredited laboratory. The range is from -196 ^{o}C to 1600 ^{o}C. The scope of accreditation and measuring capacity can be seen in the figure below. The temperatures are achieved in a set of thermostats depending on temperature as shown in the figure above.

3.6.2 Calibration of voltage, resistance current and pressure measuring equipment

M. Kirkegaard, F. Andersen and F. Eliasen
mogens.kirkegaard@risoe.dk

In connection with temperature measurements it was found necessary to perform measurements of voltage, resistance and current. For that reason these parameters have been accredited in a smaller area (Scope of accreditation and measuring capacity). In measurements at autoclaves it has also been found advantageous to measure pressure; therefore this parameter has been accredited in the area from 0 to 4 BarA.

3.6.3 Process measurement

F. Andersen, S. Clausen, M. Kirkegaard and F. Eliasen
finn.andersen@risoe.dk

The Thermometry Laboratory performs accredited "in situ" measurements, especially with respect to demanding temperature measurements in all kinds of process plants such as medical sterilisation, large power plants and incinerators. This service includes process measurements and visualisation with advanced measuring techniques developed by the research activities and not generally available.

For further information and quotations, please contact Mogens Kirkegaard, Finn Eliasen or Finn Andersen. For further information on infrared temperature, please contact Sønnik Clausen.

4. Plasma and fluid dynamics

4.1 Introduction

H. Bindslev
henrik.bindslev@risoe.dk

The year 2003 saw our activities in plasma physics and technology expand while activities in fluid dynamics were scaled back and pursued principally where direct synergy with our efforts in plasma science exist. This shift in emphasis is reflected in the fact that with the New Year 2003/2004 the research programme changes name from *Plasma and Fluid Dynamics* to *Plasma Physics and Technology*. As a follow-on from that, the department changes name to *Optics and Plasma Research Department.* With this shift we concentrate and build on our core competence in plasma physics, spanning the field from the high temperature plasmas required for fusion energy to low temperature plasmas for a broad range of current and near term environmental and industrial applications. The latter include cleaning of exhaust gasses, sterilisation, material synthesis, and modification of surfaces for instance to improve adhesion.

A plasma is a dense collection of free ions and electrons. The transitions from solids to fluids to gases are associated with increases in internal energy, the breaking of bonds and changes of physical properties. The same is true of the transition from a gas to a plasma; in fact the plasma is rightfully described as the fourth state of matter, its physics differing as much from that of gases as that of solids does. Just as solid state physics is involved in a broad range of applications, so it should be no surprise that plasmas have a broad range of applications, that their physics and chemistries are rich, and that the methods of generation and diagnosis are wide and complex.

Our activities in high temperature plasmas, aimed at developing fusion energy, are coordinated with the European EURATOM fusion programme through an agreement of association on equal footing with other fusion laboratories in Europe. Our EURATOM association facilitates extensive collaboration with other fusion research laboratories in Europe, crucial in the ongoing build-up of competences at Risø, and gives us access to placing our experimental equipment on large fusion facilities at the Max-Planck Institute for Plasma Physics in Garching and at the Research Centre Jülich, both in Germany. Our association with EURATOM also provides the basis for our participation in the exploitation of the European fusion research centre, JET, located in England. The European fusion programme, with its organisation of national programmes as EURATOM associations, is a successful example of a large *European Research Area.* Our activities in high temperature plasma research and the development of fusion energy are introduced in subsection 4.1.1, and described in further detail in subsection 4.2 discussing turbulence and transport in fusion plasmas, and in subsection 4.3 discussing our use of millimetre waves for investigating the dynamics of fast ions in fusion plasmas.

The scope for our new activities in low temperature plasmas is sketched in subsection 4.1.2. These activities were initiated this year with a project to reduce NOx emissions from gas power stations as reported in subsection 4.4. Activities in the fields of sterilisation, material synthesis and surface modifications are under preparation. The latter is pursued in collaboration with the Materials Research Department and the Danish Polymer Centre, both at Risø.

Activities in the field of fluid dynamics are discussed in subsection 4.5 and in the fields of optics and acoustics in subsection 4.6. The latter include remote sensing of defects in rail track by opto-acoustic methods described in subsection 4.6.5.

4.1.1 Fusion plasma physics

H. Bindslev
henrik.bindslev@risoe.dk, www.risoe.dk/euratom

Producing significant amounts of fusion energy requires a plasma with a temperature of 100 to 200 million degrees and densities of 1 to 2 times 10^{20} particles per cubic metre, corresponding to a pressure of 1 to 5 atmosphere. Unlike gases, plasmas can be confined and compressed by magnetic fields. At the required temperatures the plasma must be lifted off material walls to prevent the plasma from rapidly cooling. This is done by suspending the plasma in a toroidally shaped magnetic field which also acts to balance the plasma pressure. The required temperature and densities have been achieved in the joint European fusion experiment, JET. The production of net energy adds the requirement that the energy in the plasma be confined at least on the order of 6 seconds. The confinement time is the characteristic time for cooling off if heating was switched off, or equivalently the ratio of plasma energy to required heating power to sustain that energy content. Achieved confinement times are on the order of 1 second. Higher density could compensate shorter confinement time and visa versa; so a simplified statement of the target is that the product of temperature, density and confinement time should be 6 atmosphere seconds and is currently 1 atmosphere seconds. Progress towards the goal principally involves improving the confinement time, or equivalently reducing the energy transport in the plasma. The energy transport in fusion grade plasmas is principally due to turbulence, one of our main research activities which is reported in subsection 4.2. Significant progress towards the goal is expected with the next step fusion experiment, ITER, which has been designed and currently is being negotiated between the participants, Europe, Japan, Russia, USA, China and Korea. In ITER significant fusion rates are expected and with that the fast ion populations in the plasma will dramatically increase compared with present machines. The fast ions may then significantly influence the plasma and is thus one of the central physics issues to be studied in ITER. It is in fact also one of our main research topics in fusion as reported in subsection 4.3.

The fields of turbulence, transport and fast ions are closely knit. With steep gradients in plasma equilibrium parameters and with populations of energetic ions far from thermal equilibrium, fusion plasmas have considerable free energy. This energy drives turbulence, which in turn acts back on the equilibrium profiles and on the dynamics of the fast ions. The turbulence naturally gives rise to enhanced transport, but also sets up zonal flows that tear the turbulent structures apart and give rise to edge transport barriers; most likely at the root of the poorly understood, but experimentally reliably achieved, high confinement mode (H-mode). This non-linear interplay between turbulence and equilibrium also supports transient events reminiscent of edge localized modes (ELMs) where energy and particles are ejected from the plasma edge in intermittent bursts.

This set of topics is the focus of our fusion plasma physics research: With first-principles based codes we seek to model the interplay between plasma turbulence, transport and equilibrium. This modelling is tested against experimental data in collaboration with other fusion plasma physics institutes. To elucidate the physics of fast ions and their interplay with turbulence, waves and transient events, we are engaged in the diagnosis of confined fast ions by collective Thomson scattering (CTS) at the TEXTOR tokamak at the Research Centre

Jülich, Germany, and at the ASDEX upgrade tokamak in the Max-Planck Institute for Plasma Physics in Garching, Germany.

Our aim is not only to understand the dynamics, but also to identify external actuators with which the turbulence and transport can be controlled. The first demonstrations of edge turbulence control with arrays of electrostatic probes have been made in a linear device in collaboration with other associations. Selective ejection of core fast ions by sawteeth, which in turn can be manipulated by a localized heating and current drive, was found in fast ion CTS data obtained at TEXTOR in collaboration with TEC[1] and MIT, USA.

1. TEC: the Trilateral Euregio Cluster, a collaboration of FOM Institute for Plasma Physics, Holland; ERM/KMS, Belgium and Forschungszentrum Jülich, Germany.

4.1.2 Low temperature plasma technology

H. Bindslev
henrik.bindslev@risoe.dk

Low temperature plasmas, unlike high temperature plasmas encountered in fusion research, are mostly partially ionised. That is, they are mixtures of electrons, ions and neutrals which can be atoms, radicals and molecules in various states of excitation. The dynamics of low temperature plasmas thus include a rich field of plasma chemistry. Low temperature plasmas can be generated by exciting and ionising gas mixtures. Excitation from fluid or solid mixtures is also possible. Excitation can be achieved by a wide variety of means ranging from lasers over microwaves and radio waves to pulsed and low frequency electromagnetic or DC excitation. The method of excitation, the gas mixture, the pressure and the ambient conditions all influence the state of the plasma and hence its properties. Low temperature plasmas can be highly aggressive and used for cutting or etching solids, or so gentle that they can be applied directly to plastics or human skin. To meet the demands of a specific application it is often essential to design the state of the plasma carefully. Here the energy distributions of electrons, ions and neutrals, which can be quite different, may be important, just as the distribution of energy states of neutrals and concentrations of radicals can. Anisotropies, induced for instance by magnetic fields, and inhomogeneities can be designed and be essential for certain applications, just as temporal variations in the plasma state can be. Diagnosing and modelling the plasma state is crucial in designing the plasma for a specific application. Diagnostic techniques include emission and absorption spectroscopy, interferometry and scattering, and material probes. For industrial exploitation there is considerable process and financial advantage to operation at atmospheric pressure. Scientific investigation and development of such plasmas has expanded dramatically in recent years, in part driven by needs of industry. Our new activities in low temperature plasmas for environmental and industrial applications, described in subsection 4.4, thus also emphasise atmospheric pressure plasmas, though not to the exclusion of low pressure plasmas.

4.2 Turbulence and transport in fusion plasmas

O. E. Garcia, V. Naulin, A. H. Nielsen and J. Juul Rasmussen
volker.naulin@risoe.dk; jens.juul.rasmussen@risoe.dk

The transport of heat and particles across the confining magnetic field of fusion plasmas is one of the most important and interesting, but also difficult areas of contemporary fusion research. It is well established that the “anomalous” transport component mediated by low frequency turbulence is far larger than the classical collisional transport. It is thus of utmost

importance to achieve a detailed understanding of this transport and the underlying turbulence for the design of an economic, advanced fusion reactor based on magnetic confinement schemes. In spite of dramatic progress in experiment, theory and computations during recent years, the quantitative understanding is still very sparse and any predictive capacity is at best rudimentary. Even with very fundamental phenomena such as transitions from low confinement regime (L-mode) to high confinement regime (H-mode), the profile resilience and the particle pinch that are routinely observed and classified experimentally have no generally accepted explanations.

We have mainly focused our activities in plasma turbulence and transport on topics related to edge turbulence. It is found that the conditions near the edge of the plasma are dictating the global performance, which seems natural since all transport has to go through the edge region. Our investigations are based on numerical solutions of first-principle models, and we aim at benchmarking results and performance with other codes and also with experimental observations when available.

Our investigations have comprised direct numerical simulations of both impurities and tritium transport in the edge plasma region (see 4.2.1), where we found strong asymmetric transport features with a dominating pinch convection on the low-field side and an anti-pinch, i.e. outward convection, at the high-field side. In the contributions 4.2.2-4.2.3 we consider the bursting and intermittency in the fluxes of particles and heat, which come about due to nonlinear energy exchange between global poloidal flows and small-scale turbulent fluctuations. It is notable that in 4.2.2 we have derived a new energy conserving global model for transport at the transition from the edge to the scrape-off-layer (SOL). Results from this model reproduce in detail recent experimental observations of plasma blobs propagating far out into the SOL. These propagating blobs are responsible for strongly intermittent bursts of hot plasma, which pose a problem to plasma facing components in next step devices.

In general, the turbulent as well as the transport in fusion devices are observed to be strongly intermittent. In 4.2.4 we describe experimental investigations of the intermittency of small-scale fluctuations in Wendelstein 7-AS during controlled transitions in the confinement. The investigations are based on collective scattering measurements of density fluctuations utilizing the equipment constructed and run by Risø. The results indicate that the characteristics of the fluctuations are independent of the path to good or bad confinement.

In the plasma edge region the turbulent transport is found to be dominated by energetic bursts. Thus, the probability distribution functions (PDFs) of the particle and heat fluxes are skewed with fat tails, and are strongly deviating from Gaussian distributions. The mean value and variance of the PDF is therefore not sufficient to make predictions about the transport and the associated heat load on plasma facing components. It is essential to have knowledge of the full PDF, or at least higher order moments. In 4.2.5 we show that the transport PDFs for a number of different models have similar structure; that is the tails of the PDFs are well described by an extreme value distribution and are consequently decaying exponentially and not as a power law, as frequently speculated elsewhere. These results are utilized in collaboration with the Innsbruck Experimental Plasma Physics Group on the evaluation of fluctuation data from emissive probe measurements. The initial phase of this collaboration is described in 4.2.6.

The final topic is concerned with the generation of global shear flows by the turbulence, and the interplay between these flows and the turbulent transport. These flows are assumed to play a crucial role in the transition from the low confinement to the high confinement regime (LH-transition). The importance of the self-generation of these flows by the turbulence has become increasingly clear. However, the exact mechanisms have not yet been quantitatively assessed. We have investigated the generic flow generation in drift-Alfvén turbulence in 4.2.7. For increasing plasma beta the so-called Maxwell stress will compete with the

Reynolds stress and limit the flow generation; however, an additional effect due to the geodesic part of the curvature comes into play and adds to the shear flow. In 4.2.8 we consider a simple model of drift waves and investigate the parametric dependence of the width of zonal flow bands. Finally, in 4.2.9 we report on our investigations of the linear instability features of interchange modes in the presence of imposed shear flows of various profiles.

4.2.1 Impurity and trace tritium transport in tokamak edge turbulence

V. Naulin (work performed while seconded to JET under the EFDA agreement)
volker.naulin@risoe.dk

The transport properties of impurities are of great concern in magnetic fusion devices. Pinching of impurities has been observed as well as fast inward transport of trace tritium in JET tritium puffs. We here investigate the transport of passive impurity species in electromagnetic edge plasma turbulence. The turbulence is generated by a fluctuation model in flux-tube geometry and for the passive species we consider cold ions of finite mass.

Impurities released at the high field side experience an anti-pinch and while diffusing is convected out of the plasma, whereas particles released on the low field side are sucked into the plasma by a pinch effect, see Figure 53.

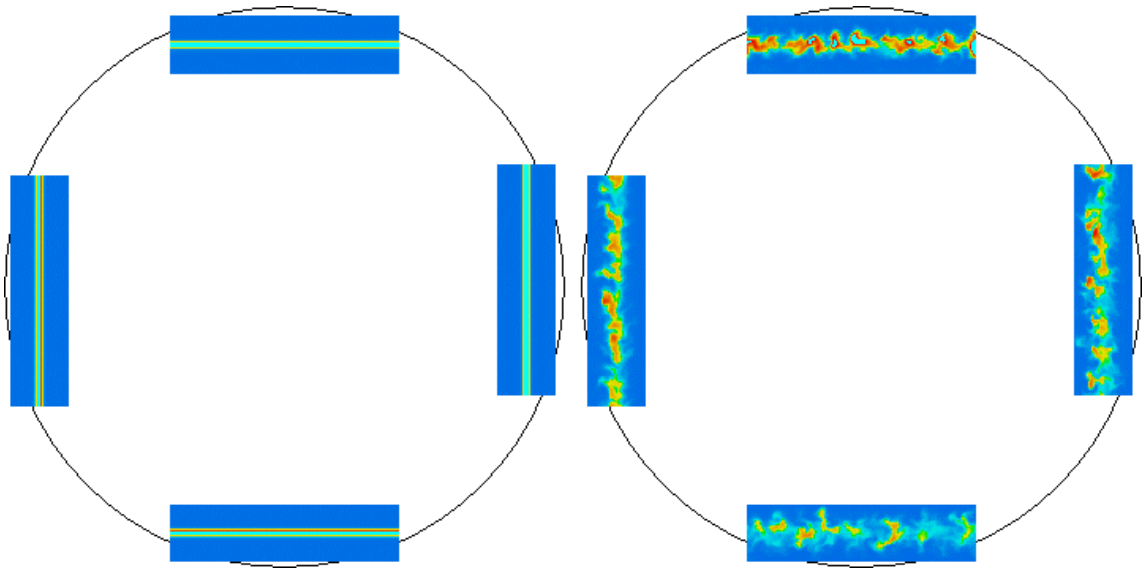

Figure 53. Impurity density in edge turbulence. Left initial distribution, right after 50 microseconds. A poloidally varying pinch effect is seen.

Initial investigations show very reasonable agreement with experiments and demonstrate that impurity transport needs at least a two-dimensional transport model resolving both radial and poloidal coordinates. This initial investigation also showed that the description of the transport Γ as given by a diffusion value D and a pinch velocity V can be justified as a first approximation.

4.2.2 Intermittent transport in scrape-off layer plasmas

O. E. Garcia, V. Naulin, A. H. Nielsen and J. Juul Rasmussen
odd.erik.garcia@risoe.dk

The radial transport of plasma and heat is universally observed to be highly intermittent in the scrape-off layer (SOL) of magnetic plasma confinement experiments. From local probe measurements it is generally observed in magnetized plasmas that the averaged density, the temperature and the electric field signals possess asymmetric waveforms with a sharp rise and slow decay, similar to the waveform from our numerical results depicted in Figure 54. Moreover, the probability distribution functions (PDFs) are positively skewed and flattened, indicating propagation of thermal structures through the SOL region. Theoretical and computational descriptions of SOL turbulence have so far assumed a local generation of turbulent fluctuations due to steep pressure gradients in the SOL region. However, experimental measurements reveal a flattened pressure profile throughout the SOL. This indicates that the observed waveforms may be due to blobs of plasma and heat ejected from the core or edge plasma and travelling through the SOL region, assuming the blob transition time through the SOL is short compared with the measurement integration time.

A new model for non-linear interchange modes has been derived which yields a conservative energy transfer between kinetic energy due to ExB drifts and thermal energy.[1] This model emphasizes the non-linear collective dynamics while a simplification is made for the dissipative processes due to particle losses along open magnetic field lines in the SOL. Forcing is invoked by means of a heat source in the edge region with closed field lines, but magnetic shear has been neglected to allow a two-dimensional description. Long-run numerical solutions of this model covering the longest time scales reveal a regulation process due to self-sustained sheared flows, which results in bursting in the fluctuation level in the edge region and relaxation oscillations in the confined heat and the total mean flow energy. The repetitive generation of sheared flows by fluctuating motions leads to ‘‘flapping’’ of the edge pressure gradient whereby blobs of hot plasma are ejected into the SOL. Also the statistical properties of the propagating structures are in excellent agreement with experimental observations. In particular, we observe asymmetric waveforms, positively skewed and flattened PDFs, and radial propagation velocities up to one tenth of the sound speed. In Figure 54 we show the conditionally averaged density signal, using the trigger condition $n > 4n_{rms}$, and the PDF of the density signal at different radial positions. The highly intermittent transport events set the heat load which the plasma facing components in next generation confinement experiments must withstand.

1. O. E. Garcia, V. Naulin, A. H. Nielsen and J. Juul Rasmussen, ‘‘Intermittent transport in scrape-off layer plasmas’’, http://arxiv.org/abs/physics/0309020.

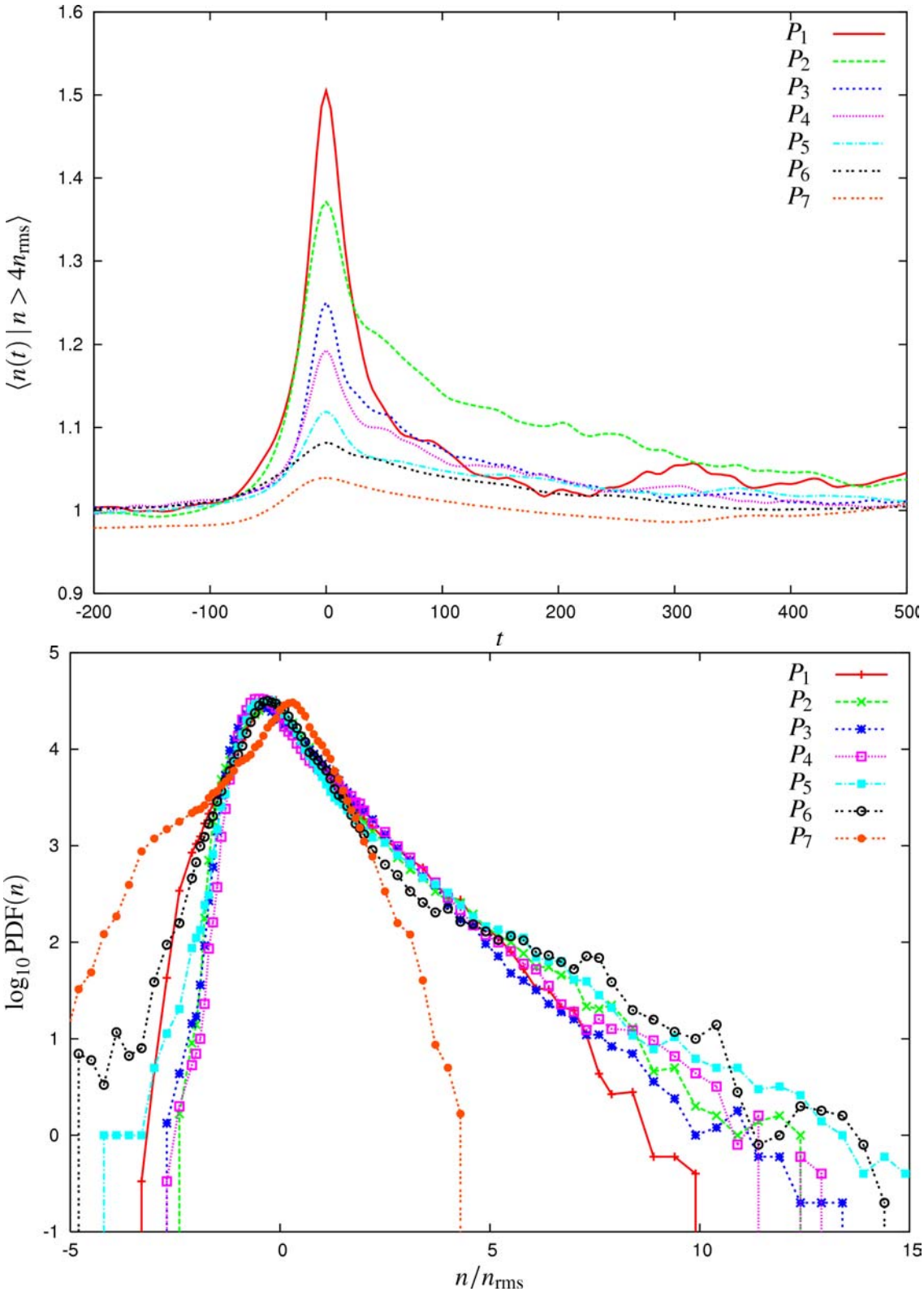

Figure 54. Results of the long time numerical simulations: Upper panel: Conditionally averaged density signals as measured at seven different radial positions. P1 is inside the last closed flux surface and P7 is in the far SOL. Lower panel: The probability distribution functions of the density fluctuations measured at the same positions.

4.2.3 Self-regulation, bursting and large-scale intermittency in convective turbulence

O. E. Garcia and N. H. Bian (Istituto Nazionale Fisica della Materia, Department of Energetics, Politecnico di Torino, Italy)
odd.erik.garcia@risoe.dk

Rotating fluids and magnetically confined plasmas are prone to quasi-two-dimensional fluctuations which lead to substantial radial transport of particles and heat. The fluctuating motions may undergo secondary instability that results in the formation of differential rotation in the azimuthal directions, which can strongly reduce the non-linear transport and thus improve the heat confinement. Examples include thermonuclear fusion experiments and atmospheres of rotating planets.[1-3] Commonly observed in such systems are low frequency bursting in the fluctuation level and relaxation oscillations in the mean flow energy level as well as in the heat confinement when the latter is allowed to vary.

The net turbulent transport therefore appears as quasi-periodic bursts separated by quiet phases. The prevailing theory for such self-regulating behaviour is based on the shearing effect due to differential advection by the mean azimuthal flows. This shearing is essentially a spectral expulsion of fluctuation energy to large radial wave numbers, leading to enhanced dissipation of convective structures and, hence, less turbulent transport.

The work reported here has demonstrated that an alternative interpretation may be given simply in terms of the energy conserving interaction between fluctuating and mean flows.[1-3] This interpretation readily explains the formation of improved confinement regimes due to sheared flows, observed in experiments and computer simulations. This point of view emphasizes the intrinsic dynamical nature of convective systems and precludes the wide-spread interpretation in terms of linear stabilization of convective modes by sheared flows. A variety of computations demonstrate the essential role of energetics for transport regulation by self-sustained sheared flows.[1,2] The bursting regime has further been demonstrated by phenomenological predator-prey-like models, which also show that the collisional dissipation of the mean profiles determines the time scale for the low frequency relaxation oscillations.[2,3]

Another regulation mechanism resulting in transport bursting is shown to result from the quasi-linear modification of the pressure profile from the turbulent heat transport.[3] The frozen-profile approximation, frequently applied in massive computations, rules out this important effect. For both regulation mechanisms, numerical simulations have demonstrated that the low frequency bursting gives rise to large-scale intermittency, manifested by exponential tails in the probability distribution functions of single-point recording of the fluctuating fields.[1,2] Moreover, this leads to high spectral energy content at low frequencies, which is frequently confused with self-organized critical behaviour.

1. O. E. Garcia, N. H. Bian, J.-V. Paulsen, S. Benkadda and K. Rypdal, ‘‘Confinement and bursty transport in a flux-driven convection model with sheared flows’’, *Plasma Phys. Control. Fusion* **45**, 919 (2003).
2. O. E. Garcia and N. H. Bian, ‘‘Bursting and large-scale intermittency in turbulent convection with differential rotation’’, *Phys. Rev.* E **68,** 047301 (2003).
3. N. H. Bian and O. E. Garcia, ‘‘Confinement and dynamical regulation in two-dimensional convective turbulence’’, *Phys. Plasmas* **10**, 4696 (2003).

4.2.4 Study of intermittent small-scale turbulence in Wendelstein 7-AS plasmas during controlled confinement transitions

N.P. Basse (Plasma Science and Fusion Center, Massachusetts Institute of Technology, MA, USA), S. Zoletnik (CAT-Science, Budapest, Hungary), P.K. Michelsen and W7-AS Team (IPP, Garching, Germany)
poul.michelsen@risoe.dk

The role of plasma turbulence in confinement transitions, both induced and spontaneous, is currently being investigated in most magnetic confinement fusion devices. This work is part of that continual effort, and focuses on internally and externally induced confinement transitions.

It is a well known fact that confinement in the Wendelstein 7-AS (W7-AS) stellarator[1] is very sensitive to the boundary value of the rotational transform, ι_a. Here, a is the minor radius of the plasma. Optimum confinement is found in narrow ι_a-windows close to (but not at) low-order rationals $\iota_a = 1/2, 1/3$, etc. The special significance of these windows is that they are free from the otherwise densely spaced higher-order rational ι_a-values. Therefore it has been assumed that perturbations arising at higher-order rational surfaces enhance the electron transport. These perturbations could be either static (due to the magnetic field) or dynamic (due to turbulence or magneto-hydrodynamic activity). We are investigating the changes in electron density fluctuations associated with the varying confinement quality at different ι_a.

The diagnostics available for our analysis are Mirnov coil measurements of magnetic fluctuations and the collective scattering measurements of density fluctuations using an infrared light source, constructed and operated by Risø till the closure of W7-AS.

We have analysed discharge types in plasmas with edge rotational transforms ι_a close to 1/3, where confinement is very sensitive to small changes in ι_a. Good (bad) stationary confinement is achieved at $\iota_a \sim 0.34$ (0.36) with zero net plasma current, and the transient good to bad confinement transition is obtained by having the external $\iota_a \sim 0.34$, while ramping up the net plasma current from zero to raise the total ι_a.

Our analysis has shown that the major spectral characteristics of the density fluctuations are independent of the path to good or bad confinement. This includes auto- and cross-power spectra and the speed of the density fluctuations. However, auto-power spectra of magnetic fluctuations display differences between transient and stationary discharges.

Correlation calculations between band auto-powers in the two density fluctuation measurement volumes showed that the correlation increases for both the stationary and the transient good to bad confinement transition. The density fluctuation power is intermittent, and the bursts are correlated between the bottom and the top of the plasma. Correlations between magnetic and density fluctuations confirmed the analysis performed with only density fluctuation measurements. The correlation time of the bursts is on the order of 100 μs, similar to the lifetime observed during edge localized modes. It is possible that the correlated fluctuations are due to large-scale zonal flows; that is a topic for future works.

1. H. Renner et al., *Plasma Phys. Control. Fusion,* **31,** 1579 (1989)

4.2.5 Statistical properties of transport in plasma turbulence

V. Naulin, O. E. Garcia, A. H. Nielsen and J. Juul Rasmussen
volker.naulin@risoe.dk

In hot magnetized plasmas the cross-field transport of particles and heat is mainly mediated by low frequency turbulence and is far larger than that expected from collisional diffusive transport. Additionally, the transport near the plasma edge is generally observed to be strongly intermittent and dominated by strong bursts. Thus, the probability distribution functions (PDFs) of the particle and heat fluxes are skewed with fat tails and are strongly deviating from Gaussian distributions. The mean value and variance of the PDF is therefore not sufficient to make predictions of the transport and of the associated heat load on plasma facing components. It is essential to have knowledge of the full PDF, or at least higher order moments.

We have investigated the statistical properties of the turbulent particle flux in different types of plasma turbulence models. These models are solved numerically and the particle flux is characterized by the PDF. The physics included in the applied models range from two-dimensional drift wave turbulence to three-dimensional MHD dynamics. We have considered local fluctuation type models, based on separation of the scale length of the background pressure gradient and the fluctuations as well as global models without scale separations and accounting for full evolution of the background. The aim is to address the essential question on how the transport PDF depends on the driving mechanism behind the turbulence, and ultimately: will it be possible to devise a generic transport PDF that is governed by a few parameters only?

The PDFs of the flux measured at one point, which mimics the experimental measurements of the flux by probe arrays (see 4.2.6), show a strongly skewed PDF with a tail toward positive (outward) flux events. For the local models, where the PDF of potential and density fluctuations are close to Gaussians, the flux PDF is well described by a PDF of a random variable that results from the product of two correlated Gaussian distributed random variables.[1] Both for the global and the local models the tails of the PDF are decaying exponentially and not as a power law, as frequently speculated elsewhere.

We also investigated the flux-surface averaged flux, and again the PDFs were skewed with a fat tail towards positive events. For the local models these PDFs are generally in good agreement with extreme value distributions (EVDs), which implies that the tail decays exponentially. This may be interpreted as a signature of strong vortical structures that dominate the transport on individual flux surfaces. The global models exhibit properties distinctly different from those observed in the local models. Specifically, the flux-surface averaged particle fluxes from the former models have a sharp peak at low transport values. This is due to the bursting of the global fluctuation level (see, e.g., 4.2.2 and 4.2.3). The bursty behaviour is caused by a regulation mechanism due to self-sustained sheared mean flows. However, also for these global models the tails of the PDFs are well fitted to EVDs as seen in Figure 55.

1. B.A. Carreras, C. Hidalgo, E. Sánchez, M. Pedrosa, R. Balbín, L. García-Cortés, B. van Milligen, D.E. Newman and V.E. Lynch, *Phys. Plasmas* **3**, 2664 (1996).

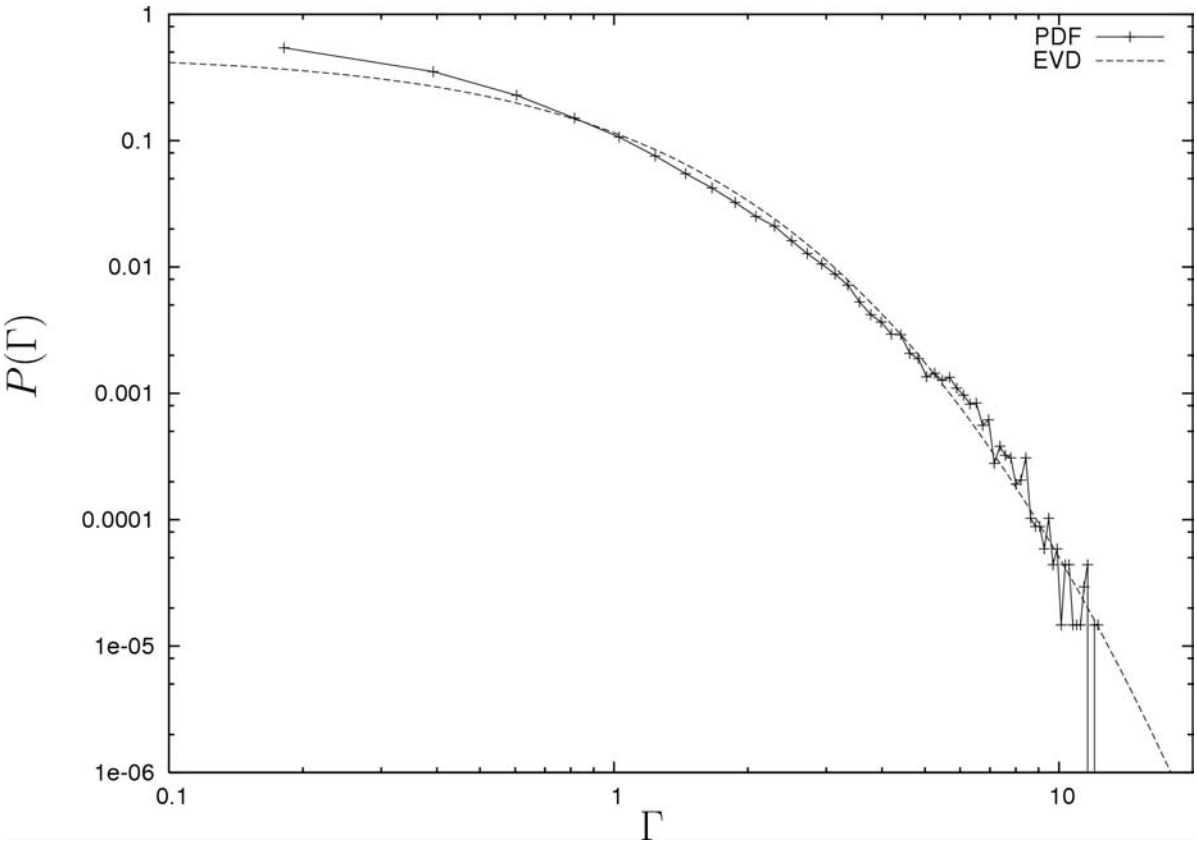

Figure 55. Tail of the flux-surface averaged particle transport fitted with an extreme value distribution for the global interchange model.

4.2.6 Evaluation of measured turbulent particle fluxes in toroidal devices

P.C. Balan, R.W. Schrittwieser*, C. Ionita* (*Institute for Ion Physics, University of Innsbruck, Austria), O. E. Garcia, V. Naulin, A. H. Nielsen and J. Juul Rasmussen*
jens.juul.rasmussen@risoe.dk

A collaborative project has been established between the Innsbruck Experimental Plasma Physics Group at the University of Innsbruck and Risø. The aim is to contribute to the evaluation of measurements of potential and density fluctuations, and of fluctuation driven particle flux and Reynolds stress performed by the Innsbruck group. The measurements are carried out by using arrays of emissive probes. Comparison of the measurements with results obtained from simulations of plasma turbulence is an important element in this collaboration. In the initial phase, we have mainly considered the evaluation of the particle flux, which can be obtained directly from measurements of the density fluctuations and the fluctuations in the radial velocity component (proportional to the poloidal electric field). It is generally found that single point measurements of the particle flux show strong non-Gaussian features, revealing probability distribution functions (PDFs), with a strong tail towards positive (outward) flux events. This is in agreement with results obtained in simulations (see 4.2.5) and expected for Gaussian density and electric field fluctuations. In order to obtain a quantity that may be compared with the flux-surface-averaged particle flux (see 4.2.5), we average the flux signal, measured at a single position, over some time interval comparable with the correlation time, to create a new series of random variables that consist of these "short-time" averaged fluxes. The underlying assumption is that the fluctuations are mainly propagating in the poloidal direction. The PDF of this quantity is found to be well described by the extreme

value distribution as was found for the flux-surface averaged flux in the simulations (see 4.2.5), although more data and in particular longer experimental time series will be needed for a detailed comparison.

4.2.7 Shear flow generation in electromagnetic plasma edge turbulence

V. Naulin, O. E. Garcia, A. H. Nielsen, J. Juul Rasmussen and A. Kendl
volker.naulin@risoe.dk

Shear flows play a crucial role in the transition from the low confinement to the high confinement regime in magnetically confined fusion plasmas (LH-transition). The importance of turbulence as an ingredient to their formation has over the last years become increasingly clear. The exact way the small-scale turbulence is capable of setting up flows and thereby to interact with the meso-scale is, however, not yet completely understood and a self-consistent model of the LH-transition is consequently lacking.

The flow generation in turbulence is due to a number of different mechanisms, the most well known being the Reynolds stress that describes the momentum transport by the turbulence. In electromagnetic turbulence the Reynolds stress is accompanied by the Maxwell stress, which reflects the momentum transport along perturbed magnetic field lines. To complicate the situation for complex magnetic field geometry a third contribution arises from the geodesic part of the curvature.

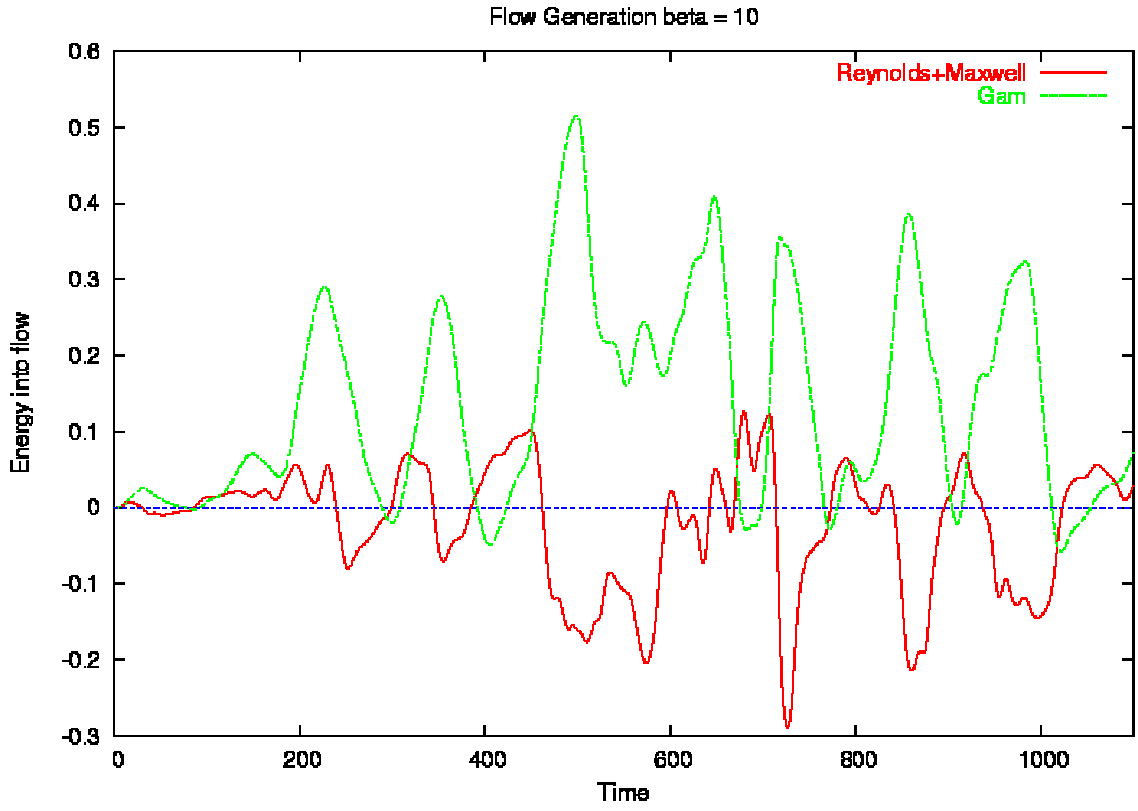

Figure 56. Energy input into the flow from the Reynolds and Maxwell stresses and from the geodesic acoustic modes.

The relative importance of these three mechanisms is investigated for drift-Alfvén turbulence by following the detailed energy transfers into the flow component. Initial results indicate that for higher plasma beta the Reynolds stress is dwarfed by the Maxwell stress. Furthermore, the geodesic curvature results in a transfer of energy into the flow component for large values of the plasma beta. In Figure 56 we show the energy input into the flow from the Reynolds and Maxwell stresses and from the geodesic acoustic modes.

4.2.8 Numerical investigations of large-scale zonal flows in drift wave turbulence

A.H. Nielsen, S. Delaux (MATMECA, Université Bordeaux, France), V. Naulin, O.E. Garcia and J. Juul Rasmussen
anders.h.nielsen@risoe.dk

The self-consistent generation of large-scale flows by the rectification of small-scale turbulent fluctuations is of great importance both in magnetically confined plasmas and in geophysical flows.[1,2] These flows regulate the turbulence that suppresses the small-scale structures and set-up transport barriers.

We have modelled the generation of zonal flows by drift wave turbulence in a magnetized plasma as described by the Hasegawa-Mima-Charney equation on a cylinder:

$$\frac{\partial}{\partial t}\left(\nabla^2\phi-\phi\right)+\frac{1}{r}\left[\phi,\nabla^2\phi\right]-\beta\frac{1}{r}\frac{\partial\phi}{\partial\theta}=\nu\Delta^2\phi-\eta\Delta\phi+F(\vec{r})\sin(\gamma t),$$

where ν is the kinematic viscosity and η a sheath damping. The last term in the equation is a body forcing term, where $F(\vec{r})$ is an array of vortices with opposing signs, illustrated in the first frame in Figure 57.

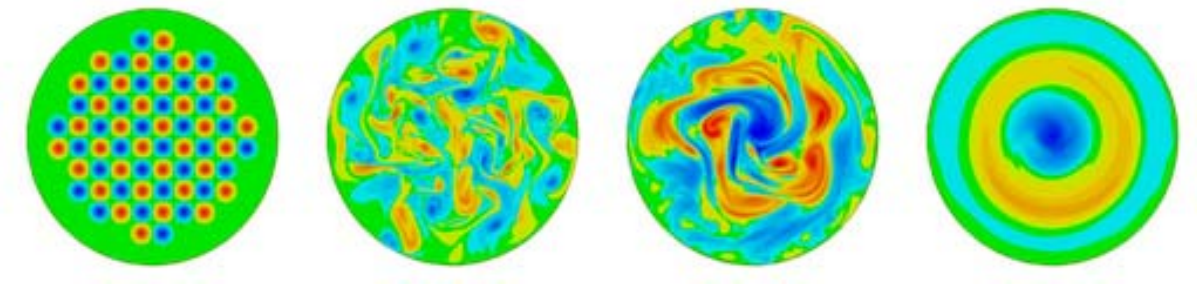

Figure 57. Temporal evolution of the electric potential, ϕ, for t=0, t=100, t=500 and t=1000. Parameters: ν=0.00001, β=0.256 and η=0.

We have numerically integrated the differential equation for different values of β on a disk applying a stress-free boundary condition.[3] In Figure 57 we display the temporal evolution of the electric potential, ϕ, where we have used an array of vortices as initial condition. After a turbulent phase, where larger structures are created by vortex-vortex merging, the flow settles into a regular pattern that consists of bands of potentials with opposing signs. For increasing values of β we generally observe more, but weaker bands.

1. P.W. Terry, *Rev. Mod. Phys.* **72**, 109 (2000).
2. P.B. Rhines, *Ann. Rev. Fluid Mech.* **11**, 401 (1979).
3. V. Naulin et al, *AIP Conf. Proc*. **669**, 662 (2003).

4.2.9 Do sheared flows inhibit interchange instability?

E.S. Benilov (Dept. Mathematics, University of Limerick, Ireland),
V. Naulin and J. Juul Rasmussen
jens.juul.rasmussen@risoe.dk

The suppression of turbulence and thereby of the associated transport by externally imposed or self-generated poloidal ExB-shear flows seems by now to be so widespread in the plasma context that it is believed to be universal.[1] This is in contrast to the general consensus in the hydrodynamics community, where it is well established that shear flows (with a finite curvature of the flow velocity profile) are generally unstable and that added shear flows act destabilizing rather than stabilizing, although there are examples of stabilizing effects in nonionized flows, in particular in geophysical flows.

To contribute to this standing discussion we have examined the particular example of shear flow effects on the interchange instability, which is unavoidable in a plasma with curved magnetic field lines. The investigations are performed by direct solutions of the eigen-problem for the linear instability on a bounded domain modelling the edge region in a toroidal plasma. We have examined the stability properties for several shear flow profiles. Generalizing the obtained results, we draw the following conclusions:

The stabilizing effect of variable shear is much weaker than that of the uniform one. Flows with sufficiently large shear anomaly cannot be stabilized no matter how strong the mean shear is.

Flows in a large slab are generally more unstable than those in a small one. There are strong indications that, in the absence of walls, flows with variable shear are all unstable - no matter how strong the mean shear is, and how weak the shear anomaly is.

All examples of flows with non-monotonic profiles turned out to be unstable.

Overall, given that realistic plasma flows always have variable shear, they appear to be unable to eliminate interchange instability (although they can still weaken it). We should, however, note that in all examples considered the instability had a short-wave cutoff, i.e., disturbances with $k>k_0$ are stable. Hence, if the poloidal length, L_y, is so that $L_y<2\pi/ k_0$, the flow should become stable. However, to explore this possibility in detail one should examine a full toroidal problem.

1. P. W. Terry, “Suppression of turbulence and transport by sheared flow”, *Rev. Mod. Phys*. 72, 109 (2000).

4.3 Millimetre waves used for diagnosing fast ions in fusion plasmas

H. Bindslev, S.B. Korsholm, F. Meo, P.K. Michelsen, S. Michelsen,
S.K. Nielsen and E.L. Tsakadze
henrik.bindslev@risoe.dk, www.risoe.dk/euratom/cts

Millimetre waves, corresponding to frequencies in the 100 GHz range, permit probing and imaging on the centimetre scale and transmission of signals with bandwidths in excess of 10 GHz. Coherent sources are now available from the micro- to Megawatt range, CW. These technologies, widely used in fusion research, and in many cases specifically developed for fusion research, are now being considered for a broader range of commercial applications. These include new GigaBit wireless Internet highways and wide area networks which avoid expensive trenching of optical fibres.

In the world of fusion, the millimetre waves are used extensively both as a diagnostic tool and as an actuator for manipulating the plasma locally as well as globally. Central to achieving these objectives is the fact that millimetre waves, like laser light, can be projected in narrow focused beams and, unlike laser light, the millimetre waves can interact strongly with the plasma.

At Risø we are developing millimetre wave diagnostics for measuring the velocity distribution of the most energetic ions in fusion plasmas. The measurements will be resolved in space on the centimetre scale and in time on the millisecond scale.

The most energetic (or fast) ions are the result of fusion reactions and auxiliary heating. Their interaction with the bulk plasma is the main mechanism by which the fusion plasmas reach and sustain the high temperatures of 100-200 million degrees Kelvin, required for fusion. The considerable energy associated with the fast ions can also drive turbulence in the plasma, and degrade the confinement of the plasma and of the fast ions themselves. Understanding and controlling the dynamics of fast ions are central tasks in the development of fusion energy, and one of the main research topics for the next large fusion facility, ITER. It is a task we seek to tackle by developing and exploiting the unique diagnostic capability of millimetre wave based collective Thomson scattering (CTS).

The group is currently developing fast ion CTS diagnostics for the TEXTOR and ASDEX-Upgrade tokamaks, which are located at the Research Centre Jülich in Germany and at the Max-Planck Institute for Plasma Physics in Garching, also in Germany. Further details of this work are given in subsections 4.3.1 and 4.3.2.

Construction and pre-installation testing of the ASDEX CTS system was completed and the system was installed in Garching in December 2003. The system for TEXTOR is under construction and testing at Risø. These projects are conducted in collaboration with MIT, the Max-Planck Institute for Plasma Physics in Garching and the TEC[1] consortium.

The CTS efforts at Risø in 2003 included a study of the feasibility of measuring the fast ion phase space distribution in ITER by CTS, described in further detail in subsection 4.3.6. The study covers the full range of potential probe frequencies from gyrotron based millimetre waves to the infrared light of the CO_2 laser. It was assessed whether the systems can meet the ITER measurement requirements and which technological developments may be required. The relative merits of the systems were compared. The study reveals that a CTS system based on a 60 GHz probe has the highest diagnostic potential, and is the only system expected to be capable of meeting all the ITER fast ion measurement requirements with existing or near term technology. A conceptual design was developed and costs estimated, details of which are given in subsection 4.3.7. With modest additions this system may also provide measurements of the fuel ion ratio.

On the basis of the millimetre wave activities for diagnosing fusion plasmas, the group responded to a call for solutions for private wireless AV transmission for music festivals and other venues. A system, using 94 GHz mm waves, was successfully demonstrated as discussed in subsection 4.3.8.

"Implementation of Fast Ion Millimeter Wave CTS Diagnostics on TEXTOR and ASDEX Upgrade", S. B. Korsholm, H. Bindslev, J. Egedal, J. A. Hoekzema, F. Leuterer, F. Meo, P. K. Michelsen, S. Michelsen, E. L. Tsakadze and P. Woskov, *45th Annual Meeting of the Division of Plasma Physics, American Physical Society* (DPP-APS), Albuquerque, New Mexico, October 27 – 31, USA, 2003.

[1] TEC: the Trilateral Euregio Cluster, comprising Association EURATOM-Forschungszentrum Jülich GmbH, Institut für Plasmaphysik, Jülich, Germany; Association EURATOM-FOM, Institute for Plasma Physics, Rijnhuizen, the Netherlands; and Association EURATOM-ERM/KMS, Belgium.

”Fast Ion Millimeter Wave CTS Diagnostics on TEXTOR and ASDEX Upgrade”, S. B. Korsholm, H. Bindslev, J. Egedal, J. A. Hoekzema, F. Leuterer, F. Meo, P. K. Michelsen, E. Tsakadze and P. Woskov, *30th EPS Conference on Controlled Fusion and Plasma Physics*, St Petersburg, Russia, July 7-11, 2003.
"Fast Ion Millimeter Wave CTS Diagnostics on TEXTOR and ASDEX", S. B. Korsholm, H. Bindslev, J. Egedal, J. A. Hoekzema, F. Leuterer, P. K. Michelsen, E. Tsakadze and P. Woskov, *44th Annual Meeting of the Division of Plasma Physics, American Physical Society* (DPP-APS), Orlando, Florida, USA (2002). Bulletin of American Physical Society (APS), p. 84, vol. 47, No. 9, November, 2002.

4.3.1 Construction of the collective Thomson scattering diagnostic upgrade for TEXTOR

S. B. Korsholm (also at MIT Plasma Science and Fusion Center, Massachusetts, USA), H. Bindslev, J. Egedal, J. A. Hoekzema (Association EURATOM-Forschungszentrum Jülich GmbH, Institut für Plasmaphysik, Jülich, Germany), F. Meo, P. K. Michelsen, S. Michelsen, E. L. Tsakadze and P. Woskov**
*(*MIT Plasma Science and Fusion Center, Massachusetts, USA)*
soeren.korsholm@risoe.dk, www.risoe.dk/euratom/cts/textor

In 2000-2001 the pilot version of the CTS system at TEXTOR, a collaborative effort between FOM, the Netherlands, and MIT, USA, obtained many useful data using a 100 kW, 0.2 s, 110 GHz gyrotron. However, due to the location of the CTS electronics close to the tokamak and configuration changes on TEXTOR itself, noise became an increasing problem. Furthermore, an upgrade of the antenna and receiver electronics was desirable, and a new data acquisition system was required.

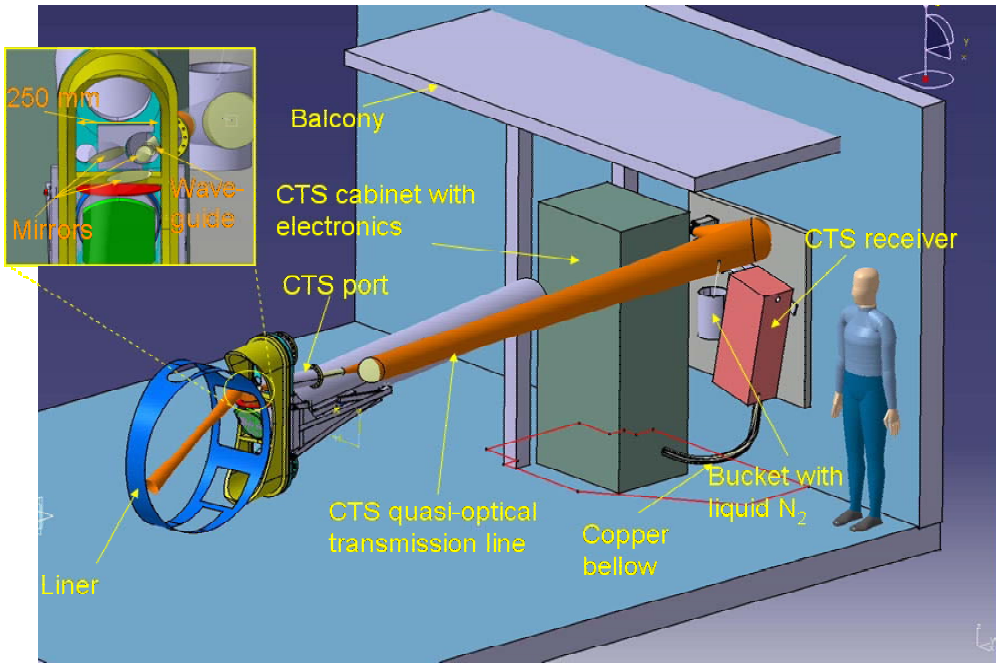

Figure 58. Overview of the TEXTOR CTS system. The quasi-optical beam is shown in orange.

In 2002 and 2003 a new quasi-optical transmission line was designed and constructed at Risø. The work on the transmission line is described in more detail in subsection 4.3.3. The main advances are a steerable (±30°) quasi-optical antenna mirror, a universal polarizer and that the quasi-optical transmission line permits locating the electronics far (3-4 m) from the tokamak (see Figure 58).

The receiver electronics has also been upgraded and a new data acquisition system constructed with 40 channels sampled at 100 kHz with 24-bit resolution. The data acquisition system will allow complete coverage of the double sideband scattered spectrum for localised (<10 cm), time resolved (~4 ms) ion velocity distribution measurements corresponding to an ion deuterium energy range of approximately 0.5 to 200 keV.

Installation of the diagnostic is scheduled for the beginning of March 2004, with operation and full system tests (including the 110 GHz gyrotron) commencing in May 2004.

4.3.2 Construction and installation of the collective Thomson scattering diagnostic at ASDEX Upgrade

S. B. Korsholm (also at MIT Plasma Science and Fusion Center, Massachusetts, USA), H. Bindslev, J. Egedal, F. Leuterer (Max-Planck-Institut für Plasmaphysik, EURATOM Association, Garching, Germany), F. Meo, P. K. Michelsen, S. Michelsen, E. L. Tsakadze and P. Woskov* (*MIT Plasma Science and Fusion Center, Massachusetts, USA)*
soeren.korsholm@risoe.dk, www.risoe.dk/euratom/cts/aug

Besides the upgrade of the existing TEXTOR CTS system (described in subsection 4.3.1), a new system has been designed, built and installed at ASDEX Upgrade at the Max-Planck Institute for Plasma Physics in Garching, Germany.

A major upgrade of the ASDEX Upgrade ECRH system is currently under way. It will contain four gyrotrons of 1 MW each, operating at 105 GHz and 140 GHz. This will bring the total heating power of ASDEX Upgrade above 30 MW (incl. more than 20 MW ion heating). The substantial ion heating produces large populations of fast ions.

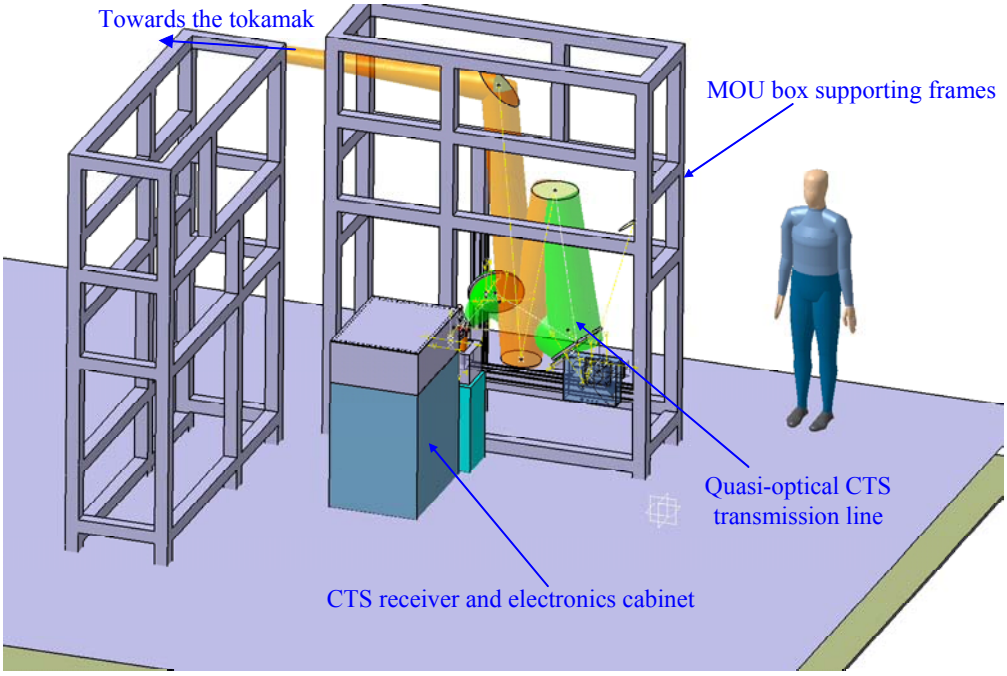

Figure 59. Overview of the CTS diagnostic for ASDEX Upgrade.

The ASDEX Upgrade CTS diagnostic will use the new ECRH system, in particular the new dual frequency gyrotron (105 GHz, 1 MW, 10 sec pulse length) and the transmission lines. One of the quasi-optical transmission lines from the vessel to the gyrotron will be modified for the optional use of the CTS antenna or the gyrotron. The design of the transmission line modification is further described in subsection 4.3.3, while an outline sketch of the system is presented in Figure 59.

The ASDEX Upgrade CTS system was installed in early December 2003 (see Figure 60). The time schedule for the exploitation of the diagnostic is dependent on the installation of the gyrotron and the relevant parts of the ECRH system. It is expected that operation of the system will commence in the summer of 2004.

Figure 60. The CTS diagnostic for ASDEX Upgrade after installation, December 2003.

4.3.3 Quasi-optical transmission line of the fast ion millimetre wave collective Thomson scattering diagnostics on TEXTOR and ASDEX Upgrade

E. L. Tsakadze, H. Bindslev and S. Michelsen
erekle.tsakadze@risoe.dk

The CTS diagnostic system includes quasi-optical transmission lines and antennae for sending the probing radiation into the plasma and collecting the scattered radiation. The measurement volume in the plasma is the intersection between the probe and the receiver antenna patterns, or beams. The directions and shapes of the beams determine the size and location of the scattering volume. The orientations of the beams, which are variable, in fact also determine which direction in ion velocity space is resolved. Careful design, construction, alignment and quality assurance of the transmission lines and antennae are thus important not only to achieve low loss transmission, but also to provide good spatial localisation of the measurement and accurate definition of the location of the movable measurement volume and resolved velocity direction.

At Risø the desired steerable beam patterns and quasi-optical transmission lines are designed using quasi-optics design tools written in MatLab. These define the quasi-optical mirror shapes, typically ellipsoidal and hyperboloidal surfaces, as well as overmoded corrugated waveguides and scalar horns. For adding engineering details and easy interface with CNC cutting tools, the numerical definitions of reflecting surfaces, waveguides and horns are transferred to the design tool, CATIA. The whole procedure of the mirror production from MatLab to metal can take as little as a few hours. Produced mirror shapes can be characterized by the surface analyser at Risø workshop (see Figure 61).

After construction, the transmission line is aligned with the use of a laser beam co-linear with the millimetre wave beam centre. For that purpose each mirror contains an optical quality pin located where the centre of the beam should hit the mirror. Properties of the beam are measured at two different locations along each beam section with a measuring rig constructed at Risø (see Figure 62).

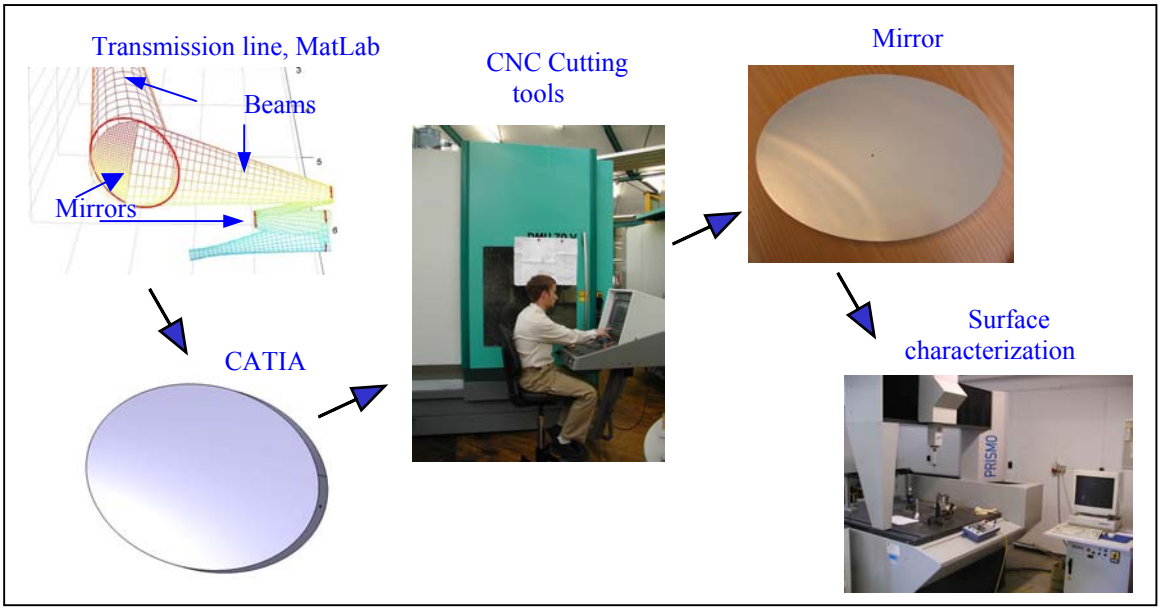

Figure 61. Production of the quasi-optical mirrors from MatLab to metal.

By the process outlined here, the elements required to intercept the new ECRH transmission line at ASDEX Upgrade for use as a CTS receiver line were designed, constructed and tested at Risø. In December 2003 the components were shipped and installed at ASDEX Upgrade at IPP Garching (see Figure 59 and Figure 60 in subsection 4.3.2). The complete alignment of the CTS system will be performed after completion and alignment of the ECRH transmission line (see also subsection 1.1.2).

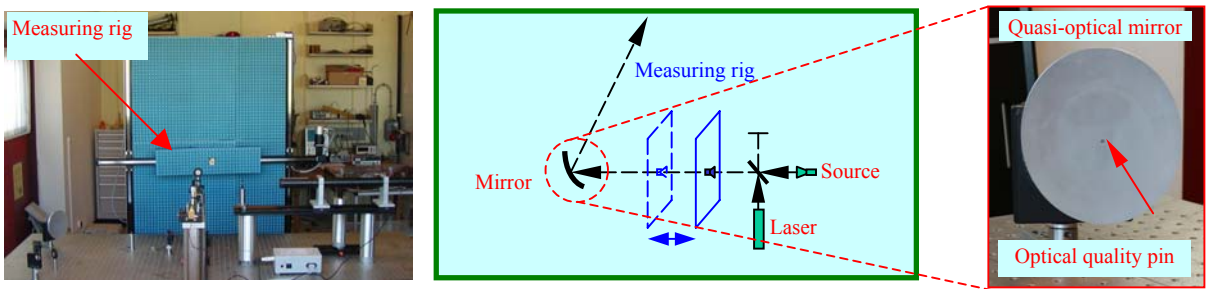

Figure 62. Alignment of the quasi-optical transmission line.

For the upgrade of the TEXTOR CTS system, described in subsection 1.1.1, a full quasi-optical transmission line, including invessel steerable antenna, has been designed, and is currently being constructed and tested at Risø.

4.3.4 Electronics for the CTS diagnostics at ASDEX Upgrade and TEXTOR

S. B. Korsholm (also at MIT Plasma Science and Fusion Center, Massachusetts, USA), H. Bindslev, P. K. Michelsen and P. Woskov (MIT Plasma Science and Fusion Center, Massachusetts, USA)
soeren.korsholm@risoe.dk

While the probe power for a CTS diagnostic is in the order of 100 kW to 1 MW, the power of interest in the scattered spectrum is in the order of 1 nW. The background noise is 10-1000 times the CTS signal. These circumstances set high requirements for the electronics in the CTS receiver.

The electronics of the pilot project TEXTOR CTS system needed an upgrade. A diagram of that receiver is presented in Figure 63. The items marked in blue have been installed as new, while some other components have been upgraded.

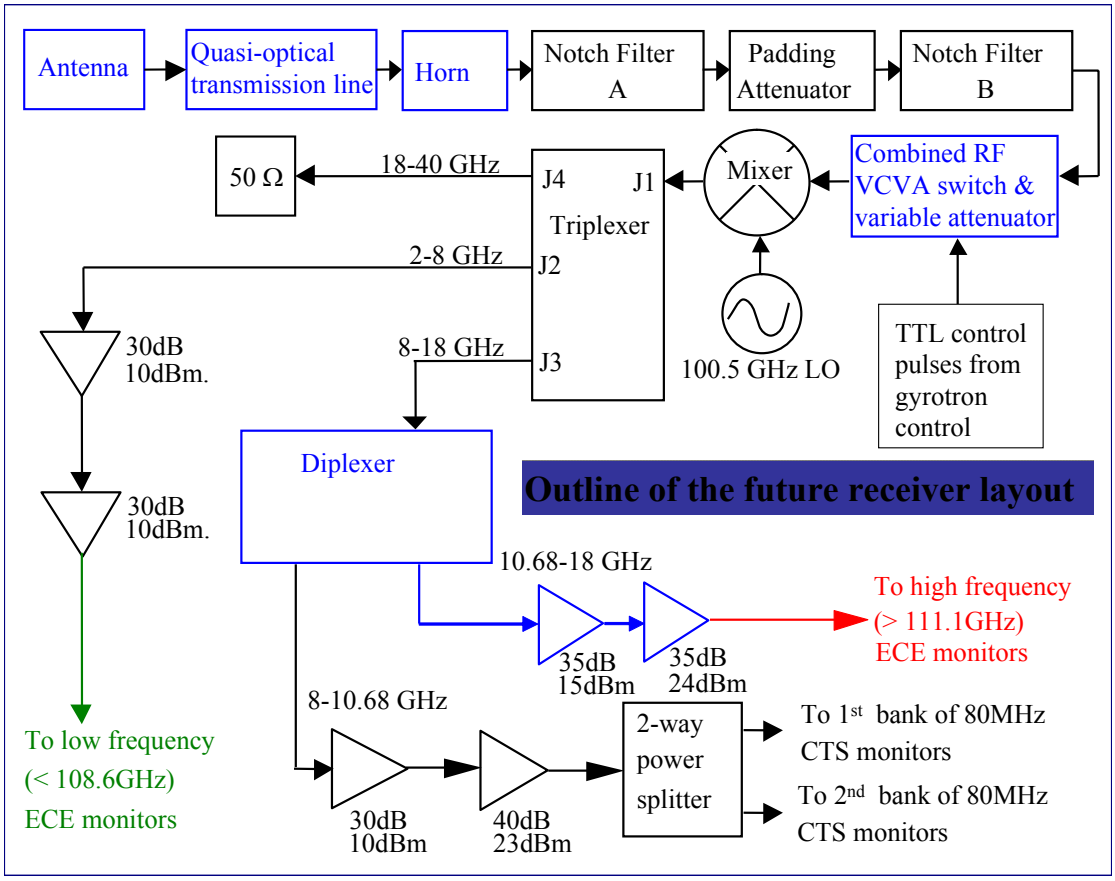

Figure 63. Layout of the electronics in the TEXTOR CTS receiver. Items marked in blue are new for the upgrade of the system.

Some of the main components are the notch filters, following immediately after the horn that interfaces the quasi-optical transmission line and the receiver box. The notch filters attenuate the stray light by damping a 250 MHz band around 110 GHz by 120 dB. After the waveguide components the signal is down-converted by 100.5 GHz, and then split into three bands by a triplexer (actually two diplexers combined), one being the centre part of the

spectrum, containing most of the energy, and the other two bands for the lower and upper frequencies. The splitting is done in order to avoid saturation of the amplifiers, which amplifies the signal in each frequency band by 60-70 dB, and to spectrally separate the sensitive wings of the CTS spectrum from the stray light from the probe. Finally, the signal enters the filter banks and the data acquisition system described in subsection 4.3.5. The amplifiers are the most delicate parts with specifications like: frequency band 10 to 16 GHz, gain 35 to 40 dB, output power of +15.9 dBm at 1 dB gain compression and a noise figure below 1.8 dB.

The receiver for the ASDEX Upgrade CTS system was designed and built at Risø. The scheme is very similar to that of the TEXTOR system though the physical layout is somewhat different. Figure 64 shows a photograph of the receiver box for the ASDEX Upgrade CTS.

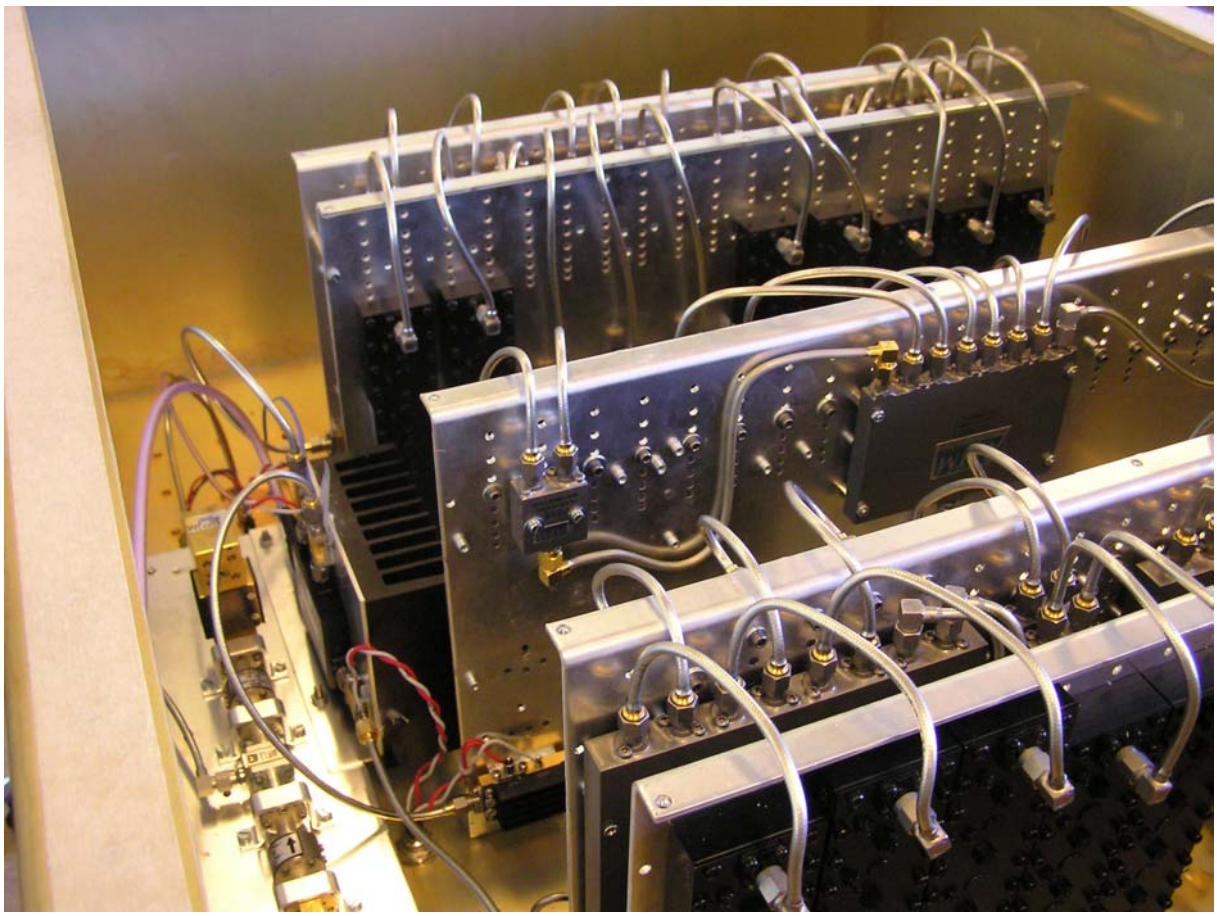

Figure 64. Photo of the ASDEX Upgrade CTS receiver. The filter banks are located to the right and the high frequency (105 GHz) waveguide components to the left.

4.3.5 Data acquisition software and calibration for collective Thomson scattering

S.K. Nielsen, J. Fold von Bülow and P. Michelsen
stefan.kragh.nielsen@risoe.dk

The collective Thomson scattering systems presently being installed on the fusion research devices ASDEX and TEXTOR (se subsections 4.3.1 and 4.3.2) require a high resolution and synchronized fast scan rate data acquisition system. The hardware and software interaction is therefore crucial.

Two data acquisition systems have been developed using National Instruments NI-4472 PCI cards (eight cards for ASDEX and seven for TEXTOR), each card with eight channels with 24-bit resolution and a sampling rate of 102400 Hz. All channels sample synchronously. Each system has an additional NI-6040 card with 16 channels for monitoring system settings such as antenna orientations.

Data acquisition software to control the two systems has been developed in "Labview". The software controls the acquiring of data (up to 500 MB per plasma discharge) and may run independently of user interaction. The software is capable of performing system calibration and controlling secondary devices such as mirror positions.

The system calibration is carried out by measuring the black body radiation emitted by a warm and a cold source. The difference in signal then yields both the signal gain and the noise in the various channels induced by the system. This noise is expressed as a noise temperature and varies for different channels. The warm source can be a room temperature object or the machine vessel itself. The cold source used is *EchoSorb* submersed in liquid nitrogen. The alternation between the two sources is done automatically by inserting a mirror just after the horn (see subsections 4.3.1 and 4.3.2).

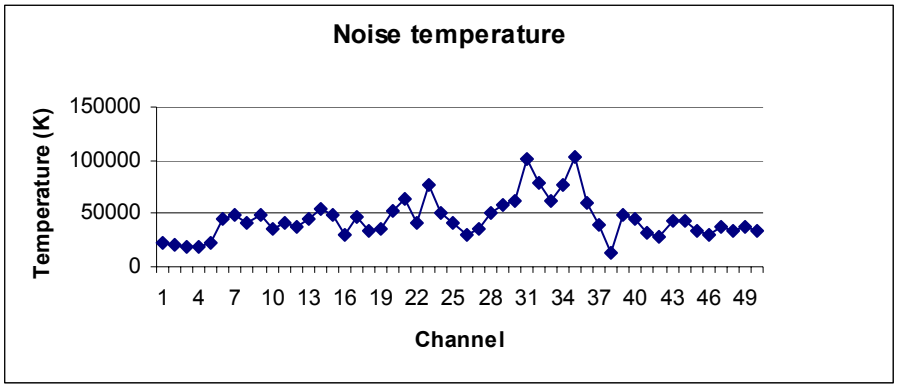

Figure 65. Noise temperature for ASDEX detection system.

An example of measured noise temperature of the ASDEX detection system is given in Figure 65. Here *EchoSorb* in liquid nitrogen was used as the cold source and room temperature *EchoSorb* was used as the warm source.

4.3.6 Diagnosing fast ions in ITER by collective Thomson scattering, feasibility study covering systems from millimetre waves to far infrared

H. Bindslev, F. Meo and S. Korsholm
henrik.bindslev@risoe.dk, www.risoe.dk/euratom/cts/ITER

The group has conducted an extensive study of the feasibility of measuring the fast ion phase space distribution in ITER by collective Thomson scattering (CTS). The study includes the full range of potential probe frequencies from the gyrotron based mm-wave range, over the far infrared with sources such as optically pumped molecular lasers and free electron lasers, to the infrared range of the CO_2 laser. It is assessed whether the systems can meet the ITER measurement requirements and which technological developments may be required. The relative merits of the systems are compared. These include both the achievable resolutions in space, velocity space and time, and accuracies with which these measurements can be obtained. Comparison of systems was preceded by conceptual designs of individual systems

to optimise for robustness, resolution and sensitivity, taking technical constraints and potential future enhancements into account.

The study reveals that a CTS system based on a 60 GHz probe frequency, which is below the lower frequency limit of the electron cyclotron emission (ECE) spectrum, has the highest diagnostic potential, and is the only system expected to be capable of meeting all the ITER fast ion measurement requirements with existing or near term technology.

Collective Thomson scattering cannot distinguish between alpha particles and deuterons travelling at the same velocity, though the signal per alpha particle is four times that of a deuteron. In the direction of the magnetic field and perpendicular to the field deuterons injected by the neutral beam heating system will give rise to fast deuteron populations which will be indistinguishable from the alpha particle population in the velocity range where they overlap. In the direction opposite to the magnetic field (actually opposite to the plasma current), the so-called *counter direction*, the beam deuteron population is negligible. While the dynamics of deuterons and alphas are much alike and both important, it is valuable also to be able to observe the alpha population solely. This is possible in the counter direction. If as expected the population is near isotropic, observation in just one direction defines the full alpha distribution. With these considerations in mind it is significant that the 60 GHz CTS system permits the counter passing part of the fusion alpha distribution, not obscured by beam ions, to be measured with a spatial resolution of one tenth the minor radius. The conceptual design is presented below in subsection 4.3.7. On the basis of this design costs have been estimated following ITER standard procedures. With modest additions this system may also provide measurements of the fuel ion ratio.

4.3.7 Preliminary design studies of a 60 GHz CTS diagnostic for ITER

F. Meo and H. Bindslev
fernando.meo@risoe.dk

The feasibility study reported in subsection 4.3.6 concludes that a fast ion collective Thomson scattering (CTS) diagnostic with a probe frequency below the electron cyclotron emission spectrum is the only CTS diagnostic capable of meeting the ITER measurement requirements for the fusion alphas, with present or near term technology. The CTS diagnostic for ITER at the 60 GHz range is capable of measuring the fast ion distribution parallel and perpendicular to the magnetic field at different radial locations simultaneously. The design is robust technologically with no moveable components near the plasma. The fast ion CTS diagnostic proposed consists of two separate systems. Each system has its own probe launcher and separate sets of receiving antennae and receivers. The first system, shown in Figure 66, measures the fast ion velocity distribution resolved in the direction perpendicular to the confining magnetic field. For this system the probe and receiver beams are near perpendicular to the magnetic field. The antennae of the probe and receivers are located in the equatorial port on the low field side (LFS)[2].

The receiver consists of a fixed quasi-optical mirror that measures backscattered radiation and couples it to a distributed set of receiver horns. This system is referred to by the acronym LFS-BS system referring to the location of the receiver and the fact that it measures backscattered radiation. Figure 67 gives a schematic presentation of the front-end of the probe launcher and the receiver of the LFS-BS system. It shows the receiver consisting of a quasi-optical mirror coupled to an array of horns mounted in a stainless steel frame that houses a series of fundamental waveguides connected to the horns. The waveguides are directed to

[2] The low field side is the side of the plasma or vacuum vessel which has the largest distance to the machine centre and hence the largest major radius.

tapers coupled to over-moded waveguides. Each horn is located at a different distance from the mirror and collects scattered radiation from a different radial position in the plasma, as shown by the dotted and solid blue lines in Figure 67.

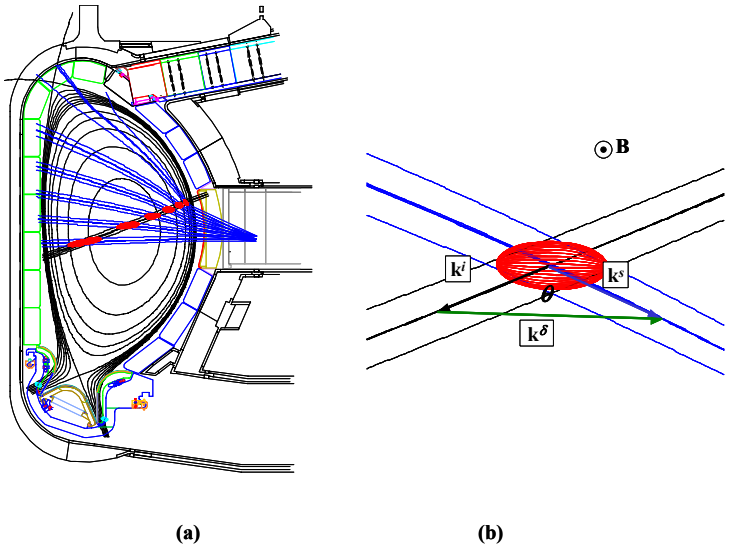

Figure 66. Poloidal view of the LFS-BS set-up: (a) Beam traces of the LFS-BS system with respect to the ITER vessel components. The probe is in black, the receiver beam traces in blue, and the calculated scattering volume in red. (b): A close-up view of the probe beam (black), one of the receiver beams (blue) and the scattering volume (red). The drawing shows the wave vectors of the received scattered radiation k^s, probe radiation k^i, and the fluctuation wave vector k^δ. ($k^\delta = k^s - k^i$).

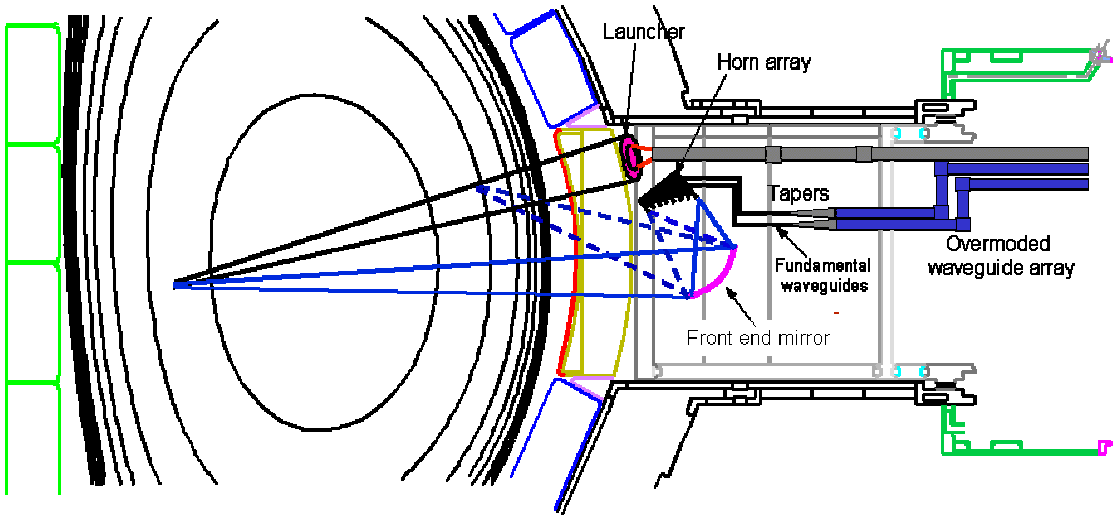

Figure 67. Schematic drawing of the side view of the LFS-BS components. The probe launchers are located in the same poloidal plane as the detectors.

The second part of the CTS diagnostic, shown in Figure 68, measures fast ion velocity distribution resolved in the direction parallel to the confining magnetic field. It consists of a probe launcher located in the low field side mid-plane port and a receiver array located on high field side. This system will be referred to as HFS-FS referring to the location of the receivers and that they measure forward scattered radiation.

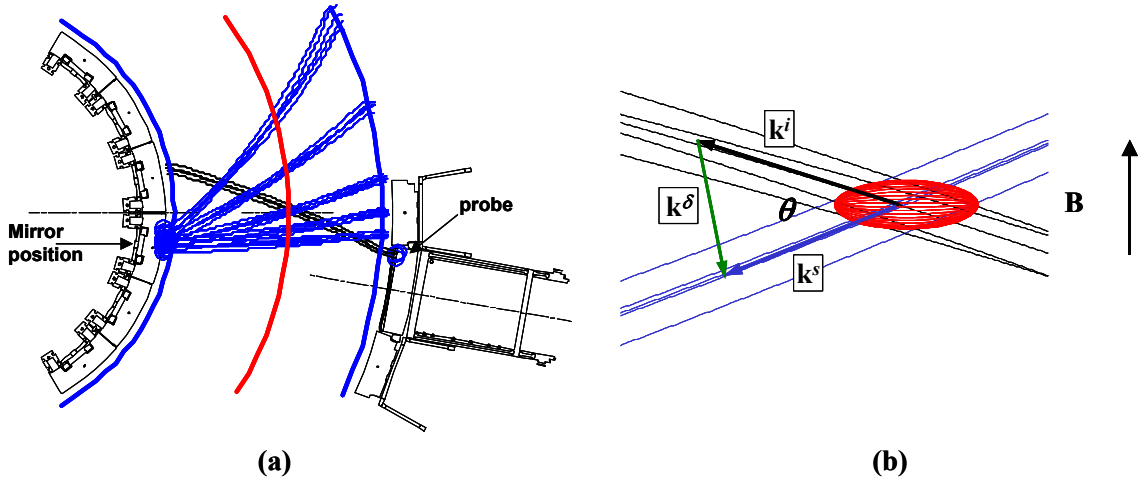

Figure 68. (a) Top view of beam traces for the HFS-FS with an LFS probe launcher (black) and HFS detectors (blue). The red curve indicates the plasma centre. (b) Close-up view of the probe beam and one of the receiver beams with the scattering volume in red. Shown are the wave vectors of the received scattered radiation k^s, the incident probe radiation k^i, and the fluctuation vector $k^\delta = k^s - k^i$, which is near parallel to B.

The hardware of the HFS receivers consists of a quasi-optical mirror mounted on the inner vessel wall below the blanket module key as shown in the side view sketch in Figure 69a. Toroidally the mirror is located between the cooling manifolds (Figure 69b). The mirror collects scattered radiation from a narrow horizontal slot between blanket modules that form the first wall against the plasma. The mirror relays the radiation to a series of horns. The horns are distributed toroidally, each representing a different toroidal angular view in the plasma. The horns are encased inside a cast, housing fundamental waveguides that are routed upwards along the inner vessel wall. These are in turn coupled to over-moded waveguides that run up along the vacuum vessel wall behind the blanket modules toward the upper port.

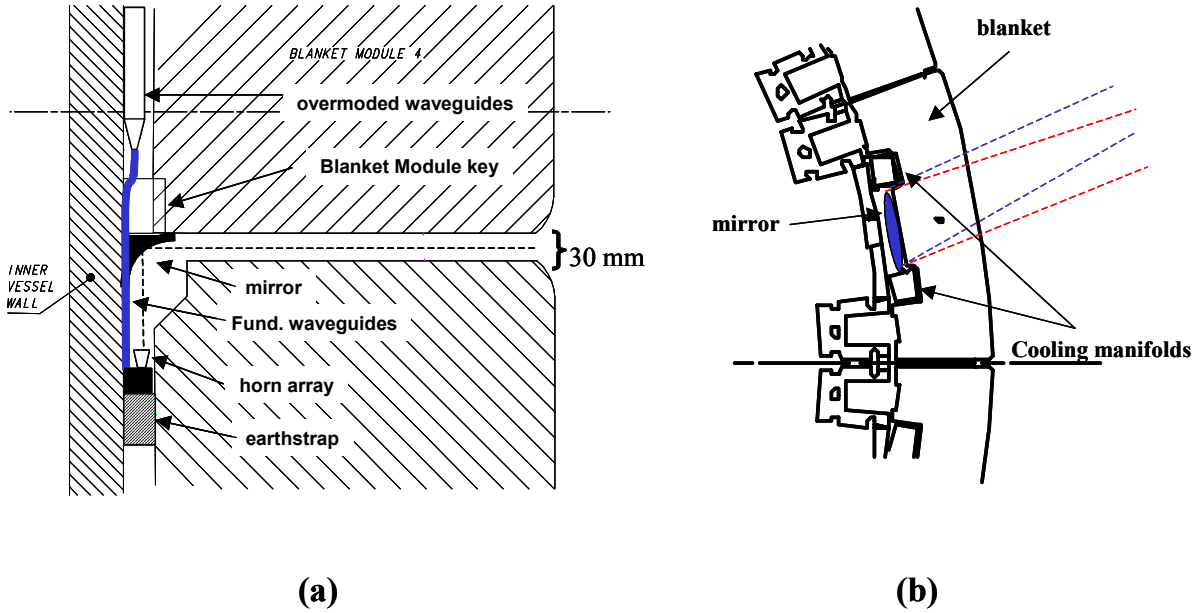

Figure 69. (a) Cross section of blanket modules 3 and 4 with mirror, horn array and waveguide assembly. The vertical distance between the blanket modules gap diameter is 30 mm as shown. (b) Top view of mirror located behind the blanket module between the cooling manifolds.

In close collaboration with the ITER International Team, the preliminary phase of the hardware design for the CTS on ITER has been completed. The 3D CATIA drawings in Figure 70(a) show the view of ITER's equatorial port #12 with the blanket and the apertures for the CTS. In Figure 70(b), the blanket module is not shown and the plug front plate was made semi-transparent in this illustration for a better view of the front-end optics and the port plug waveguides. The launcher for both the LFS-BS and HFS-FS system consists of two fixed quasi-optical ellipsoidal mirrors fed by a corrugated high power waveguide. The purple and orange dash-dotted line shows the beam centre of the LFS-BS probe and the HFS-FS probe, respectively. Also shown are the first mirror and the horn array of the LFS-BS receiver. The enclosure in blue contains the fundamental waveguides that are directed to tapers and are coupled to the over-moded waveguides. Not shown in this report is the preliminary hardware design for the HFS-FS receiver located on the inner vessel wall. There is no integration issues with other diagnostics yet identified in port #12. A relatively low-cost upgrade to the LFS-BS system of CTS has the potential to provide temporally and spatially resolved measurements of the fuel ion ratio.

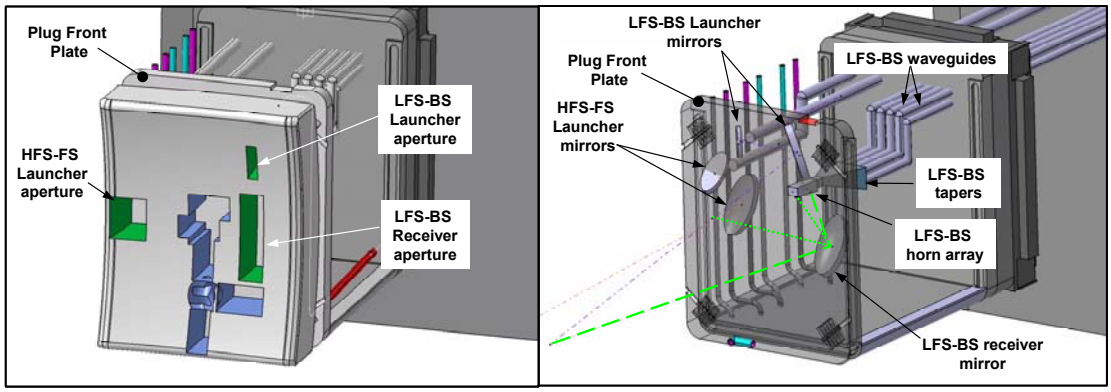

Figure 70. (a) View from the plasma side of the mid plane port plug #12. The apertures for the CTS diagnostic are shown in green. The apertures in blue are for the other diagnostics that share the same port. (b) View of the CTS in port plug from the plasma side without the blanket module.

4.3.8 Microwave transmission system for audio signals

P.K. Michelsen, H. Bindslev, J. Holm, J.P. Lynov, S.B. Korsholm, B. Sass and J. Thorsen
poul.michelsen@risoe.dk

At large outdoor music concerts and other large public events a major problem is to draw cables between the stage, the mixer and the loudspeakers. In connection with the Musicon Valley Project, it was suggested that the cables could be replaced by microwave transmission of the audio signals. Microwave beams are already used for wireless transmission of data, for instance for satellite communication around 12 GHz and connections of pc-equipment at 2.4 GHz. For private communication at shorter distances higher frequencies are preferable. The frequencies of interest are: 40-44, 59-64 and 92-96 GHz, which are bands allocated for wireless services. The higher the frequency the smaller the antennas (parabolas) which can be used, but the cost of microwave components increases with frequency. Signals around 60 GHz are absorbed heavily by atmospheric oxygen. The power absorption is 98% per km. It may be a disadvantage for some applications, but for private communication over short distances it may be an advantage. A system for TV-transmission using 92 GHz, which was demonstrated at Risø, has been sketched in Figure 71.

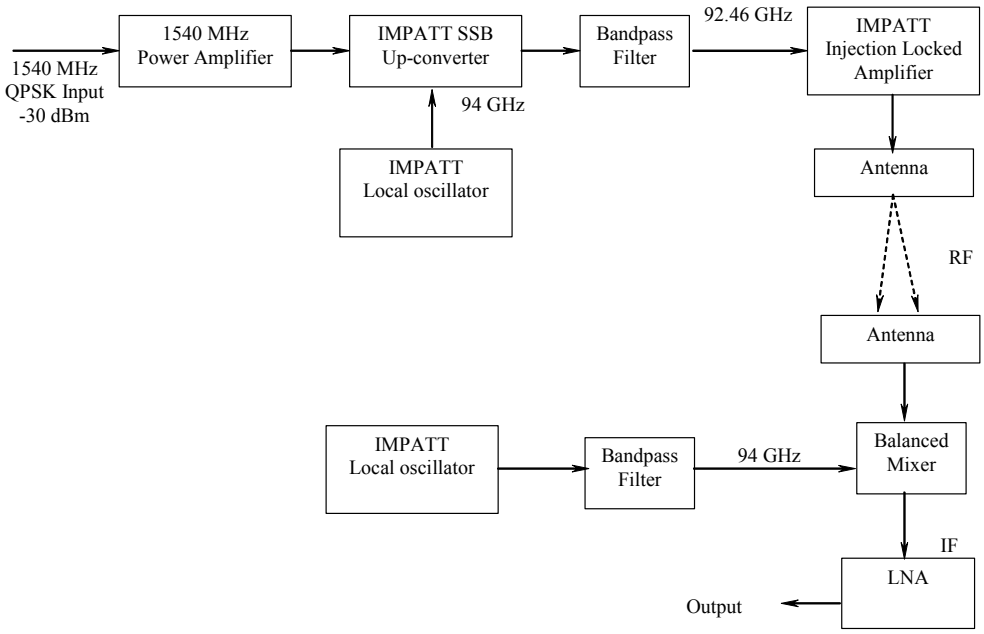

Figure 71. Block diagram of system for transmission of digital television by micro waves at 92 GHz.

Microwave signals can propagate in narrow beams permitting private transmission of information: Reception of the signals is only possible with antennae placed inside the beam. The signal beam can be terminated a given distance from the transmitter by inserting a microwave absorbing material, a dump, the size of the beam into the path of the beam. In the following table estimates are given of transmission range, antenna and dump size for private transmission and cost of microwave systems.

Frequency	10 GHz	42 GHz	62 GHz	94 GHz	Comments
Max range	> 10 km	10 km	2 km	5 km	Depends on power, antenna diameter, bit-rate and weather condition.
Beam size* as a function of frequency and range					The width of that fraction of the beam, which contains 99 % of the power.
Range = 20 m	0.71 m	0.35 m	0.3 m	0.2 m	
Range = 100 m	1.6 m	0.8 m	0.6 m	0.5 m	
Range = 500 m	3.5 m	1.7 m	1.4 m	1.1 m	
Cost	Low	Medium	Medium	High	Low means < 10 kkr, High means ≈ 50 kkr
**Beam size* is also the size of the launching antenna required to keep the beam size below the indicated size over the indicated range. The receiver antenna can be smaller. Good reception is possible inside the beam. To ensure that no reception is possible beyond a certain point, the beam can be dumped on a pad the size of the beam.					

For all the transmission frequencies 10 to 100 Mbps can be achieved. The demonstration system, for transmission of television signals, used a DVB-S (QPSK) modulation system, for which the modulator and demodulator systems are commercially available. Modulation systems for Internet transmission are also available. Typical and sufficient microwave output power is 10 – 100 mW.

4.4 Low temperature plasmas with environmental and industrial applications

H. Bindslev, A. Fateev, Y. Kusano, F. Leipold, P.K. Michelsen, B. Stenum and E. Tsakadze
henrik.bindslev@risoe.dk

In low temperature plasmas, the electron temperature (a few tens of thousands of degrees) can differ greatly from the temperature of the ions and of the neutrals, which can be close to room temperature. Due to this low gas temperature, interaction of low temperature plasma with heat sensitive material can be non-destructive. If, in addition, the plasma is operated at atmospheric pressure process advantages generally ensue and expensive pumping and vacuum equipment is not required. This opens a wide field of industrial applications for low temperature plasma sources such as surface treatment, pollution remediation, and sterilization.

4.4.1 Remediation of nitrogen oxide (NO) in the flue gas of a gas power plant

H. Bindslev, A. Fateev, Y. Kusano, F. Leipold, P. Michelsen, B. Stenum, E. Tsakadze, H. Egsgaard (Plant Research Dept, Risø National Laboratory) and P. Kristensen (Danish Gas Technology Center, Hørsholm, Denmark)
henrik.bindslev@risoe.dk

This project seeks to develop a method for reducing the nitrogen oxide emissions from gas power plants by injecting reducing radicals into the flue gas. A central milestone is the development of an atmospheric pressure low temperature discharge for efficient production of the reducing radicals. Combustion of fossil fuel (in power plants or automotive engines) produces nitrogen oxides, commonly referred to as NO_x. NO_x causes acid rain and generates ozone. Effort thus needs to be put into reducing NO_x emission. Several techniques are known to reduce the NO_x in the flue gas from power plants. One of these techniques is the addition of NH_2 radicals to the flue gas. The NH_2 radical serves as a reducing agent for NO. The reaction products, N_2 and H_2O, can be released in the air. In order to generate the required NH_2 radicals, an atmospheric pressure dielectric barrier discharge (DBD) with NH_3 as operating gas is utilized. Argon serves as carrier gas.

A DBD consists of two electrodes with one or more layers of dielectric in between. The plasma is generated by applying a high AC or pulsed voltage between the electrodes (see Figure 72).

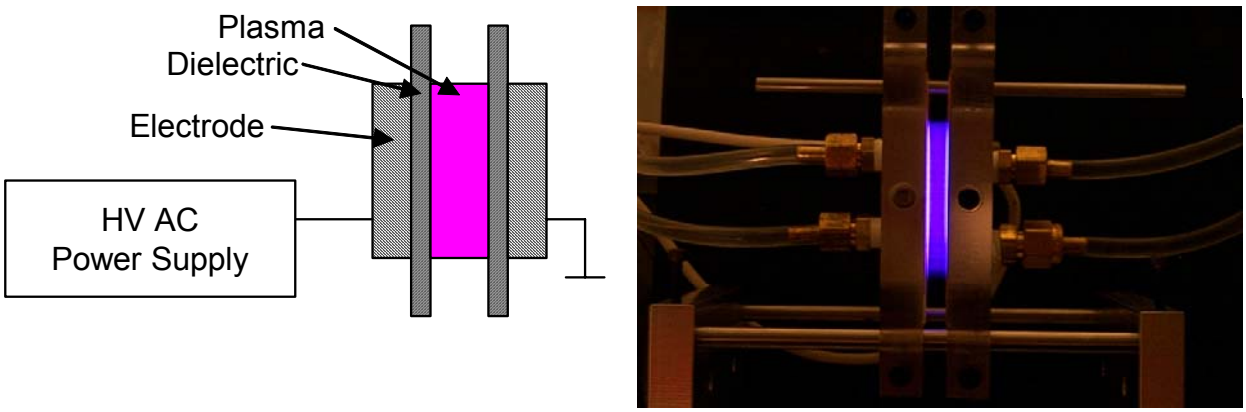

Figure 72: Schematic presentation and photography of a dielectric barrier discharge (DBD).

The electrodes of our DBD have a size of 5 cm by 5 cm. Alumina (Al_2O_3) plates serve as dielectric barriers. The distance between the electrodes is 3 mm. The electrode temperature is kept at 15 degree C by means of external cooling. The power consumption of the DBD has been varied from a few watts up to 70 W.

The characterization of the DBD was performed by means of emission spectroscopy in UV-IR spectral ranges. In addition, electrical measurements (current, voltage) were performed. Optical emission spectra of excited NH($c^1\Pi$, $A^3\Pi$) radicals in the range between 322 nm and 345 nm at various ammonia concentrations (0.1%...10%) were recorded. The presence of NH in the plasma plays an important role for the plasma chemistry in the discharge. Typical emission spectra for ammonia concentrations of 3% and 8% are shown in Figure 73.

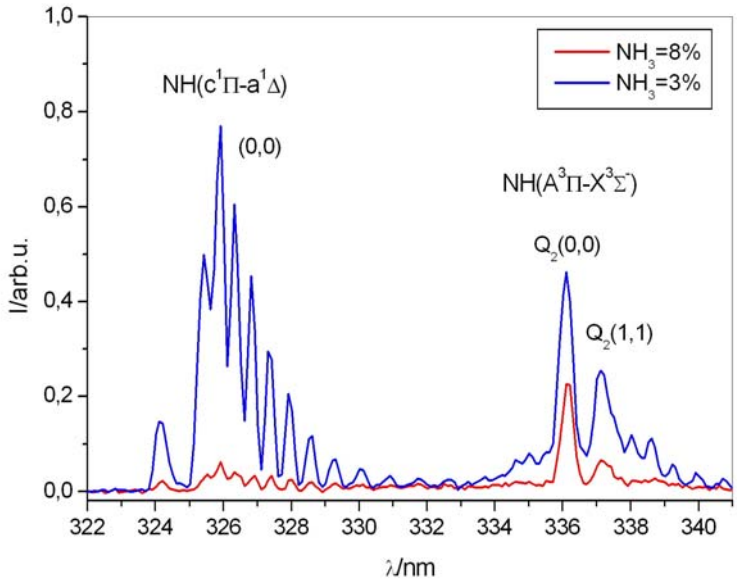

Figure 73. Emission spectrum of the NH_3/Ar DBD for various NH_3 concentrations.

The maximum emission of NH was found for an NH_3/Ar concentration of approximately 0.5%. These measurements indicate also that the state of excitation can be controlled by the ammonia concentration of the feed gas. Measurements are in good agreement with modelling. Due to strong quenching of $NH_2(A^2A_1)$ by argon and ammonia, optical emission from

$NH_2(A^2A_1)$ radicals could not be detected. Experiments for detection of NH_2 radicals by means of IR absorption spectroscopy are currently under investigation.

This is a collaborative project with participants from the Department of Optics and Fluid Dynamics, the Plant Research Department, both at Risø, and the Danish Gas Technology Center. This work is funded by the public service obligation (PSO) from Elkraft Systems (Order – 103159, FU 3401).

4.5 Fluid dynamics

J. Juul Rasmussen
jens.juul.rasmussen@risoe.dk

The studies in fluid dynamics comprise investigations of the evolution of vortex structures and the stability of a falling liquid thread. A general Hamiltonian formalism for the dynamics of bubble vortices, or "air-core vortices", is derived in 4.5.1. This formalism has been applied to the formation and dynamics of cavities in fluids and in particular to describe the stability and motion of vortex ring bubbles. The interaction of vortex lines plays an essential role near the onset of turbulence, and in 4.5.3 we have initiated studies of the interaction of three vortex lines. Theoretical and experimental investigations of the classical problem on stability and dynamics of a falling liquid thread are discussed in 4.5.2.

4.5.1 Toroidal bubbles with circulation in ideal hydrodynamics: a variational approach

V. P. Ruban (Landau Institute for Theoretical Physics, Moscow, Russia)
and J. Juul Rasmussen
jens.juul.rasmussen@risoe.dk

Vortex ring bubbles in water are like usual vortex rings with circulation, but the core is filled with air; thus they are also termed "air-core vortex rings". The higher velocity fluid surrounding the core of the ring is at lower pressure than the fluid farther away due to the Bernoulli effect. Vortex ring bubbles can be generated in various ways naturally or artificially, and they are interesting objects both from experimental and theoretical points of view. Amazing examples of the natural beauty are vortex ring bubbles blown by dolphins for amusement.

The vortex ring bubble is a special example of a general class of fluid dynamical problems involving the free surface separating the fluid and air (or generally two different fluids). The aim of this work is to develop a Hamiltonian formalism for these systems, and we have formulated a general variational principle that determines the evolution of the bubble shape. For a two-dimensional (2D) cavity with a constant area, exact pseudo-differential equations of motion are derived, based on variables that determine a conformal mapping of the unit circle exterior into the region occupied by the fluid. A closed expression for the Hamiltonian of the 2D system in terms of canonical variables is obtained. The stability of a stationary drifting 2D hollow vortex is demonstrated when the effect of gravity is small. For a circulation-dominated regime of three-dimensional flows a simplified Lagrangian is suggested, employing that the bubble shape is well described by the centre line and by an approximately circular cross-section with a relatively small area. For an axially symmetric rising and spreading vortex ring bubble our variational approach provides a finite-dimensional approximate system that is a generalization of the model discussed by Lundgren and Mansour.[1]

1. T. S. Lundgren and N. N. Mansour, *J. Fluid Mech*. **224**, 177 (1991).

4.5.2 The shape and stability of a falling liquid thread

T. Bohr (Physics Dept., Technical University of Denmark, Lyngby), S. Senchenko (also at Physics Dept., Technical University of Denmark, Lyngby) and J. Eggers (School of Mathematics, University of Bristol University, Bristol, United Kingdom)
senchen@fysik.dtu.dk

When a viscous fluid, like oil or sirup, streams from a small orifice and falls freely under gravity, it forms a long slender thread which can be maintained in a stable, stationary state with lengths up to several metres. We have performed both analytical and experimental investigations of the shape and stability of a freely falling thread. It turns out that the strong advection of the falling fluid can almost outrun the Rayleigh-Plateau instability and change the usual exponential growth of small perturbations to the stretched exponential form $\exp(ct^{1/4})$

We have measured the shape of the falling jet of a silicon oil (kinematic viscosity: $\mu = 600$ cm^2/s) and the measured profile was found to be in a good agreement with the theoretical prediction, though the best fit was achieved for the far downstream region (from 40 cm to 100 cm along the jet). We have initialized a numerical investigation of the falling thread by solving directly the model equations. We have been able to investigate a vide range of viscosity values and have observed the predicted local damping of the perturbations in the presence of viscosity.

4.5.3 Dynamics of vortex lines

S. Senchenko (also at Physics Dept., Technical University of Denmark, Lyngby), V.P. Ruban (Landau Institute for Theoretical Physics, Moscow, Russia) and J. Juul Rasmussen
senchen@fysik.dtu.dk

It is commonly believed that the interaction of vortex lines plays an essential role at the onset of developed turbulence. We have initiated investigations of a set of models, where initially parallel (i.e. effectively 2D) vortex lines interact through a weak potential. The inviscid dynamics of the vortex lines are investigated by the Hamiltonian method. In particular, we take advantage of the complete integrability of systems with two- and three- point vortices in the plane. This allows us to perform a reduction of the dynamical equations for the interaction of the vortex lines. We explore both analytically and numerically different features of the models. In particular, we are interested in the process of collapse of vortex lines; the latter is expected for the interaction dynamics of three lines initialized in a specific configuration.

4.6 Optics and acoustics

J. Juul Rasmussen and B. Stenum,
jens.juul.rasmussen@risoe.dk, bjarne.stenum@risoe.dk,

The investigations within optics are concentrated on nonlinear propagation of light in various media. In particular, we have investigated the dynamics of dark solitons in media, where the nonlinear response is non-local (4.6.1). The nonlocallity introduces a new type of attractive interaction, and stable bound states of dark solitons are realized. Then in 4.6.2 it is demonstrated that the soliton structures in quadratic nonlinear material may be described as soliton solutions for nonlocal cubic nonlinearities. Furthermore, in 4.6.3 we discuss the possibility for stabilizing optical beams in nonlinear media by means of an attractive potential. We have generalized the classical Ginzburg-Landau theory for second-order phase

transitions in 4.6.4. We consider media with long-range correlations and nonlocal interactions and have derived a fractional version of the Ginzburg-Landau equation. Finally, we describe (4.6.5) investigations of laser-generated ultrasound that has proved to be an effective tool for remote non-contact inspections of material characteristics and defects.

4.6.1 Interaction of nonlocal dark optical solitons

N. Nikolov (also at Informatics and Mathematical Modelling, Technical University of Denmark, Lyngby), W. Krolikowski (Australian Photonics Cooperative Research Centre, Australian National University, Canberra, Australia), O. Bang (COM, Technical University of Denmark, Lyngby), J. Juul Rasmussen and P.L. Christiansen (Informatics and Mathematical Modelling, Technical University of Denmark, Lyngby)
jens.juul.rasmussen@risoe.dk

The continuing interest in fundamental studies of temporal and spatial solitons is motivated by their collisional properties. The solitons are robust objects that display particle-like behaviour in their mutual interaction. In different non-linear systems the details of their interactions may vary, but the generic features remain basically universal. It appears that dark solitons, i.e. entities having the form of an intensity dip in the otherwise uniform background, which are also topological objects because of their nontrivial phase structure, almost always *repel* each other.

We study theoretically the formation and interaction of spatial dark optical solitons in materials with a nonlocal non-linear Kerr-like response. We show that the presence of nonlocality drastically modifies the interaction of the dark solitons by inducing long-range attraction between them, which allows for the formation of bound states. These states are stable when propagating and can withstand even strong perturbations. The bound states can be created using a beam with a finite width as background. They evolve adiabatically maintaining their soliton properties even as the background beam deforms during propagation. We also demonstrate numerically that bound states of dark solitons can be created dynamically by the nonlocality-mediated collision of dark solitons.

4.6.2 Quadratic solitons as nonlocal solitons

N. Nikolov (also at Informatics and Mathematical Modelling, Technical University of Denmark, Lyngby), O. Bang (COM, Technical University of Denmark, Lyngby), D. Neshev and W. Krolikowski* (*Australian Photonics Cooperative Research Centre, Australian National University, Canberra, Australia)*
nikola.i.nikolov@risoe.dk

Quadratic nonlinear (or $\chi(2)$-) materials have strong and fast electronic nonlinearity, which makes them excellent materials for the study of nonlinear effects such as solitons. The main properties of quadratic solitons are well-known and both (1+1)- and (2+1)-dimensional bright spatial solitons have been observed experimentally. Unlike conventional solitons, which form due to a self-induced refractive index change, the formation of quadratic solitons does not involve a change of the refractive index. Thus, the underlying physics of quadratic solitons is often obscured by the complex mathematical model. Certain features of quadratic solitons, such as the formation of bound states, are still without a physical interpretation. We have used the analogy between parametric interaction and nonlocality to present a physically intuitive nonlocal theory. This method is exact in predicting the properties of stationary quadratic solitons. We provide a broad physical picture in the whole regime of existence of the solitons and discuss, e.g., dark solitons and bound states of out-of-phase bright solitons.[1]

1. N.I. Nikolov, D. Neshev, O. Bang and W.Z. Krolikowski, "Quadratic solitons as nonlocal solitons", Phys. Rev. E 68, 036614 (2003)

4.6.3 Beam stabilization in the 2D nonlinear Schrödinger equation by attractive potentials and radiation

B. leMesurier (College of Charleston, Charleston, USA), P. L. Christiansen (Informatics and Mathematical Modelling, Technical University of Denmark, Lyngby, Denmark), Yu. B. Gaididei (Institute for Theoretical Physics, Kiev, Ukraine) and J. Juul Rasmussen
jens.juul.rasmussen@risoe.dk

The effect of attractive linear potentials on self-focusing in wave fields modelled by the nonlinear Schrödinger equation is considered. Variants of the nonlinear Schrödinger equation with attractive potentials arise in several models of weakly nonlinear, dispersive waves. Specific examples are: models of optical fibres with narrow cores of different refractive index or waveguides induced in a nonlinear medium by another beam, in models of the behaviour near impurities in two-dimensional molecular structures and in the Gross-Pitaevskii model of Bose-Einstein condensates.

By means of direct numerical solutions it is demonstrated that the attractive potential can prevent both singular collapse and dispersion that are generic in the nonlinear Schrödinger equation in the critical dimension, and can lead to a stable oscillating beam. This is observed to involve a splitting of the beam into an inner part that is oscillatory and of sub-critical power, and an outer dispersing part. This behaviour is explained by means of collective coordinate calculation and in terms of rate competition between the nonlinear and the linear (mediated by the potential) focusing effects, radiation losses and stable periodic behaviour of specific solutions in the presence of attractive potentials.

4.6.4 Fractional generalization of the Ginzburg-Landau equation: implications for high-temperature superconductivity

A.V. Milovanov (Department of Space Plasma Physics, Space Research Institute, Moscow, Russia) and J. Juul Rasmussen
jens.juul.rasmussen@risoe.dk

The classical Ginzburg-Landau theory for second-order phase transitions is generalized to media with long-range correlations and nonlocal interactions. It is suggested that interaction between the local ψ-order (ψ denotes the condensate wave function) and a coexisting nonlocal symmetry can be described by a fractional generalization of the free energy expansion. The ensuing fractional Ginzburg-Landau equation is incorporating the effect of nonlocality and long-range correlations. This equation leads among other features to intriguing implications regarding the nature of high-temperature superconductivity in complex materials such as copper-oxide compounds and their derivatives, which may support a long-range, nonlocal ordering in addition to the superconducting ψ-order. The model allows for a self-consistent estimate of the superconducting transition temperature Tc with a characteristic numerical value around 180 K.

4.6.5 Inspection of steel bars with laser-generated ultrasound at high scanning velocities

A. Bardenstheín), A. M. Thommesen*, B. Stenum and S. Arnfred Nielsen (*FORCE Technology, Brøndby, Denmark)*
steen.arnfred.nielsen@risoe.dk

Laser ultrasound (LU) is a promising technology for remote, non-contact inspection of material characteristics and defects. A pulsed laser is used to generate an ultrasonic pulse in the material, and an optical interferometer is used to detect the ultrasonic pulses in the material. LU has a number of unique applications: the high bandwidth of the laser-generated pulses enhances spatial resolution and provides more reliable defect detection compared with traditional ultrasonic techniques. Since LU is a non-contact technique, it is suitable for scanning objects.

In this project, a new robust LU-inspection system has been built for scanning steel bars at high velocities. The system has been tested in industrial environments at scanning velocities up to about 10 m/s. Known defects were located in samples with poor reflection of the probe laser beam at velocities up to 3 m/s.

The project is a part of the Centre for On-Line, Non-Contact Sensing, Monitoring and Control of Industrial Processes and Systems (BIPS). The participants are FORCE Technology, Risø National Laboratory, Technical University of Denmark, Junckers Industrier A/S, Coloplast A/S, Danish National Railway Agency and SCITEQ-Hammel A/S.

5. Publications and educational activities

5.1 Laser systems and optical materials

International publications

Apitz, D.; Svanberg, C.; Jespersen, K.G.; Pedersen, T.G.; Johansen, P.M., Orientational dynamics in dye-doped organic electro-optic materials. *J. Appl. Phys.* (2003) v. 94 p. 6263-6268

Baragiola, R.A.; Vidal, R.A.; Svendsen, W.; Schou, J.; Shi, M.; Bahr, D.A.; Atteberry, C.L., Sputtering of water ice. *Nucl. Instrum. Methods Phys. Res. B* (2003) v. 209 p. 294-303

Bubb, D.M.; Toftmann, B.; Haglund Jr., R.F.; Horwitz, J.S.; Papantonakis, M.R.; McGill, R.A.; Wu, P.W.; Chrisey, D.B., Resonant infrared pulsed laser deposition of thin biodegradable polymer films. *Appl. Phys. A* (2002) v. 74 p. 123-125

Horvath, R.; Lindvold, L.R.; Larsen, N.B., Fabrication of all-polymer freestanding waveguides. *J. Micromech. Microeng.* (2003) v. 13 p. 419-424

Horvath, R.; Pedersen, H.C.; Skivesen, N.; Selmeczi, D.; Larsen, N.B., Optical waveguide sensor for on-line monitoring of bacteria. *Opt. Lett.* (2003) v. 28 p. 1233-1235

Jespersen, K.G.; Pedersen, T.G.; Johansen, P.M., Electro-optic response of chromophores in a viscoelastic polymer matrix to a combined dc and ac poling field. *J. Opt. Soc. Am. B* (2003) v. 20 p. 2179-2188

Johansen, P.M., Photorefractive space-charge field formation: Linear and nonlinear effects. *J. Opt. A* (2003) v. 5 p. S398-S415

Kjærgaard, N.; Drewsen, M., Observation of a structural transition for coulomb crystals in a linear Paul trap. *Phys. Rev. Lett.* (2003) v. 91 p. 095002.1-095002.4

Mingjun Chi; Thestrup, B.; Mortensen, J.L.; Nielsen, M.E.; Petersen, P.M., Improvement of the beam quality of a diode laser with two active broad-area segments. *J. Opt. A* (2003) v. 5 p. S338-S341

Nedelchev, L.L.; Matharu, A.S.; Hvilsted, S.; Ramanujam, P.S., Photoinduced anisotropy in a family of amorphous azobenzene polyesters for optical storage. *Appl. Opt.* (2003) v. 42 p. 5918-5927

Ramanujam, P.S., Evanescent polarization holographic recording of sub-200-nm gratings in an azobenzene polyester. *Opt. Lett.* (2003) v. 28 p. 2375-2377

Ramanujam, P.S.; Nedelchev, L.; Matharu, A., Polarization holographic and surface-relief gratings at 257 nm in an amorphous azobenzene polyester. *Opt. Lett.* (2003) v. 28 p. 1072-1074

Sajti, S.; Kerekes, A.; Lorincz, E.; Ramanujam, P.S., Description of photoinduced anisotropy in azobenzene side-chain polyesters. *Synth. Met.* (2003) v. 138 p. 79-83

Samsøe, E.; Malm, P.; Andersen, P.E.; Petersen, P.M.; Andersson-Engels, S., Improvement of brightness and output power of high-power laser diodes in the visible spectral region. *Opt. Commun.* (2003) v. 219 p. 369-375

Sanchez, C.; Alcala, R.; Hvilsted, S.; Ramanujam, P.S., Effect of heat and film thickness on a photoinduced phase transition in azobenzene liquid crystalline polyesters. *J. Appl. Phys.* (2003) v. 93 p. 4454-4460

Skivesen, N.; Horvath, R.; Pedersen, H.C., Multimode reverse-symmetry waveguide sensor for broad-range refractometry. *Opt. Lett.* (2003) v. 28 p. 2473-2475

Thestrup, B.; Toftmann, B.; Schou, J.; Doggett, B.; Lunney, J.G., A comparison of the laser plume from Cu and YBCO studied with ion probes. *Appl. Surf. Sci.* (2003) v. 208 p. 33-38

Toftmann, B.; Schou, J.; Lunney, J.G., Dynamics of the plume produced by nanosecond ultraviolet laser ablation of metals. *Phys. Rev. B* (2003) v. 67 p. 104101.1-104101.5

Danish publications

Jespersen, K.G., Dynamics in nonlinear optical polymers. Risø-R-1397(EN) (2003) 126 p. (ph.d. thesis)

Conference lectures

Petersen, P.M.; Thestrup, B.; Chi, M., Improving the spatial and temporal coherence of high-power diode lasers using four-wave mixing in the gain material. In: Photorefractive effects, materials, and devices. 9. International conference, La Colle sur Loup (FR), 17-21 Jun 2003. Delaye, P.; Denz, C.; Mager, L.; Montemezzani, G. (eds.), (Optical Society of America, Washington, DC (US), 2003) (Trends in Optics and Photonics, vol. 87) p. 529-534

Ramanujam, P.S.; Berg, R.H., Photochromic processes for high-density optical storage. In: Optical data storage 2003. 6. International sumposium on optical storage, Vancouver (CA), 11-14 May 2003. O'Neill, M.; Miyagawa, N. (eds.), (International Society for Optical Engineering, Bellingham, VA, 2003) (SPIE Proceedings Series, 5069) p. 57-63

Publications for a broader readership

Kristensen, P.K.; Pedersen, T.G.; Johansen, P.M., Polymer light emitting diodes. *DOPS-Nyt* (2003) v. 18 (no.2) p. 9-11

Unpublished Danish lectures

Thestrup, B.; Petersen, P.M.; Chi, M., Improving the focusing properties of a near-infrared high-power broad-stripe diode laser (poster). Danish Physical Society annual meeting 2003, Nyborg (DK), 12-13 Jun 2003. Unpublished. Abstract available (AF23P)

Unpublished international lectures

Amoruso, S.; Bruzzese, R.; Velotta, R.; Wang, X.; Toftmann, B.; Schou, J., Diagnostics of laser ablated plasma plumes. E-MRS 2003 Spring meeting, Strasbourg (FR), 10-13 Jun 2003. Unpublished.

Amoruso, S.; Toftmann, B.; Schou, J., Expansion of a laser-produced silver plume in light and heavy background gases. 7. International conference on laser ablation, Hersonissos (GR), 5-10 Oct 2003. Unpublished.

Apitz, D.; Svanberg, C.; Jespersen, K.G.; Pedersen, T.G.; Johansen, P.M., Orientational dynamics in dye-doped organic electro-optic materials. 9. International conference on photorefractive effects, materials, and devices (PR'03), post-deadline paper, La Colle sur Loup (FR), 17-21 Jun 2003. Unpublished.

Berg, R.H.; Ramanujam, P.S., Photodimerization in peptides for high-density optical data storage (P466) , Biopolymers (2003) v. 71 p. 403

Berg, R.H.; Ramanujam, P.S., Optical data storage using peptides (invited lecture). 10. Congress of the European Society for Photobiology, Vienna (AT), 6-11 Sep 2003. Unpublished. Abstract available

Holmelund, E.; Thestrup, B.; Schou, J.; Tougaard, S.; Nielsen, M.M.; Johnson, E., Deposition and characterization of aluminum-doped ZnO films produced by pulsed laser deposition. 7. International conference on laser ablation, Hersonissos (GR), 5-10 Oct 2003. Unpublished.

Horvath, R., Refractive index dependent incoupled light inbtensity in planar optical waveguides and the detection of living cells. Biomedical optics '03 (BIOP 2003), Lyngby (DK), 28 Oct 2003. Unpublished.

Horwitz, J.S.; Callahan, J.A.; Houser, E.J.; McGill, R.A.; Bubb, D.M.; Papantonakis, M.R.; Haglund Jr., R.F.; Toftmann, B., Resonant-infrared pulsed laser deposition of organic thin films. 7. International conference on laser ablation, Hersonissos (GR), 5-10 Oct 2003. Unpublished.

Janik, K.; Toftmann, B.; Schou, J.; Pedrys, R., Laser ablation at 355 nm of organic materials embedded in matrices. NATO Advanced Study Institute, Laser processing of biological tissues and bio-compatible materials, Hersonissos (GR), 24 Sep - 3 Oct 2003. Unpublished.

Johansen, P.M., Dynamics of electro-optic polymers. Visit to University of Osnabrück, Osnabrück (DE), 23 May 2003. Unpublished.

Johansen, P.M.; Apitz, D.; Jespersen, K.G.; Pedersen, T.G., Dynamics of electro-optic polymers. In: Proceedings. Northern optics 2003, Espoo (FI), 16-18 Jun 2003. Noponen, E. (ed.), (Helsinki University of Technology, Department of Engineering Physics and Mathematics, Espoo, 2003) p. 11

Pedersen, T.G.; Lynge, T.B.; Kristensen, P.K.; Johansen, P.M., Theoretical study of conjugated porphyrin polymers. International conference on materials for advanced technologies (ICMAT 2003), Singapore (SG), 7-12 Dec 2003. Unpublished.

Skivesen, N., Reverse-symmetry multimode waveguide sensors. Biomedical optics '03 (BIOP 2003), Lyngby (DK), 28 Oct 2003. Unpublished.

Toftmann, B., Photon irradiation of organic materials in ice. 4. Nordic workshop on surface physics in planetary and astrophysical environments, Odense (DK), 19 Sep 2003. Unpublished.

Toftmann, B.; Budtz-Jørgensen, C.; Doggett, B.; Schou, J.; Lunney, J.G., Plume dynamics of UV laser ablation of silver in vacuum with fs-pulses. 7. International conference on laser ablation, Hersonissos (GR), 5-10 Oct 2003. Unpublished.

Toftmann, B.; Schou, J.; Doggett, B.; Budtz-Jørgensen, C.; Lunney, J.G., The angular distribution of plume ions from fs-laser irradiation. E-MRS 2003 Spring meeting, Strasbourg (FR), 10-13 Jun 2003. Unpublished. Abstract available

Toftmann, B.; Schou, J., Matrix assisted pulsed laser evaporation (MAPLE) of polyethylene glycol (PEG). E-MRS 2003 Spring meeting, Strasbourg (FR), 10-13 Jun 2003. Unpublished. Abstract available

Internal reports

Kjærgaard, N., Second harmonic generation in a two-mirror travelling wave resonator. (2003) p.

Schou, J., Monitoring for pulsed plasma processing - New plasma probes for advanced manufacturing. Final technical report. Risø-Dok-760 (2003) 51 p.

5.2 Optical diagnostics and information processing

International publications

Angelsky, O.V.; Burkovets, D.N.; Maksimyak, P.P.; Hanson, S.G., Applicability of the singular-optics concept for diagnostics of random and fractal rough surfaces. *Appl. Opt.* (2003) v. 42 p. 4529-4540

Daria, V.R.M.; Eriksen, R.L.; Glückstad, J., Dynamic optical manipulation of colloidal systems using a spatial light modulator. *J. Mod. Opt.* (2003) v. 50 p. 1601-1614

Daria, V.R.M.; Eriksen, R.L.; Sinzinger, S.; Glückstad, J., Optimizing the generalized phase contrast method for a planar optical device. *J. Opt. A* (2003) v. 5 p. S211-S215

Eriksen, R.L.; Daria, V.R.M.; Rodrigo, P.J.; Glückstad, J., Computer-controlled orientation of multiple optically-trapped microscopic particles. *Microelectr. Eng.* (2003) v. 67-68 p. 872-878

Eriksen, R.L.; Rodrigo, P.J.; Daria, V.R.; Glückstad, J., Spatial light modulator-controlled alignment and spinning of birefringent particles optically trapped in an array. *Appl. Opt. OT* (2003) v. 42 p. 5107-5111

Glückstad, J.; Daria, V.R.M.; Eriksen, R.L., Comment: Influence of illuminating beyond the object support on zernike-type phase contrast filtering. *Appl. Opt.* (2003) v. 42 p. 792-793

Glückstad, J.; Daria, V.R.M.; Rodrigo, P.J., Comment on interferometric phase-only optical encryption system that uses a reference wave. *Opt. Lett.* (2003) v. 28 p. 1075-1076

Hansen, R.S., Modeling of the nonlinear response of the intrinsic HgCdTe photoconductor by a two-level rate equation with a finite number of carriers available for photoexcitation. *Appl. Opt.* (2003) v. 42 p. 4819-4826

Jakobsen, M.L.; Osten, S.; Kitchen, S.R.; Dam-Hansen, C.; Hanson, S.G., Multiple-beam time-of-flight sensor based on a vertical cavity surface emitting laser diode array. *Meas. Sci. Technol.* (2003) v. 14 p. 329-335

Jensen, P.S.; Bak, J.; Andersson-Engels, S., Influence of temperature on water and aqueous glucose absorption spectra in the near- and mid-infrared regions at physiologically relevant temperatures. *Appl. Spectrosc.* (2003) v. 57 p. 28-36

Kitchen, S.R.; Dam-Hansen, C., Holographic common-path interferometer for angular displacement measurements with spatial phase stepping and extended measurement range. *Appl. Opt.* (2003) v. 42 p. 51-59

Kitchen, S.R.; Dam-Hansen, C.; Jakobsen, M.L., Quasi-achromatic laser Doppler anemometry systems based on a diffractive beam splitter. *Appl. Opt.* (2003) v. 42 (no.28) p. 5642-5648

Martiny, A.C.; Jørgensen, T.M.; Albrechtsen, H.-J.; Arvin, E.; Molin, S., Long-term succession of structure and diversity of a biofilm formed in a model drinking water distribution system. *Appl. Environ. Microbiol.* (2003) v. 69 p. 6899-6907

Rodrigo, P.J.; Daria, V.R.; Glückstad, J., Multiple dynamic optical traps facilitate active microscopy. *Opt. Photonics News* (2003) v. 14 p. 20

Rodrigo, P.J.; Eriksen, R.L.; Daria, V.R.M.; Glückstad, J., Interactive light-driven and parallel manipulation of inhomogeneous particles. *Opt. Express* (2002) v. 10 p. 1550-1556

Rodrigo, P.J.; Eriksen, R.L.; Daria, V.R.M.; Glückstad, J., Shack-Hartmann multiple-beam optical tweezers. *Opt. Express* (2003) v. 11 p. 208-214

Samsøe, E.; Malm, P.; Andersen, P.E.; Petersen, P.M.; Andersson-Engels, S., Improvement of brightness and output power of high-power laser diodes in the visible spectral region. *Opt. Commun.* (2003) v. 219 p. 369-375

Sørensen, H.S.; Pranov, H.; Larsen, N.B.; Bornhop, D.J.; Andersen, P.E., Absolute refractive index determination by microinterferometric backscatter detection. *Anal. Chem.* (2003) v. 75 p. 1946-1953

Yura, H.T.; Hanson, S.G., Comment: Absolute measurement of roughness and lateral-correlation length of random surfaces by use of ths Simplified model of image-speckle contrast. *Appl. Opt.* (2003) v. 42 p. 2521-2522

Yura, H.T.; Hanson, S.G., Variance of intensity for Gaussian statistics and partially developed speckle in complex ABCD optical systems. *Opt. Commun.* (2003) v. 228 p. 263-270

Danish publications

Andersen, P.E.; Thrane, L.; Bjerring, P.; Hougaard, J.L.; Hansen, P.R., Optisk kohærenstomografi. *Ugeskr. Læger* (2003) v. 165 p. 1546-1550

Kitchen, S.R., Optical sensors based on dedicated diffractive optical elements. Risø-R-1381(EN) (2003) 122 p. (ph.d. thesis) www.risoe.dk/rispubl/ofd/ris-r-1381.htm

Conference lectures

Andersen, P.E.; Thrane, L.; Yura, H.T.; Tycho, A.; Jørgensen, T.M., Modeling the optical coherence tomography geometry using the extended Huygens-Fresnel principle and Monte Carlo simulations. In: Proceedings. Saratov Fall meeting 2002: Optical technologies in biophysics and medicine 4, Saratov (RU), 1-4 Oct 2002. Tuchin, V.V. (ed.), (The International Society for Optical Engineering, Bellingham, WA, 2003) (SPIE Proceedings Series, 5068) p. 170-181

Choma, M.A.; Yelbuz, T.M.; Thrane, L.; Kirby, M.L.; Izatt, J.A., Three-dimensional OCT imaging of the embryonic chick heart. In: Proceedings. Coherence domain optical methods and optical coherence tomography in biomedicine 7, San Jose, CA (US), 27-29 Jan 2003. Tuchin, V.V.; Izatt, J.A.; Fujimoto, J.G. (eds.), (The International Society for Optical Engineering, Bellingham, WA, 2003) (SPIE Proceedings Series, 4956; Progress in Biomedical Optics and Imaging, v. 4, no. 8) p. 259-262

Daria, V.R.; Rodrigo, P.J.; Glückstad, J., Controllable coupling to the second-order mode of photonic crystal fibers. In: Photonics North 2003. International conference on applications of photonics technology, Montreal (CA), 25-29 May 2003. (Conference Organizing Committee, Montreal, 2003) (W-PM-OF1) 3 p.

Daria, V.R.; Rodrigo, P.J.; Glückstad, J., All-optical manipulation of microstructures for lab-on-a-scope applications. In: Creating essential bridges uniting physics, society, and industry. Proceedings. 21. SSP physics congress, Cebu City (PH), 22-25 Oct 2003. (University of San Carlos, Cebu City, 2003) 2 p.

Daria, V.R.; Rodrigo, P.J.; Glückstad, J., Controllable launching of high-order guided modes of microstructured fibres using a spatial light modulator. In: Topical meeting digest. Diffractive optics 2003, Oxford (GB), 17-19 Sep 2003. (Institute of Physics, London, 2003) (Topical Meeting Digest Series) p. 72-73

Falldorf, C.; Hanson, S.G.; Osten, W.; Jüptner, W., Fringe compensation in multiband speckle shearography using a wedge prism. In: Proceedings. Speckle metrology 2003, Trondheim (NO), 18-20 Jun 2003. Gastinger, K.; Løkberg, O.J.; Winther, S. (eds.), (International Society for Optical Engineering, Bellingham, WA, 2003) (SPIE Proceedings Series, 4933) p. 82-89

Glückstad, J.; Daria, V.R.; Eriksen, R.L.; Rodrigo, P.J., Vision-guided manipulation of colloidal structures (invited paper). In: Proceedings. Optical pattern recognition 14, Orlando, FL (US), 21-25 Apr 2003. Casasent, D.P.; Tien-Hsin Chao (eds.), (International Society for Optical Engineering, Bellingham, WA, 2003) (SPIE Proceedings Series, 5106) p. 46-52

Glückstad, J.; Daria, V.R.; Rodrigo, P.J., Generalized phase contrast facilitated encryption, wavefront sensing and optical micro-manipulation (invited paper). In: Proceedings. International conference on laser applications and optical metrology (ICLAOM-03), New Delhi (IN), 1-4 Dec 2003. Shakher, C.; Mehta, D.S. (eds.), (Anamaya Publishers, New Delhi, 2003) p. 135-141

Hansen, R.S., Handheld ESPI-speckle interferometer. In: Proceedings. Speckle metrology 2003, Trondheim (NO), 18-20 Jun 2003. Gastinger, K.; Løkberg, O.J.; Winther, S. (eds.), (International Society for Optical Engineering, Bellingham, WA, 2003) (SPIE Proceedings Series, 4933) p. 246-249

Jensen, L.K.; Thrane, L.; Andersen, P.E.; Tycho, A.; Pedersen, F.; Andersson-Engels, S.; Bendsøe, N.; Svanberg, S.; Svanberg, K., Optical coherence tomography in clinical examinations of nonpigmented skin malignancies. In: Proceedings. Conference on optical coherence tomography and coherence techniques, Munich (DE), 22-24 Jun 2003. Drexler, W. (ed.), (The International Society for Optical Engineering, Bellingham, WA, 2003) (SPIE Proceedings Series, 5140) p. 160-167

Levitz, D.; Andersen, C.B.; Frosz, M.H.; Thrane, L.; Hansen, P.R.; Jørgensen, T.M.; Andersen, P.E., Assessing blood vessel abnormality via extracting scattering coefficients from OCT images. In: Proceedings. Conference on optical coherence tomography and coherence techniques, Munich (DE), 22-24 Jun 2003. Drexler, W. (ed.), (The International Society for Optical Engineering, Bellingham, WA, 2003) (SPIE Proceedings Series, 5140) p. 12-19

Michelsen, P.K.; Bindslev. H.; Hansen, R.S.; Hanson, S.G., Position control of ECRH launcher mirrors by laser speckle sensor. In: Proceedings. 12. Joint workshop on electron cyclotron emission and electron cyclotron resonance heating, Aix-en-Provence (FR), 13-16 May 2002. (World Scientific, Singapore, 2003) p. 553-558

Rodrigo, P.J.; Daria, V.R.; Glückstad, J., Generation of multiple dynamic optical tweezers using microlens array and spatial light modulator. In: Topical meeting digest. Diffractive optics 2003, Oxford (GB), 17-19 Sep 2003. (Institute of Physics, London, 2003) (Topical Meeting Digest Series) p. 70-71

Rodrigo, P.J.; Lentge, H.; Daria, V.R.; Glückstad, J., Optical tweezers based on polarized beams from a reconfigurable diffractive optical element. In: Topical meeting digest. Diffractive optics 2003, Oxford (GB), 17-19 Sep 2003. (Institute of Physics, London, 2003) (Topical Meeting Digest Series) p. 94-95

Rodrigo, P.J.R.; Eriksen, R.L.; Daria, V.R.M.; Glückstad, J., Manipulation of mesoscopic particles with dynamic multiple-beam optical tweezers. In: Proceedings. 1. Humanoid, nanotechnology, information technology, communication and control, environment and management (HNICEM) international conference, Manila (PH), 27-30 Mar 2003. (Robautronix, Manila, 2003) 5 p.

Rodrigo, P.J.R.; Eriksen, R.L.; Daria, V.R.M.; Glückstad, J., Interactive light-powered lab-on-a-chip: Simultaneous actuation of microstructures by optical manipulation. In: Proceedings. Bioengineered and bioinspired systems, Maspalomas (ES), 19-21 May 2003. Rodríguez-Vázquez, A.; Abbott, D.; Carmona, R. (eds.), (International Society for Optical Engineering, Bellingham, WA, 2003) (SPIE Proceedings Series, 5119) p. 54-59

Sørensen, T.; Glückstad, J.; Bjarklev, A., Transversal non-destructive test principle for photonic crystal fibres. In: Proceedings. Photonic crystal materials and devices, San Jose, CA (US), 28-30 Jan 2003. Adibi, A.; Scherer, A.; Lin, S.Y. (eds.), (International Society for Optical Engineering, Bellingham, WA, 2003) (SPIE Proceedings Series, 5000) p. 287-296

Publications for a broader readership

Andersen, P.E.; Andersson-Engels, S., New beginnings in bio-photonics. *SPIE OE Mag.* (2003) (no.Oct.) p. 30

Hanson, S.G., ABCD for SDU. Kompendium udarbejdet for studerende ved SDU efteråret 2003. (Forskningscenter Risø, Risø, 2003) 31 p.

Jakobsen, M.L.; Hanson, S.G., Vertical cavity surface emitting lasers in optical sensors. *DOPS-Nyt* (2003) v. 17 (no.3) p. 12-15

Unpublished Danish lectures

Andersen, F., Introduction to Risø National Laboratory and the Thermometry Laboratory. Lecture to customers from Korea, Japan and Sweden, Risø (DK), 13 Jan 2003. Unpublished.

Andersen, F., Introduction to Risø National Laboratory and the Thermometry Laboratory. Lecture to customers from Korea, Japan and Sweden, Risø (DK), 3 Mar 2003. Unpublished.

Andersen, F., Introduction to Risø National Laboratory and the Thermometry Laboratory. Lecture to customers from Korea, Japan and Sweden, Risø (DK), 17 Mar 2003. Unpublished.

Andersen, F., Introduction to Risø National Laboratory and the Thermometry Laboratory. Lecture to customers from Korea, Japan and Sweden, Risø (DK), 7 Apr 2003. Unpublished.

Andersen, F., Introduction to Risø National Laboratory and the Thermometry Laboratory. Lecture to customers from Korea, Japan and Sweden, Risø (DK), 22 Apr 2003. Unpublished.

Andersen, F., Introduction to Risø National Laboratory and the Thermometry Laboratory. Lecture to customers from Korea, Japan and Sweden, Risø (DK), 10 Jun 2003. Unpublished.

Andersen, F., Introduction to Risø National Laboratory and the Thermometry Laboratory. Lecture to customers from Korea, Japan and Sweden, Risø (DK), 23 Jun 2003. Unpublished.

Andersen, F., Introduction to Risø National Laboratory and the Thermometry Laboratory. Lecture to customers from Korea, Japan and Sweden, Risø (DK), 15 Sep 2003. Unpublished.

Andersen, F., Introduction to Risø National Laboratory and the Thermometry Laboratory. Lecture to customers from Korea, Japan and Sweden, Risø (DK), 20 Oct 2003. Unpublished.

Andersen, F., Introduction to Risø National Laboratory and the Thermometry Laboratory. Lecture to customers from Korea, Japan and Sweden, Risø (DK), 8 Dec 2003. Unpublished.

Andersen, F.; Kaiser, N.E., Temperatur. Måling af temperatur og kalibrering af termometre. Seminar hos Bie og Berntsen A/S, Rødovre (DK), 10 Apr 2003. Unpublished.

Andersen, F.; Kaiser, N.E., Temperatur. Måling af temperatur og kalibrering af termometre. Seminar hos Bie og Berntsen A/S, Århus (DK), 18 Nov 2003. Unpublished.

Clausen, S., Non-intrusive gas analysis at high temperature (invited talk). Meeting on non-intrusive gas analysis at high temperature, Risø (DK), 29 Sep 2003. Unpublished. Abstract available

Jakobsen, M.L.; Hanson, S.G., VCSEL'er og deres anvendelse indenfor optiske sensorer. Final conference on Centre for Miniaturisation of Optical Sensors (MINOS), Risø (DK), 19 Mar 2003. Unpublished.

Jakobsen, M.L.; Osten, S.; Kitchen, S.R.; Dam-Hansen, C.; Hanson, S.G., Multiple-beam time-of-flight sensor based on a VCSEL array (poster). Final conference on Centre for Miniaturisation of Optical Sensors (MINOS), Risø (DK), 19 Mar 2003. Unpublished.

Jørgensen, T.M., Et kig bag computerens øjne - maskinsyn og active appearence modeller. Arrangementet 'Fra ide til produkt' for Musicon Valleys medlemsklub Backstage, Risø (DK), 27 Aug 2003. Unpublished.

Jørgensen, T.M., Quantification of biofilm structure from confocal imaging. Medicinsk vision dag, Lyngby (DK), 11 Jun 2003. Unpublished.

Nielsen, F.D., Bio-optik. Besøg af Amtsgymnasiet i Roskilde, Risø (DK), 6 Mar 2003. Unpublished.

Rodrigo, P.J.R., Optical tweezers (optiske pincetter). Besøg af Amtsgymnasiet i Roskilde, Risø (DK), 6 Mar 2003. Unpublished.

Unpublished international lectures

Andersen, P.E.; Tycho, A.; Jørgensen, T.M.; Yura, H.T., Monte Carlo modelling of optical coherence tomography systems (invited talk). International conference on advanced laser technologies (ALT '03), Silsoe (GB), 19-23 Sep 2003. Unpublished.

Andersen, P.E.; Tycho, A.; Jørgensen, T.M.; Thrane, L.; Yura, H.T., Monte Carlo modeling of optical coherence tomography systems (invited lecture). Saratov Fall meeting 2003. Internet session, Saratov (RU), 7-10 Oct 2003. Unpublished.

Bak, J.; Jensen, P.S., Measurement of glucose in aqueous solutions with dual-beam FTIR. Pittsburgh conference 2003. Session: Infrared spectroscopy: Method development and applications, Orlando, FL (US), 9-14 Mar 2003. Unpublished.

Choma, M.A.; Yelbuz, T.M.; Thrane, L.; Kirby, M.L.; Izatt, J.A., Three-dimensional optical coherence tomography: Applications to chick embryo cardiac development and drosophila melanogaster circulatory function. The Fitzpatrick Center for Photonics and Communication Systems 3. Annual symposium, Durham, NC (US), 27-28 May 2003. Unpublished. Abstract available

Choma, M.A.; Yelbuz, T.M.; Thrane, L.; Kirby, M.L.; Izatt, J.A., Three-dimensional optical coherence tomography: Applications to chick embryo cardiac development and drosophila melanogaster circulatory function. 3. World congress on heart disease, Washington, DC (US), 12-15 Jul 2003. Unpublished.

Daria, V.R.; Rodrigo, P.J.; Glückstad, J., Independently controlled multiple doughnut beams for trapping low-index microstructures (poster). In: Northern optics 2003. Joint conference of the Optical Societies of Denmark, Finland, Norway and Sweden, Espoo (FI), 16-18 Jun 2003. Noponen, E. (ed.), TKK-F-A822 (2003) p. 89

Falk, P.; Frosz, M.H.; Sanz, L.P.; Thrane, L.; Tycho, A., Compact, portable and modular OCT system. Biomedical optics '03 (BIOP 2003), Lyngby (DK), 28 Oct 2003. Unpublished. Abstract available

Frosz, M.H., Modelling of active fibres. In: Program. Book of abstracts. Bio-photonics '03. graduate Summer school, Ven (SE), 15-21 Jun 2003. (Risø National Laboratory, Roskilde, 2003) p. 6

Glückstad, J.; Daria, V.R.; Rodrigo, P.J., The potential for an all-optically assembled, powered and controlled micro-fluidic lab-on-a-chip system. In: Digest of papers. 2003 International microprocesses and nanotechnology conference, Tokyo (JP), 29-31 Oct 2003. (Japan Society of Applied Physics, Tokyo, 2003) 2 p.

Hanson, S.G., Velocity measurement in the atmosphere based on optical tracking of refractive index fluctuations (invited paper). 6. International conference "Correlation optics" (CorrOpt '03), Chernivtsi (UA), 16-19 Sep 2003. Unpublished.

Jakobsen, M.L.; Larsen, H.E.; Hanson, S.G., Compact optical system for measuring linear and angular displacement of solid structures. 6. International conference "Correlation optics" (CorrOpt '03), Chernivtsi (UA), 16-19 Sep 2003. Unpublished.

Jakobsen, M.L.; Osten, S.; Kitchen, S.R.; Dam-Hansen, C.; Hanson, S.G., VCSEL array for compact time-of-flight sensor. In: Photonics North 2003. International conference on applications of photonics technology, Montreal (CA), 25-29 May 2003. (Conference Organizing Committee, Montreal, 2003) (M-PM-D2) 1 p.

Jensen, P.S.; Bak, J.; Ladefoged, S.; Andersson-Engels, S., On-line measurement of trace components in dialysate with dual-beam FTIR spectroscopy. Pittsburgh conference 2003. Session: Biomedical analysis, Orlando, FL (US), 9-14 Mar 2003. Unpublished.

Jensen, S.B., Four-wave mixing in broad area semiconductor lasers. In: Program. Book of abstracts. Bio-photonics '03. graduate Summer school, Ven (SE), 15-21 Jun 2003. (Risø National Laboratory, Roskilde, 2003) p. 8

Jørgensen, T.M.; Hougaard, J.L.; Sander, B.; Thrane, L.; Larsen, M., Image processing scheme for enhancing retinal oct scans. 3. International Workshop on Computer Assisted Fundus Image Analysis (CAFIA 2003), Turin (IT), 28-30 Mar 2003. Unpublished. Abstract available

Larsen, M.; Thrane, L.; Hougaard, J.L.; Sander, B.; Jørgensen, T.M., Enhanced-resolution optical coherence tomographic imaging of ischemic and edematous retinal damage. 3. International Workshop on Computer Assisted Fundus Image Analysis (CAFIA 2003), Turin (IT), 28-30 Mar 2003. Unpublished. Abstract available

Nielsen, F.D., Frequency chirped Yb3+ fibre laser for OCT. In: Program. Book of abstracts. Bio-photonics '03. graduate Summer school, Ven (SE), 15-21 Jun 2003. (Risø National Laboratory, Roskilde, 2003) p. 12

Rodrigo, P.J.; Daria, V.R.M.; Glückstad, J., Active microscopy: User-interface SLM-driven optical micaromanipulation. Biomedical optics '03 (BIOP 2003), Lyngby (DK), 28 Oct 2003. Unpublished.

Rodrigo, P.J.; Eriksen, R.L.; Daria, V.R.; Glückstad, J., Powering microfluidic systems with optically trapped colloidal microspheres (poster). In: Northern optics 2003. Joint conference of the Optical Societies of Denmark, Finland, Norway and Sweden, Espoo (FI), 16-18 Jun 2003. Noponen, E. (ed.), TKK-F-A822 (2003) p. 25

Samsøe, E., Diode laser systems for photodynamic therapy and diagnosis. In: Program. Book of abstracts. Bio-photonics '03. graduate Summer school, Ven (SE), 15-21 Jun 2003. (Risø National Laboratory, Roskilde, 2003) p. 15

Sørensen, H.S., Microstructure fabrication for an optical polymer based bio-chip sensor. Biomedical optics '03 (BIOP 2003), Lyngby (DK), 28 Oct 2003. Unpublished. Abstract available

Thrane, L., Multiple scattering effects in optical Doppler tomography. In: Program. Book of abstracts. Bio-photonics '03. graduate Summer school, Ven (SE), 15-21 Jun 2003. (Risø National Laboratory, Roskilde, 2003) p. 18

Thrane, L., Multiple scattering effects in optical Doppler tomography. Biomedical optics '03 (BIOP 2003), Lyngby (DK), 28 Oct 2003. Unpublished. Abstract available

Thrane, L.; Frosz, M.H.; Tycho, A.; Jørgensen, T.M.; Levitz, D.; Yura, H.T.; Andersen, P.E., OCT modelling: From theory towards clinical applications (invited paper). In: Conference digest book. International conference on advanced laser technologies. 11. Annual meeting, Cranfield (GB), 19-23 Sep 2003. (Cranfield University at Silsoe, Cranfield, 2003) p. 25

Internal reports

Andersen, P.E.; Black, J.; Thrane, L., A continuously swept frequency laser source. US patentansøgning

Clausen, S.; Jensen, P.S.; Jørgensen, T.M., Optiske målinger på Enstedværkets Biokedel november 2002. (2003) 27 p.

Hansen, R.S., An optical system. DK patentansøgning PA 2003 00651

5.3 Plasma and fluid dynamics

International publications

Andersen, A.; Bohr, T.; Stenum, B.; Juul Rasmussen, J.; Lautrup, B., Anatomy of a bathtub vortex. *Phys. Rev. Lett.* (2003) v. 91 p. 104502.1-104502.4

Andersen, A.; Lautrup, B.; Bohr, T., An averaging method for nonlinear laminar Ekman layers. *J. Fluid Mech.* (2003) v. 487 p. 81-90

Bache, M.; Gaididei, Y.B.; Christiansen, P.L., Nonclassical statistics of intracavity coupled chi2 waveguides: The quantum optical dimer. *Phys. Rev. A* (2003) v. 67 p. 043802.1-043802.15

Basse, N.P.; Zoletnik, S.; Baumel, S.; Endler, M.; Hirsch, M.; McCormick, K.; Werner, A., Turbulence at the transition to the high density H-mode in Wendelstein 7-AS plasmas. *Nucl. Fusion* (2003) v. 43 p. 40-48

Basse, N.P.; Zoletnik, S.; Antar, G.Y.; Baldzuhn, J.; Werner, A., Characterization of turbulence in L- and ELM-free H-mode Wendelstein 7-AS plasmas. *Plasma Phys. Control. Fusion* (2003) v. 45 p. 439-453

Basu, R.; Jessen, T.; Naulin, V.; Juul Rasmussen, J., Turbulent flux and the diffusion of passive tracers in electrostatic turbulence. *Phys. Plasmas* (2003) v. 10 p. 2696-2703

Basu, R.; Naulin, V.; Juul Rasmussen, J., Particle diffusion in anisotropic turbulence. *Commun. Nonlinear Sci. Num. Simul.* (2003) v. 8 p. 477-492

Bian, N.H.; Garcia, O.E., Confinement and dynamical regulation in two-dimensional convective turbulence. *Phys. Plasmas* (2003) v. 10 p. 4696-4707

Garcia, O.E.; Bian, N.H.; Paulsen, J.V.; Benkadda, S.; Rypdal, K., Confinement and bursty transport in a flux-driven convection model with sheared flows. *Plasma Phys. Control. Fusion* (2003) v. 45 p. 919-932

Garcia, O.E.; Bian, N.H., Bursting and large-scale intermittency in turbulent convection with differential rotation. *Phys. Rev. E* (2003) v. 68 p. 047301.1-047301.4

Guio, P.; Børve, S.; Daldorff, L.K.S.; Lynov, J.P.; Michelsen, P.; Pecseli, H.L.; Juul Rasmussen, J.; Saeki, K.; Truelsen, J., Phase space vortices in collisionless plasmas. *Nonlinear Process. Geophys.* (2003) v. 10 p. 75-86

Krolikowski, W.; Bang, O.; Wyller, J.; Juul Rasmussen, J., Optical beams in nonlocal nonlinear media. *Acta Phys. Pol. A* (2003) v. 103 p. 133-147

Lomholt, S.; Maxey, M.R., Force-coupling method for particulate two-phase flow: Stokes flow. *J. Comput. Phys.* (2003) v. 184 p. 381-405

Naulin, V., Electromagnetic transport components and sheared flows in drift-Alfven turbulence. *Phys. Plasmas* (2003) v. 10 p. 4016-4028

Naulin, V.; Juul Rasmussen, J.; Nycander, J., Transport barriers and edge localized modes-like bursts in a plasma model with turbulent equipartition profiles (Erratum in Phys. Plasmas v. 9, 3804 (2003)). *Phys. Plasmas* (2003) v. 10 p. 1075-1082

Naulin, V.; Nielsen, A.H., Accuracy of spectral and finite difference schemes in 2D advection problems. *SIAM J. Sci. Comput.* (2003) v. 25 p. 104-126

Nikolov, N.I.; Neshev, D.; Bang, O.; Krolikowski, W.Z., Quadratic solitons as nonlocal solitons. *Phys. Rev. E* (2003) v. 68 p. 036614.1-036614.5

Nikolov, N.I.; Sørensen, T.; Bang, O.; Bjarklev, A., Improving efficiency of supercontinuum generation in photonic crystal fibers by direct degenerate four-wave mixing. *J. Opt. Soc. Am. B* (2003) v. 20 p. 2329-2337

Ostrikov, K.N.; Tsakadze, E.L.; Xu, S.; Vladimirov, S.V.; Storer, R.G., Nonlinear electromagnetic fields in 0.5 MHz inductively coupled plasmas. *Phys. Plasmas* (2003) v. 10 p. 1146-1151

Ruban, V.P.; Juul Rasmussen, J., Toroidal bubbles with circulation in ideal hydrodynamics: A variational approach. *Phys. Rev. E* (2003) v. 68 p. 056301.1-056301.11

Verhoeven, A.G.A.; Bongers, W.A.; Elzendoorn, B.S.Q.; Graswinckel, M.; Hellingman, P.; Kooijman, W.; Kruijt, O.G.; Maagdenberg, J.; Ronden, D.; Stakenborg, J.; Sterk, A.B.; Tichler, J.; alberti, S.; Goodman, T.; Henderson, M.; Hoekzema, J.A.; Oosterbeek, J.W.; Fernandez, A.; Likin, K.; Bruschi, A.; Cirant, S.; Novak, S.; Piosczyk, B.; Thumm, M.; Bindslev, H.; Kaye, A.; Fleming, C.; Zohm, H., The design of an ECRH system for JET-EP. *Nucl. Fusion* (2003) v. 43 p. 1477-1486

Danish publications

Bindslev, H.; Singh, B.N (eds.), Association Euratom - Risø National Laboratory annual progress report 2002. Risø-R-1414(EN) (2003) 53 p. www.risoe.dk/rispubl/ofd/ris-r-1414.htm

Published conference papers

Bindslev, H., Operations space diagram for ECRH and ECCD in JET and ITER. In: Proceedings. 12. Joint workshop on electron cyclotron emission and electron cyclotron resonance heating, Aix-en-Provence (FR), 13-16 May 2002. (World Scientific, Singapore, 2003) p. 119-124

Garcia, O.E.; Bian, N.H.; Naulin, V.; Nielsen, A.H.; Juul Rasmussen, J., Bursting and intermittency in two-dimensional convective turbulence (poster). In: Contributed papers (on CD-ROM). 30. European Physical Society conference on controlled fusion and plasma physics, St. Petersburg (RU), 7-11 Jul 2003. (European Physical Society, Paris, 2003) (Europhysics Conference Abstracts, vol. 27A) P-1.173 (4 p.)

Korsholm, S.B.; Bindslev, H.; Egedal, J.; Hoekzema, J.A.; Leuterer, F.; Meo, F.; Michelsen, P.K.; Tsakadze, E.L.; Woskov, P., Fast ion millimeter wave CTS diagnostics on TEXTOR and ASDEX upgrade (poster). In: Contributed papers (on CD-ROM). 30. European Physical Society conference on controlled fusion and plasma physics, St. Petersburg (RU), 7-11 Jul 2003. (European Physical Society, Paris, 2003) (Europhysics Conference Abstracts, vol. 27A) P-1.53 (4 p.)

Michelsen, P.K.; Bindslev. H.; Hansen, R.S.; Hanson, S.G., Position control of ECRH launcher mirrors by laser speckle sensor. In: Proceedings. 12. Joint workshop on electron cyclotron emission and electron cyclotron resonance heating, Aix-en-Provence (FR), 13-16 May 2002. (World Scientific, Singapore, 2003) p. 553-558

Naulin, V., Electromagnetic transport components and sheared flows in plasma edge turbulence (invited topical talk). In: Proceedings (CD-ROM). 11. International congress on plasma physics (ICPP 2002), Sydney (AU), 15-19 Jul 2002. Falconer, I.S.; Dewar, R.L.; Khachan, J. (eds.), (American Institute of Physics, New York, 2003) (AIP Conference Proceedings, 669) p. 626-629

Naulin, V.; Garcia, O.E.; Nielsen, A.H.; Juul Rasmussen, J., Statistics of SOL and drift-wave turbulence transport events. In: Contributed papers (on CD-ROM). 30. European Physical Society conference on controlled fusion and plasma physics, St. Petersburg (RU), 7-11 Jul 2003. (European Physical Society, Paris, 2003) (Europhysics Conference Abstracts, vol. 27A) O-2.4A (4 p.)

Naulin, V.; Juul Rasmussen, J., Aspects of turbulent transport (invited paper). In: Proceedings. Vol. 4. International conference on phenomena in ionized gases (26. ICPIG), Greifswald (DE), 19-20 Jul 2003. Meichsner, J.; Loffhagen, D.; Wagner, H.-E. (eds.), (Local Organizing Committee, Greifswald, 2003) p. 237-238

Naulin, V.; Juul Rasmussen, J.; Stenum, B.; Bokhoven, L.J.A. van; Konijnenberg, J. van de, Modelling the formation of large scale zonal flows in drift wave turbulence in a rotating fluid experiment (poster). In: Proceedings (CD-ROM). 11. International congress on plasma physics (ICPP 2002), Sydney (AU), 15-19 Jul 2002. Falconer, I.S.; Dewar, R.L.; Khachan, J. (eds.), (American Institute of Physics, New York, 2003) (AIP Conference Proceedings, 669) p. 662-665

Naulin, V.; Nycander, J.; Juul Rasmussen, J., Dynamics of transport barriers and ELM-like behaviour in electrostatic turbulence (poster). In: Proceedings (CD-ROM). 11. International congress on plasma physics (ICPP 2002), Sydney (AU), 15-19 Jul 2002. Falconer, I.S.; Dewar, R.L.; Khachan, J. (eds.), (American Institute of Physics, New York, 2003) (AIP Conference Proceedings, 669) p. 659-661

Verhoeven, A.G.A.; Bongers, W.A.; Elzendoorn, B.S.Q.; Graswinckel, M.; Hellingman, P.; Kamp, J.J.; Kooijman, W.; Kruijt, O.G.; Maagdenberg, J.; Ronden, D.; Stakenborg, J.; Sterk, A.B.; Tichler, J.; Alberti, S.; Goodman, T.; Henderson, M.; Hoekzema, J.A.; Oosterbeek, J.W.; Fernandez, A.; Likin, K.; Bruschi, A.; Cirant, S.; Novak, S.; Piosczyk, B.; Thumm, M.; Bindslev, H.; Kaye, A.; Fleming, C.; Zohm, H., The 113 GHz ECRH system for JET. In: Proceedings. 12. Joint workshop on electron cyclotron emission and electron cyclotron resonance heating, Aix-en-Provence (FR), 13-16 May 2002. (World Scientific, Singapore, 2003) p. 511-516

Westerhof, E.; Hogeweij, G.M.D.; Hoekzema, J.A.; Schüller, F.C.; Barth, C.J.; Bindslev, H.; Donné, A.J.H.; Dumortier, P.; Gorkom, J.V. van; Jaspers, R.J.E.; Kalupin, D.; Koslowski, H.R.; Krämer-Flecken, A.; Cardozo, N.J.L.; Meiden, H.J. van der; Messiaen, A.; Oyevaar, T.; Polman, R.W.; Porte, L.; Udintsev, V.S.; Unterberg, B.; Vervier, M.; Eester, D. van; Wassenhove, G. van, Electron cyclotron resonance heating on TEXTOR: Results from the preliminary 110 GHz system. In: Proceedings. 12. Joint workshop on electron cyclotron emission and electron cyclotron resonance heating, Aix-en-Provence (FR), 13-16 May 2002. (World Scientific, Singapore, 2003) p. 395-402

Unpublished conference papers from Danish conferences incl. published abstracts

Jensen, V.O., Fusionsenergi - fremtidens uudtømmelige energikilde. Møde i Ungdommens Naturvidenskabelige forening, UNF, Aalborg (DK), 11 Feb 2003. Unpublished.

Jensen, V.O., Fusionsenergi - fremtidens uudtømmelige energikilde. Møde i Ungdommens Naturvidenskabelige forening, UNF, Århus (DK), 11 Sep 2003. Unpublished.

Unpublished conference papers from international conferences incl. published abstracts

Bindslev, H., ECW-CMA operations space diagram for ITER. IAEA technical meeting on ECRH physics and technology for ITER, Kloster Seeon (DE), 14-16 Jul 2003. Unpublished. PowerPoint presentation available

Bindslev, H., Fast ion dynamics measured by collective Thomson scattering (invited lecture). International conference: Plasma 2003, Warsaw (PL), 9-12 Sep 2003. Unpublished.

Bindslev, H., ITER: An opportunity for Europe. Dinner debate on fusion, European Parliament, Strasbourg (FR), 19 Nov 2003. Unpublished.

Bindslev, H.; Tsakadze, E.; Meo, F.; Korsholm, S.; Michelsen, P.; Woskov, P.; Hoekzema, F.; Leuterer, F.; Egedal, J.; Porte, L.; Eester, D. van, Diagnosing fast ions in ITER with collective Thomson scattering. 4. Meeting of the ITPA Topical Group on Diagnostics, Padova (IT), 17-21 Feb 2003. Unpublished. PowerPoint presentation available

Bindslev, H.; Korsholm, S.; Meo, F.; Michelsen, P.; Søgård, S.; Tsakadze, E.; Woskov, P.; Hoekzema, F.; Leuterer, F.; Egedal, J.; Porte, L.; Eester, D. van, Fast ion dynamics measured by collective Thomson scattering. Colloquium IPP Garching, Garching (DE), 16 May 2003. Unpublished. PowerPoint presentation available

Garcia, O.E.; Bian, N.H.; Naulin, V.; Nielsen, A.H.; Juul Rasmussen, J., Bursting and intermittency in two-dimensional convective turbulence. Meeting on new themes in plasma and fluid turbulence, London (GB), 13-14 May 2003. Unpublished.

Garcia, O.E.; Naulin, V.; Nielsen, A.H.; Juul Rasmussen, J., Transport statistics and intermittency in plasma turbulence. In: Book of abstracts. 10. European fusion theory conference (EFTC), Helsinki (FI), 8-10 Sep 2003. (Helsinki University of Technology, Helsinki, 2003) p. O-6 (P2-9)

Garcia, O.E.; Naulin, V.; Nielsen, A.H.; Juul Rasmussen, J., Theoretical investigation on intermittent transport in the scrape-off-layer (poster). In: Book of abstracts. 10. European fusion theory conference (EFTC), Helsinki (FI), 8-10 Sep 2003. (Helsinki University of Technology, Helsinki, 2003) p. P2-23

Juul Rasmussen, J., Self-focusing of lighe pulses, and collapse dynamics in Bose-Einstein condensates. In: Book of abstracts. 3. IMACS international conference on nonlinear evolution equations and wave phenomena: Computation and theory, Athens, GA (US), 7-10 Apr 2003. Taha, T.R. (ed.), (University of Georgia Athens, Athens, GA, 2003) p. 143

Juul Rasmussen, J., Self-focusing and wave collapse dynamics. Seminar at College of Charleston, Charleston, SC (US), 2003. Unpublished. Abstract available

Juul Rasmussen, J.; Naulin, V.; Basu, R.; Jessen, T., Particle diffusion and transport in electrostatic turbulence. Meeting on new themes in plasma and fluid turbulence, London (GB), 13-14 May 2003. Unpublished.

Korsholm, S.B., Fast ion millimeter wave CTS diagnostics on TEXTOR and ASDEX upgrade. Seminar at ELVA-1 Millimeter Wave Division (DOK Ltd.), St. Petersburg (RU), 10 Jul 2003. Unpublished.

Korsholm, S.B.; Bindslev, H.; Egedal, J.; Hoekzema, J.A.; Leuterer, F.; Michelsen, P.K.; Tsakadze, E.; Woskov, P., Fast ion millimeter wave CTS diagnostics on TEXTOR and ASDEX (poster). In: Program. 44. Annual meeting of the Division of Plasma Physics, American Physical Society, Orlando, FL (US), 11-15 Nov 2002. (American Institute of Physics, Melville, NY, 2002) (Bulletin of the American Physical Society, v. 47, no. 9) p. 84

Korsholm, S.B.; Bindslev, H.; Egedal, J.; Hoekzema, J.; Leuterer, F.; Meo, F.; Michelsen, S.; Michelsen, P.K.; Tsakadze, E.L.; Woskov, P., Implementation of fast ion millimeter wave CTS diagnostics on TEXTOR and ASDEX upgrade. 45. Annual meeting of the Division of Plasma Physics, American Physical Society, Albuquerque, NM (US), 27-31 Oct 2003. Unpublished. Abstract available

Krolikowski, W.; Bang, O.; Wyller, J.; Juul Rasmussen, J., Nonlocal solitons. In: Book of abstracts. 3. IMACS international conference on nonlinear evolution equations and wave phenomena: Computation and theory, Athens, GA (US), 7-10 Apr 2003. Taha, T.R. (ed.), (University of Georgia Athens, Athens, GA, 2003) p. 32

Krolikowski, W.; Bang, O.; Neshev, D.; Nikolov, N.I., Quadratic solitons as nonlocal solitons (contributed talk EE2-5-WED). CLEO/EQEC Europe 2003, Munich (DE), 23-27 Jun 2003. Unpublished.

Milovanov, A.V.; Juul Rasmussen, J., Topology of percolation at criticality and the Alexander-Orbach conjecture. Niels Bohr Summer Institute on complexity and criticality symposium and workshop, Copenhagen (DK), 21-29 Aug 2003. Unpublished. Abstract available

Naulin, V., Turbulence, flows, transport .... Risø's 2 cent worth. IPP Theorie meeting, Mac-Planck Gesellschaft, Zinnowitz (DE), 17-20 Nov 2003. Unpublished.

Naulin, V.; Basu, R.; Garcia, O.E.; Nielsen, A.H.; Juul Rasmussen, J., Statistics of transport in drift and drift-Alfvén turbulence (invited talk). 8. Easter plasma meeting, Torino (IT), Apr 2003. Unpublished.

Naulin, V.; Garcia, O.E.; Nielsen, A.H.; Basu, R.; Juul Rasmussen, J., Transport statistics in drift-wave turbulence. Meeting on new themes in plasma and fluid turbulence, London (GB), 13-14 May 2003. Unpublished.

Naulin, V.; Garcia, O.E.; Nielsen, A.H.; Basu, R.; Juul Rasmussen, J., Transport statistics in drift-wave turbulence (poster). Niels Bohr Summer Institute on complexity and criticality symposium and workshop, Copenhagen (DK), 21-29 Aug 2003. Unpublished. Abstract available

Nielsen, A.H.; Garcia, O.E.; Naulin, V.; Juul Rasmussen, J., Fluctuation statistics from numerical simulations of scrape-off-layer. Meeting on new themes in plasma and fluid turbulence, London (GB), 13-14 May 2003. Unpublished.

Nikolov, N.I., Effective white light generation in photonic crystal fibers. Seminar at Research School of Physical Sciences and Engineering, Australian National University, Canberra (AU), 19 Feb 2003. Unpublished.

Nikolov, N.I.; Bang, O.; Bjarklev, A., Designing the dispersion for optimum supercontinuum bandwidth using picosecond pulses (poster). 2003 Optical fiber communication conference, Atlanta, GA (US), 23-28 Mar 2003. Unpublished.

Ramponi, G.; Bindslev, H.; Farina, D.; Giruzzi, G.; Lloyd, B.; Novak, S.; Poli, E.; Shevchenko, V.; Volpe, F.; Zohm, H., Optimisation of the ITER top launcher. IAEA technical meeting on ECRH physics and technology for ITER, Kloster Seeon (DE), 14-16 Jul 2003. Unpublished. PowerPoint presentation available

Schröder, C.; Grulke, O.; Klinger, T.; Naulin, V., Investigations on drift wves in a helicon discharge (poster). Spring meeting of the German Physical Society DPG, Section Plasma Physics, Aachen (DE), 10-13 Mar 2003. Unpublished.

6. Personnel

Head of department

Jens-Peter Lynov

Heads of research programmes

Henrik Bindslev, Plasma and Fluid Dynamics
Hanson, Steen Grüner, Optical Diagnostics and Information Processing
Petersen, Paul Michael**,** Laser Systems and Optical Materials

Scientific staff

Andersen, Peter E.
Bak, Jimmy
Clausen, Sønnik
Daria, Vincent
Fateev, Alexander (from 15 September)
Glückstad, Jesper
Hansen, René Skov
Jakobsen, Michael Linde
Johansen, Per Michael
Jørgensen, Thomas Martini
Kirkegaard, Mogens
Kusano, Yukihiro (from 1 June)
Larsen, Henning Engelbrecht
Leipold, Frank (from 1 September)
Michelsen, Poul K.
Naulin, Volker
Nielsen, Anders H.
Nielsen, Birgitte Thestrup
Pedersen, Henrik Chresten
Ramanujam, P.S.
Rasmussen, Jens Juul
Schou, Jørgen
Stenum, Bjarne

Post Docs

Bardenshtein, Alexander (until 28 February)
Chi, Mingjun
Friderichsen, Anders (from 1 October)
Garcia, Odd Erik
Horvath, Robert
Jensen, Peter Snoer (until 29 August)
Jensen, Sussie Juul (until 14 January)
Kasimova, Marina
Kjærgaard, Niels (until 31 March)
Korsholm, Søren
Michelsen, Susanne (from 27 March)
Meo, Fernando (from 1 February)

Thrane, Lars
Tsakadze, Erekle

Technical staff

Andersen, Finn
Begovic, Tanja
Eilertsen, Erik
Eliasen, Finn
Holm, John
Jessen, Martin
Knudsen, Lene
Nielsen, Karsten Lindorff (from 1 August)
Nimb, Søren
Pedersen, Finn
Pedersen, Søren Peo
Petersen, Torben D.
Rasmussen, Erling
Sass, Bjarne
Stubager, Jørgen
Thorsen, Jess

Administrative staff

Andersen, Heidi (back from maternal leave on 17 February)
Andreasen, Mette (until 28 February)
Astradsson, Lone
Skaarup, Bitten

Research assistants

Jensen, Laura Køster (1 April – 30 June)
Kendl, Alexander (1 September – 31 October)

Laboratory assistant

Bülow, Jon Fold von (from 15 September)

PhD students

Andersen, Eva Samsøe
Apitz, Dirk
Christensen, Bo Toftmann
Eriksen, René Lynge (until 28 February)
Falk, Peter (from 1 November)
Frosz, Michael H. (from 1 September)
Holm, Jesper (from 13 October)
Jespersen, Kim G. (until 28 February)
Kristensen, Peter Kjær
Nielsen, Frederik Donbæk
Nielsen, Stefan Kragh (from 1 September)
Nikolov, Nikola Ivanov
Rodrigo, Peter John

Senchenko, Sergey
Skivesen, Nina
Sørensen, Henrik Schiøtt

Industrial PhD student

Kitchen, Steven R. (until 31 July)

Marie Curie student

Janik, Katarzyna (from 20 June)

MSc students

Andersen, Grith Hougaard (from 15 November)
Frosz, Michael (until 31 July)
Jensen, Laura Køster (until 31 March)
Lentge, Heidi (from 21 July – 30 November)
Levitz, David
Rytter, Malene (until 31 July)
Sanz, Laura Pastor (from 1 October)

BSc students

Bjernemose, Keld (from 9 September)
Dirksen, Kim (1 October – 20 December)
Haghighi, Navid (from 7 July)
Mousavian, Shabab (from 7 July)
Nilsson, Ronnie Thorup (from 11 August)

Visiting student

Delaux, Sebastian, MATMECA, Université Bordeaux, France

Student assistants

Christiansen, Lars (19 June – 29 August)
Jensen, Anne Marie (10 June – 31 August)
Kjær, Rasmus (10 June – 31 August)
Larsen, Sille Bendix (10 June – 31 August)
Madsen, Trine Hartvig (2 July – 30 August)
Ruminski, Wojciech (2 July – 30 August)
Sadol, Hülya (2 July – 30 August)
Søderman, Andreas (2 July – 30 August)

Guest scientists and short-term visitors

Andersen, Anders, Cornell University, Ithaca, USA
Andersson, Stefan E., Lund Institute of Technology, Lund, Sweden
Anhut, Tiemo, Swiss Federal Institute of Technology, Lausanne, Switzerland
Balan, Petru, Dept. of Ion Physics, University of Innsbruck, Austria
Benilov, Eugene, University of Limerick, Limerick, Ireland
Bornhop, Darryl, Texas Tech University at Lubbock, USA
Cecconello, Marco, Royal Institute of Technology, Stockholm, Sweden

Dhayal, Marshal, University of Manchester Institute of Science and Technology (UMIST), Manchester, United Kingdom
Dreher, Jürgen, Ruhr University, Bochum, Germany
Egedal, Jan, MIT Plasma Science and Fusion Center, Massachusetts, USA
Grauer, Rainer, Ruhr University, Bochum, Germany
Grigiene, Jurgita, Institute for Biomedical Research, Kaunas University of Medicine, Kaunas, Lithuania
Hesthaven, Jan, Brown University, USA
Kawata, Satoshi, Osaka University, Osaka, Japan
Kuznetsov, Eugenii A., Landau Institute of Theoretical Physics, Moscow, Russia
Milovanov, Alexander, Space Science Institute, Moscow, Russia
Pécseli, Hans L., Inst. Physics, University of Oslo, Norway
Rasmussen, Kim Ø., Los Alamos National Laboratory, USA
Ruban, Victor, Landau Institute for Theoretical Physics, Moscow, Russia
Shagalov, Arkadi G., Institute of Metal Physics, Ekaterinburg, Russia
Woskov, Paul, MIT Plasma Science and Fusion Center, Massachusetts, USA
Wyller, John, Agricultural University of Norway, Norway
Yamaguchi, Ichirou, Faculty of Engineering, Gunma University, Gunma, Japan
Yura, Hal, The Aerospace Corporation, Los Angeles, USA

Title and authors

Optics and Fluid Dynamics Department
Annual Progress Report for 2003

Edited by H. Bindslev, S.G. Hanson, J.P. Lynov, P.M. Petersen and B. Skaarup

ISBN	ISSN
87-550-3301-6 (Internet)	0106-2840; 0906-1797

Department or group	Date
Optics and Fluid Dynamics Department	May 2004

Pages	Tables	Illustrations	References
111	1	74	76

Abstract (max. 2000 characters)

The Optics and Fluid Dynamics Department performs basic and applied research within three scientific programmes: (1) laser systems and optical materials, (2) optical diagnostics and information processing and (3) plasma and fluid dynamics. The department has core competences in: optical sensors, optical materials, optical storage, biophotonics, numerical modelling and information processing, non-linear dynamics, fusion plasma physics and plasma technology. The research is supported by several EU programmes, including EURATOM, by Danish research councils and by industry. A summary of the activities in 2003 is presented.

Descriptors INIS/EDB

DIAGNOSTIC TECHNIQUES; DYNAMICS; FLUIDS; LASERS; NONLINEAR OPTICS; NONLINEAR PROBLEMS; NUMERICAL SOLUTION; PLASMA; PROGRESS REPORT; RESEARCH PROGRAMS; RISOE NATIONAL LABORATORY; THERMONUCLEAR REACTIONS